Development of an analytical method to quantify the oxidative deoxyribose damage product 3'-phosphoglycolaldehyde induced by radiation, iron and peroxynitrite

by

Christiane Collins

M.S. in Chemistry, Tufts University, 1999
Vorpruefung in Lebensmittelchemie, (Equivalent of Bachelor of Science in Food Chemistry), Ludwigs-Maximilians Universitaet, 1997

Submitted to the Biological Engineering Division in Partial Fulfillment of the Requirements for the Degree of

Ph.D. in Bioanalytical Chemistry
at the
MASSACHUSETTS INSTITUTE OF TECHNOLOGY

June, 2004

Signature of Author: _____
Biological Engineering Division
June, 2004

Certified by: _____
Peter C. Dedon
Professor of Biological Engineering and Toxicology
Thesis Supervisor

Accepted by: _____
Alan J. Grodzinsky
Chairman, Committee on Graduate Students
Biological Engineering Division

This doctoral thesis has been examined by a committee of the Biological Engineering Division as follows:

Dr. John S. Wishnok _____
Chairman

Professor Peter C. Dedon _____
Supervisor

Associate Professor Jeffrey A. Coderre: _____

Professor William G. Thilly _____ 18 May 2004

Professor Thomas D. Tullius _____ 5/18/04

Development of an analytical method to quantify the oxidative deoxyribose damage product 3'-phosphoglycolaldehyde induced by radiation, iron and peroxynitrite

by
Christiane Collins

Submitted to the Biological Engineering Division
on April 29th, 2004 in partial fulfillment of the
requirements for the degree of
Ph.D. in Bioanalytical Chemistry

ABSTRACT

Deoxyribose oxidation in DNA forms strongly electrophilic terminal blocking groups and abasic sites capable of stopping polymerases, forming DNA-protein cross-links and nucleobase adducts. These threats to the genetic integrity of cells are caused by exogenous and endogenous oxidizing agents and may contribute to diseases such as cancer. To better understand the role of oxidative DNA damage in these diseases, it is necessary to quantify deoxyribose oxidation both *in vitro* and *in vivo*. Current methods lack the sensitivity required to measure low concentrations of deoxyribose oxidation products. The goals of the research findings reported here is to develop a sensitive method that can accurately and reproducibly quantify 3'-phosphoglycoladehyde (PGA), one example of a deoxyribose oxidation product, and to apply the method to quantify PGA *in vitro* and in cells. Given the presence of reactive carbonyl groups in many deoxyribose oxidation products, the method should be widely applicable to other studies of oxidative DNA damage.

The analytical method exploits the reactive carbonyl moiety in PGA by derivatization as a stable oxime with pentafluorobenzylhydroxylamine, followed by solvent extraction and gas chromatography/negative chemical ionization/mass spectrometry. A stable isotopically-labeled [$^{13}C_2$]-PGA is synthesized and used as an internal standard. The method is linear in response over the range of 30 fmol to 300 pmol and precision is verified by analysis of a synthetic, PGA-containing oligodeoxynucleotide. The limit of detection in the presence of DNA is 30 fmol of PGA.

The analytical method was then applied to the quantification of PGA in purified DNA and cultured cells treated with several oxidants. γ-Radiation forms PGA in a linear dose response both *in vitro* and in cells with a 1000-fold quenching effect *in vivo*. The total quantity of deoxyribose oxidation, determined by plasmid topoisomer analysis, allows the calculation of PGA formation per deoxyribose oxidation event. PGA is formed in 1% of deoxyribose oxidation events induced by γ-radiation *versus* 7% for α-particles. PGA formation induced by Fe(II), Fe(II)/EDTA/H_2O_2, and peroxynitrite follows a nonlinear dose response best fitted to a second-order polynomial, in contrast to a linear response induced by Fe(II)/EDTA, with PGA formation representing 5% of deoxyribose

oxidation events. Peroxynitrite-induced DNA damage is studied under conditions of both hydroxyl radical and carbonate radical formation. With increasing carbonate radical formation, PGA induction is suppressed which indicates that the carbonate radical is not capable of inducing PGA.

Thesis Supervisor: Peter C. Dedon
Title: Professor of Biological Engineering Division

Acknowledgements

First and foremost I want to thank my mother, without her I would not have a high school degree, let alone a university degree. The encouragement and never-ending faith of my parents are the foundation of this thesis. There also were some outstanding teachers, who made it possible for a dyslexic girl to be able to go to high school and ultimately to university. Among those are Horst Reck and Rainer Janka, who believed in me for no apparent reason and tipped the vote in my favor so I could stay in high school. My outstanding Biology and Chemistry teacher Christine DeLorenzo taught me to use my brain. Dr. Siems, your memory will live on, even though you forced me to take German as a major in high school. You were right. Meinrad Staudiegl, your belief that people from different countries who can communicate with each other tend not to kill each other, brought me here and I treasure this memory of you. The career advisor in the Arbeitsamt Rosenheim, who made me attend the Chemieschule Elhardt to be educated as a chemical-technical assistant (instead of becoming a gardener or photographer), had everything to do with me ultimately becoming a chemist. My teacher Mr. Burger at the Chemieschule had faith in me when I did not, he gave me the self-esteem and direction I desperately needed.

I also have to thank the pharmaceutical department at the Ludwigs-Maximilians Universitaet for discontinuing my major, food chemistry, when I was in my third semester. I would not have come to the United States for a graduate degree if I had been able to finish my Master degree in Munich. Dr. Birgit Puschner is ultimately responsible for me going to the United States, without her I still would not know what a PhD is. I

want to thank Aida Herrera, who encouraged me to leave Tufts with a MS degree in search of a different graduate environment. I am very much in debt to Dr. Arthur Utz, Dr. Robert Stolow and the International Student Office at Tufts who supported my transfer to MIT above and beyond anything anyone could ever ask for. Dr. Shuguang Zhang first introduced me to my advisor and drew my attention to the toxicology program at MIT. Debra Luchanin, without you I would never have written this thesis! Scientifically I am much in debt to Elaine Plummer, Dr. Koli Taghizadeh, and Dr. Paul Skipper and my thesis committee Drs. John Wishnok, Jeffrey Coderre, William Thilly, and Thomas Tullius. I thank Rong Wang, Xinfeng Zhou, Mohamad Awada, Marita C. Barth and Tao Jiang for collaborating with me and providing results that put the content of this thesis into a greater context. All my colleagues at the Dedon lab past and present have enriched my life. My thesis advisor, Dr. Peter C. Dedon took more than one chance with me, which I will always be grateful for. His generous support and encouragement made me grow scientifically more than I ever thought I could. Dawn Erickson, you are the dream of every thesis-writing graduate student. My friends Olga Parkin and her family, Florian Sailer and Yvonne Slanz stood by me during my graduate career, some of you much longer than that, you will always have a special place in my heart. My mentor Bill Wei, your friendship and support means more to me than I can ever express.

Finally I want to thank my husband, David. You put many things into perspective for me, your optimism and faith in me and my abilities surprise me every day.

To my husband, David.

Table of Contents

List of Abbreviations
(in alphabetical order)

bp	base pair
BSTFA	*bis*(trimethylsilyl)trifluoroacetamide
Cu(OP2)	*bis*(1,10-phenanthroline)copper(I)
EDTA	ethelenediaminetetraacetic acid
GC	gas chromatography
HPLC	high pressure liquid chromatography
LET	linear energy transfer
5-MF	5-methylene-furanone
MS	mass spectrometry
NCI	negative chemical ionization
nt	nucleotide
$O_2^{\bullet}$	superoxide anion
$^{\bullet}OH$	hydroxyl radical
$ONOO^-$	peroxynitrite
$ONOOCO_2^-$	nitrosoperoxycarbonate
8-oxo-dG	8-oxo-7,8-dihydro-2'-deoxyguanosine
PFBHA	pentafluorobenzylhydroxylamine
PGA	3'-phosphoglcycolaldehyde
RNS	reactive nitrogen species
ROS	reactive oxygen species
SIM	selective ion monitoring
TBA	thiobarbituric acid

List of Figures

List of Schemes

Scheme V-2: Reaction of $ONOO^-$ with CO_2.

Scheme V-3: Oxidation of acetaldehyde by $ONOO^-$.

List of Tables

Chapter I

Introduction

Free radicals in biological systems have been associated with aging, carcinogenesis and radiation injury (reviewed in *1*). Many of these effects have been associated with the reaction of DNA with radicals, such as reactive oxygen (ROS) and nitrogen species (RNS). The former are produced by many xenobiotics (*i.e.* see reference *2*), during normal metabolism and by the indirect effects of ionizing radiation, while RNS are associated with the generation of nitric oxides for example at sites of inflammation *(i.e.* references *3, 4*). Both species attack cellular components such as lipids, proteins and carbohydrates in addition to DNA. However, DNA damage can also be therapeutic, as the treatment of cancer often involves DNA as a target for ionizing radiation and anti-tumor antibiotics such as bleomycin *(5)*. The studies presented here address the chemistry of DNA oxidation with a focus on the deoxyribose moiety and the formation of genotoxic, electrophilic products. The major goal of this thesis was to establish a sensitive and specific method to quantify deoxyribose oxidation in cells, which is discussed in Chapter II. So far no method to measure deoxyribose oxidation in cells is available, even though several methods are available to measure base lesions (*vide infra*). The developed method is applied to the quantification of the little studied C3' oxidation product 3'-phosphoglycolaldehyde, a potentially mutagenic, polymerase blocking lesion (*vide infra*).

Oxidation of DNA can involve either the nucleobases or the deoxyribose moiety, with a great deal of attention paid to the nucleobase lesions on the presumption that such lesions are directly responsible for toxicity and mutagenesis associated with ROS and RNS. However, radical-mediated oxidation of deoxyribose in DNA generates a variety of diffusible electrophiles, covalently bound fragments and oxidized abasic sites, with a unique spectrum of products derived from each position in the sugar *(6-8)* (see Figure I-1). There is growing evidence that deoxyribose oxidation plays a much larger role in the toxicity of oxidative stress than previously appreciated. For example, the deoxyribonolactone lesion arising from 1'-oxidation of deoxyribose causes the formation of protein-DNA cross-links in abortive attempts at repair by polymerase β *(9)* and endonuclease III *(10)*.

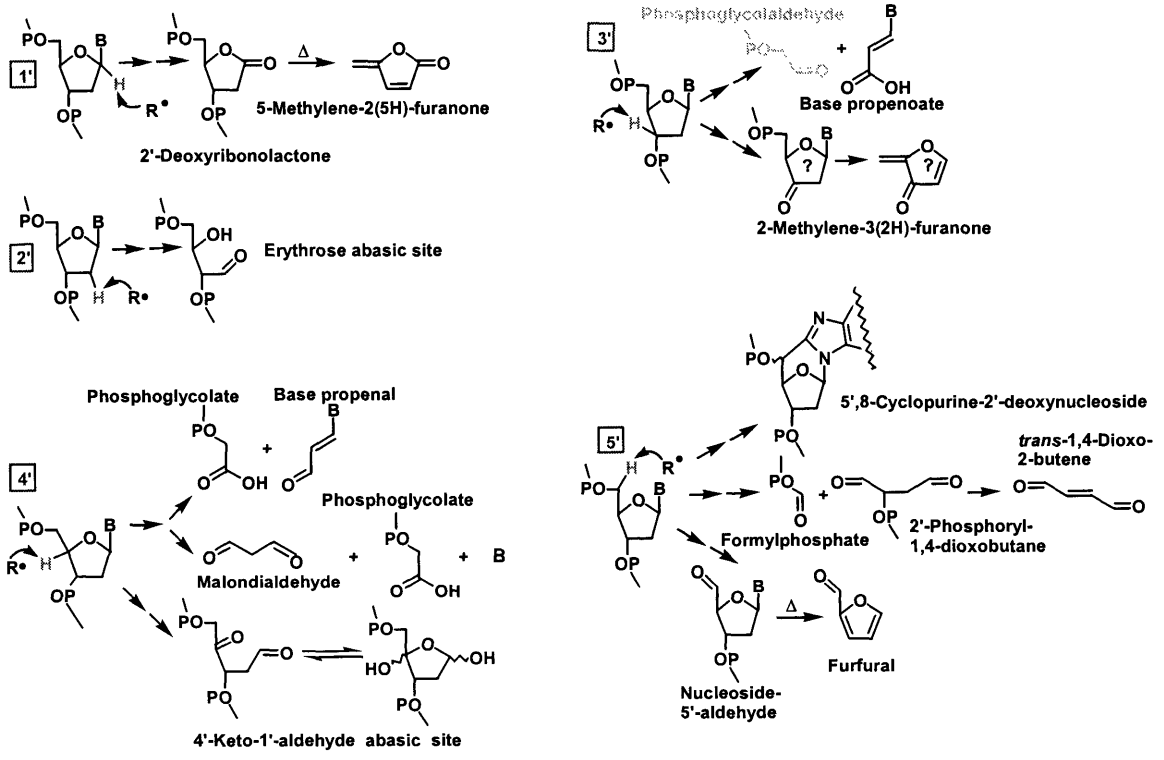

Figure I-1: Overview of deoxyribose oxidation products.

The electrophilic products of deoxyribose oxidation also have the potential to react with DNA bases to form mutagenic adducts. The first example of this phenomenon entails the reaction of base propenals, which arise from 4'-oxidation of deoxyribose, with dG to form the mutagenic pyrimidopurinone adduct, M_1G *(11)* (see Scheme I-1). More recently, we have demonstrated the formation of glyoxal and the mutagenic 1,N^2-glyoxal adducts of dG *(12, 13)* in reactions of DNA with phosphoglycolaldehyde under physiological conditions *(14)* (see Scheme I-2).

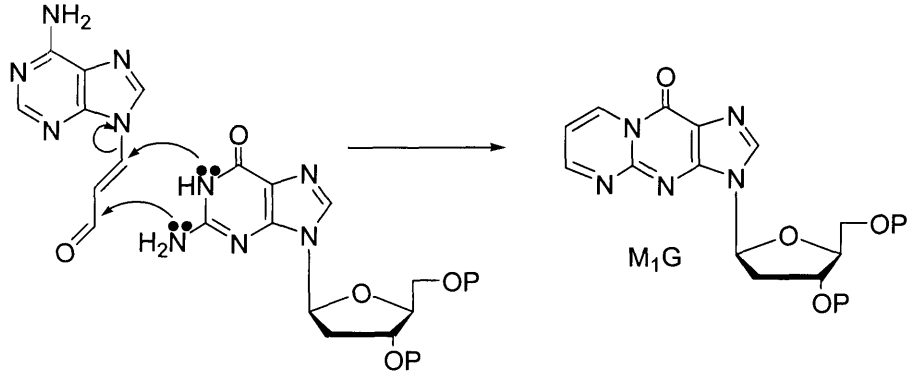

Scheme I-1: Proposed mechanism for the formation of M_1G from adenine propenal *(11)*.

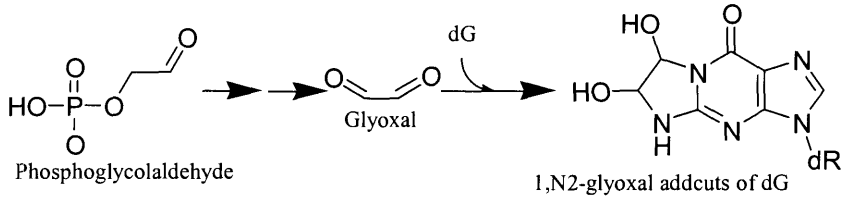

Scheme I-2: Proposed mechanism for the formation of 1,N^2-glyoxal adducts of dG from phosphoglycolaldehyde *(14)*.

These specific examples have motivated us to develop sensitive analytical methods to quantify deoxyribose oxidation products in an effort to define the spectrum of sugar-derived electrophiles and their reaction products in cells. The challenge here is that, not only do the oxidation products vary for each position in deoxyribose *(7, 8)*, the different oxidizing agents produce different proportions of products (even different products altogether) at the same sites in deoxyribose *(15)* (*vide infra*). For example, it has recently been observed that, under biological conditions of pH and ionic strength, γ-radiation produces 4'-chemistry consisting of a malondialdehyde moiety and a free nucleobase but not the base propenal observed with bleomycin and the enediynes *(7, 16)*.

In this chapter, a comprehensive review of the field of deoxyribose oxidation is presented, focusing on deoxyribose oxidation products and the responsible oxidative agent, beginning with the C3' position due to the relevance of this position for this thesis.

1. DEOXYRIBOSE OXIDATION IN GENERAL

The deoxyribose in DNA has seven carbon-bound hydrogen atoms that are available for abstraction by radicals or other one-electron oxidants. These atoms have been designated as H-5', H-5'', H-4', H-3', H-2', H-2'' and H-1' *(8)* (see Figure I-2). In addition to differences in reactivity due to inherent carbon-hydrogen bond energies, the various hydrogen atoms in deoxyribose are differentially reactive with oxidants as a result of the three dimensional structure of B-DNA. This latter feature has been explained by both chemical and computational means (see for example *17-19*). Balasubramanian *et*

al. found that Fe(II)/EDTA/H_2O_2/ascorbate caused deoxyribose oxidation with relative reactivity occurring in the following order: 5'-H > 4'-H > 3'-H ≈ 2'H ≈ 1'-H *(19)*. The authors observed a high degree of correlation between the solvent-accessibility of the deoxyribose hydrogen atoms and the reactivity towards the oxidizing agent *(19)*. Aydogan *et al.* used an atomistic stochastic model of hydroxyl radical reactions with DNA to calculate relative probabilities of hydroxyl radical attack at individual deoxyribose hydrogen atoms in a self-complementary decamer duplex oligodeoxynucleotide *(20)*. Their results, in agreement with Balasubramanian *et al. (19)*, show a preferential attack at deoxyribose hydrogen atoms in the order of 5'-H > 4'-H > 3'-H, 2'-H > 1'-H with corresponding hydroxyl radical attack probabilities of 54.6%, 20.6%, 15.0%, 8.5%, and 1.3%, respectively. The authors argue that steric hindrance from non-reacting atoms significantly influences site-specific hydroxyl attack probabilities in DNA *(20)*.

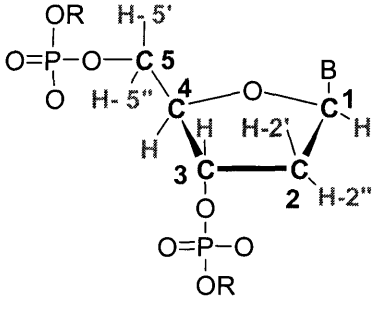

Figure I-2: The seven abstractable hydrogen atoms in deoxyribose *(8)*.

Oxidation of each position of deoxyribose produces a unique spectrum of products, a matter that has received extensive review *(5, 6, 8)*. The following sections describe deoxyribose oxidation organized by individual positions and then by oxidizing

agents. For information about the mechanistic aspects of the formation of the individual deoxyribose oxidation products, the reader is referred to other reviews *(2, 5, 6, 8, 21, 22)*.

2. C3' OXIDATION

The C3' position is of central importance for the research presented here and therefore will be discussed first. The C3'-hydrogen atom is located in the major groove of DNA and appears to be involved in few oxidative pathways investigated to date. This position is believed to be only a minor target of hydroxyl radicals *(8)*. The proposed products of deoxyribose oxidation include base propenoate and phosphoglycolaldehyde (PGA) (see Scheme I-3).

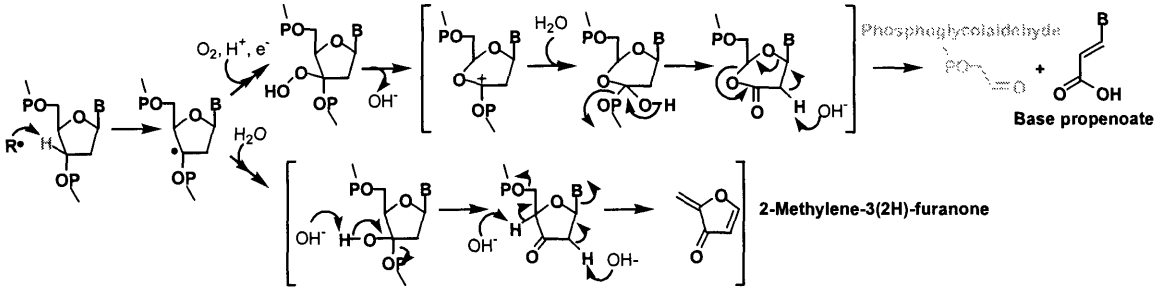

Scheme I-3. Proposed oxidation of the C3' position in deoxyribose based on work presented here as well as published work *(2, 23)*.

In order to study the C3' radical, Koerner *et al.* synthesized a C3' branched-chain nucleoside which, upon UV irradiation, produces the C3' radical (see Scheme I-4) *(24)*. HPLC analysis of the modified nucleoside after photolysis in acetonitrile in the presence of the electron acceptor tributyltin hydride revealed the formation of a 1 : 1 mixture of α-

and β-5'-*O*-tritylated thymidine. This of course does not represent physiological conditions and therefore no conclusions of products formed under those conditions can be made at this point. Debije *et al.* used electron paramagnetic resonance to prove the presence of a C3' radical in a crystalline duplex 11-mer oligodeoxynucleotide subjected to X-irradiation at 4 K *(25)*. Under these conditions, the C3' radical made up 4.5% of the total radical population trapped in the oligodeoxynucleotide crystal *(25)*.

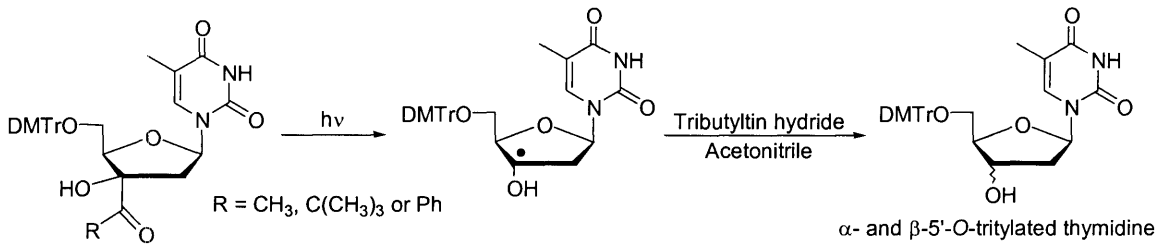

Scheme I-4. Formation of a C3' radical from C3'-branched-chain nucleosides by photoactivation *(24)*.

PGA has been shown to block DNA synthesis *(26)* and removal of related 3'-terminal blocking groups, such as phosphoglycolate, has been shown to be rate-limiting during DNA repair *(27)*. In addition, our laboratory has demonstrated the formation of glyoxal and the mutagenic 1,N^2-glyoxal adducts of dG *(12, 13)* in reactions of DNA with PGA under physiological conditions *(14)*. All these findings support a deleterious effect associated with the formation of PGA in cells.

Photoactive rhodium(III) complexes. Bis(phenanthroline)(9,10-phenanthrene-quinonediimine)rhodium(III) [$Rh(phen)_2phi^{3+}$] and bis(9,10-phenanthrenequinone diimine)(bipyridyl)rhodium(III) [$Rh(phi)_2bpy^{3+}$] were found to induce efficient DNA

strand scission after irradiation with long-wavelength UV light *(23)*. These complexes, while exhibiting similar cleavage properties and products, were found to display vastly different DNA recognition properties *(23)*. $Rh(phen)_2phi^{3+}$ shown in Figure I-3 exhibits marked sequence selectivity with a general preference for pyrimidine-pyrimidine-purine sequences, while $Rh(phi)_2bpy^{3+}$ prefers purine-pyrimidine-purine and induces DNA strand scission in a predominantly sequence-neutral fashion *(23)*. $Rh(phen)_2phi^{3+}$ targets the DNA major groove and recognizes regions that exhibit tertiary interactions, such as unusual secondary structures like triple helices in tRNA molecules *(23)*. Barton and co-workers used a sequencing gel technique to tentatively identify PGA termini attached to the 3'-ends of strand breaks arising from deoxyribose oxidation by rhodium(III) complexes *(23)*. They observed a 1:1 molar ratio for the production of PGA and base propenoates, the latter identified by co-elution with synthetic standards using HPLC *(23)*.

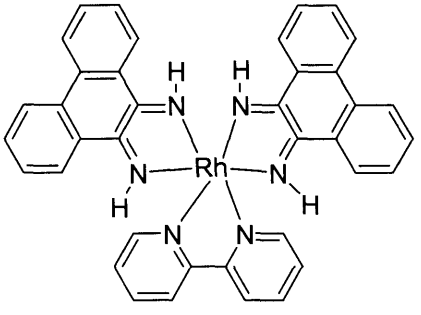

Figure I-3: The structure of bis(9,10-phenanthrenequinonediimine)-2,2'-bipyridyl-rhodium(III) *(23)*.

3. C1' OXIDATION

The formation of a C1' radical is thought to have low probability due to its solvent-inaccessible location deep in the minor groove in B-DNA *(19, 28)*. Therefore, the importance of H-1' as a reactive site is thought to be limited to minor groove-binding molecules, where the oxidant is generated in close proximity to the H-1' atom. In contrast to issues of solvent exposure, *ab initio* calculations indicate that the bond dissociation energy for the C1' hydrogen bond is the lowest of all of the carbon-hydrogen bonds in deoxyribose *(28, 29)*. Despite the low accessibility, the C1' position is a target for many minor groove-binding oxidizing agents, as discussed below.

The C1' oxidation product deoxyribonolactone has been shown to form covalent adducts with DNA repair proteins responsible for the removal of AP sites *(9, 10, 30, 31)* which suggests that the lesions are highly toxic in cells. Furthermore, the deoxyribonolactone was found to induce DNA polymerase-mediated mutagenesis *in vitro (32)*. The half-life of deoxyribonolactone in DNA under physiological conditions (pH 7.4, 37 °C) has been estimated to range from 20 to 54 h and is dependent on the sequence context of the lesion *(33)*. The most frequent decomposition products induced by heating or alkali involve β- and δ-elimination reactions, which ultimately lead to the formation of 5-methylenefuranone (5-MF) (see Scheme I-5). This double elimination product can account for up to 10–15% of the deoxyribonolactone lesions in DNA *(34)*. 5-MF can also arise directly from a C1' radical by formation and subsequent solvolysis of a 1',2'-

dehydronucleotide intermediate after one-electron oxidation of *bis*(1,10-phenanthroline)copper(I) ($Cu(OP)_2$) *(35)* (see Scheme I-5).

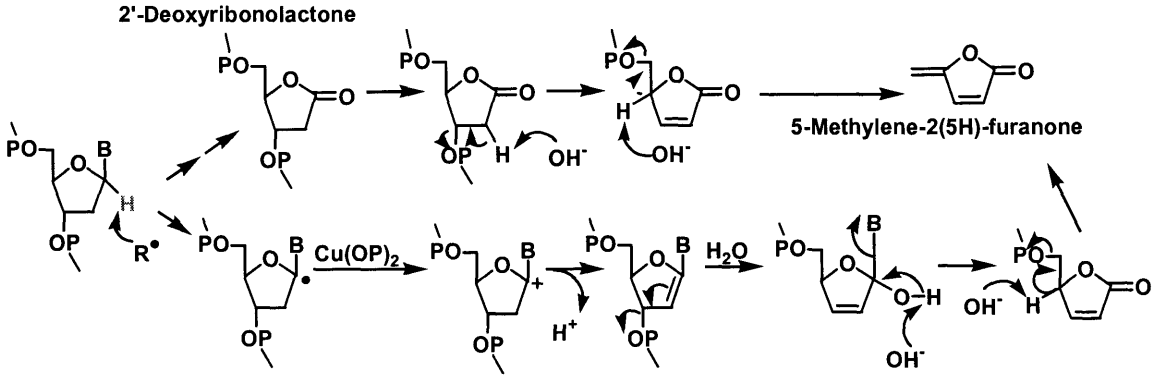

Scheme I-5. Oxidation of the C1' position in deoxyribose *(35, 36)*.

3.1 Copper complexes. Sigman *et al.* discovered that the redox active complex *bis*(1,10-phenanthroline)copper(I) ($Cu(OP)_2$) cleaves DNA by sequence-dependent binding to the minor groove followed by C1' hydrogen atom abstraction *(37, 38)* (see Figure I-4). Deoxyribonolactone and 5-MF were shown to be the major products of $Cu(OP)_2$-induced DNA damage *(39)*. The reaction efficiency at any sequence position depends on the stability of the $Cu(OP)_2$-DNA complex and the reactive copper-oxo intermediate thought to be responsible for the oxidation reaction *(39)*.

The spermine conjugate of the *bis*-phenanthroline ligand, called "Clip-Phen" (see Figure I-4), produces C1', C4' and C5' oxidation in deoxyribose without any sequence selectivity. However, C1' is the major chemical pathway, producing 5-MF after heat-induced β/δ-elimination of the deoxyribonolactone *(40)*. The authors propose the production of 50% C1' oxidation, ~15% C4' oxidation and ~15% C5' oxidation of

deoxyribose in double-stranded DNA *(40)*. Conjugating 3-Clip-Phen to a distamycin analogue drives sequence selectivity towards successive A/T base pairs and markedly influences the regioselectivity of oxidation of the three accessible deoxyribose sites *(40)*. C1' chemistry is less predominant, suggesting that this large conjugate preferentially interacts with the edge of the minor groove due to steric hindrance *(40)*.

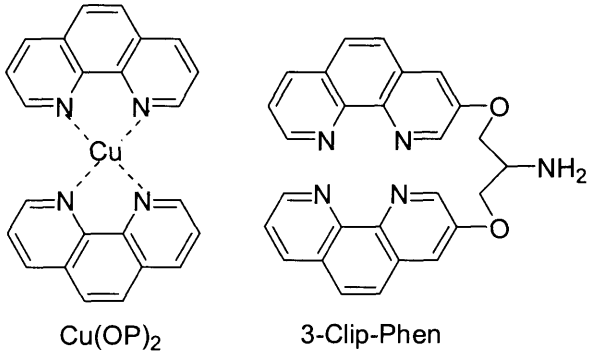

Figure I-4: Structures of *bis*(1,10-phenanthroline)copper(I) ($Cu(OP)_2$) and the spermine conjugate of *bis*-phenanthroline "Clip-Phen" *(37, 40)*.

Copper(II) complexes with benzothiazolesulfonamide cause sequence independent degradation of DNA by oxidation of C1', C4' and C5'. C1' oxidation is the major chemical pathway, as determined by quantification of 5-MF *(41)*.

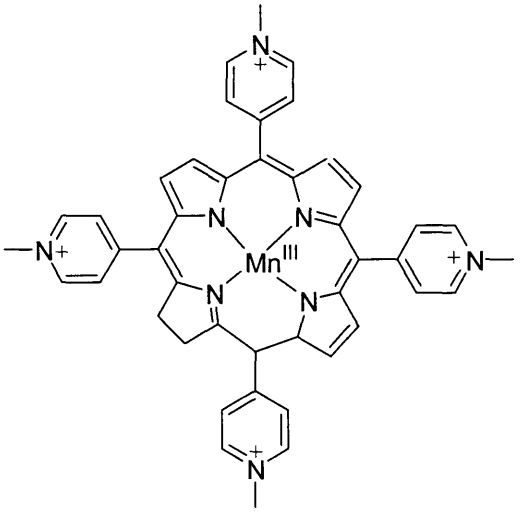

Figure I-5: Structure of tetrakis(4-*N*-methylpyridiniumyl)-porphyrin-manganese(III) (Mn-TMPyP) *(36)*.

3.2 Tetrakis(4-*N*-methylpyridiniumyl)porphyrin manganese(III) (Mn-TMPyP). Mn-TMPyP (see Figure I-5) is a powerful artificial nuclease that can be activated by an oxygen atom donor, such as potassium monopersulfate, into a very reactive high-valent porphyrin Mn(V)=O species *(36)*. 5-MF has been shown to be the major reaction product arising from Mn-TMPyP-treatment of calf thymus DNA after a heating step *(42)*. This confirms that metalloporphyrin derivatives interact with the minor groove of double-stranded DNA *(42)*. Mn-TMPyP has been proposed to induce DNA cleavage by formation of a carboncation followed by hydroxylation of deoxyribose carbons, as opposed to the reaction of the C1' radical with oxygen *(42)* as detailed in Scheme I-5 for $Cu(OP)_2$.

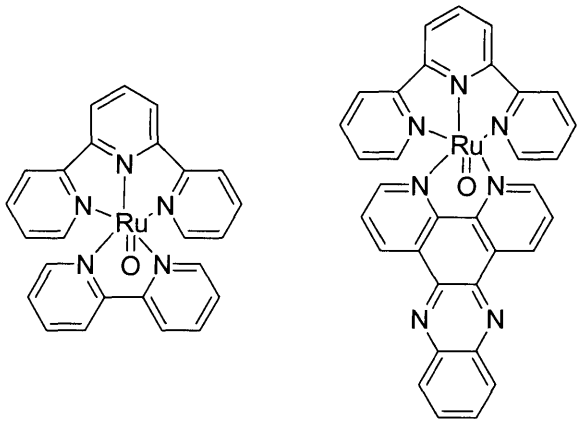

Figure I-6: Structures of (2,2',2"-terpyridine)(2,2'-bipyridine)oxoruthenium(IV) and ruthenium(2,2',2"-terpyridine)(dipyridophenanzine)oxoruthenium(IV) *(43)*.

3.3 Oxoruthenium(IV). The complexes (2,2',2"-terpyridine)(2,2'-bipyridine)oxoruthenium(IV) and ruthenium(2,2',2"-terpyridine)(dipyridophenanzine)-oxoruthenium(IV) (see Figure I-6) oxidize organic substrates *via* hydrogen atom abstraction or oxo transfer. In DNA, the complexes have been shown to cause C1' oxidation of deoxyribose, leading to 2'-deoxyribonolactone and ultimately 5-MF, as well as oxidation of guanine *(43, 44)*. The oxo ligand of the complex directly participates in the oxidation of C1', as revealed by ^{18}O labeling of recovered 5-MF *(43)*.

3.4 UV radiation. Urata *et al.* have characterized a mutagenic hot spot in the d(ApCpA) sequence in DNA exposed to UV radiation *(45)*. The DNA lesion responsible for the mutational hotspot was determined to be deoxyribonolactone using ^{1}H-nuclear magnetic resonance, Fourier transform infrared absorption and fast atom bombardment mass spectrometry *(45)*. This reaction was shown to be highly dependent on pH, with efficient formation of deoxyribonolactone at acidic pH and inefficient formation a pH 7.4

(45). Neighboring bases were shown to have no influence on the deoxyribonolactone formation from dC upon UV irradiation, but modifications of dC had profound effects *(46)*. 5-Methyl-deoxycytidine and N^3-methyl-deoxycytidine inhibited the formation of deoxyribonolactone, leading the authors to conclude that protonation of a precursor to deoxyribonolactone, and not dC itself, is of importance in the reaction mechanism *(46)*.

3.5 X-rays and γ-radiation. Single crystals of deoxycytidine hydrochloride exhibit C1' radicals, as shown by Hole *et al.* using electron paramagnetic resonance *(47)*. The authors suggest that the hydrogen atom abstraction resulted from initial one-electron oxidation of the cytidine base with subsequent intramolecular oxidation of the C1' position of the deoxyribose.

Nucleobase radicals are a major family of reactive intermediates formed when DNA is exposed to radiation. Nucleobase radicals account for as much as 90% of the reactions between pyrimidines in DNA and hydroxyl radicals produced by radiation *(48)*. Synthetic, photolabile precursors have been used to elucidate the reactivity of DNA radicals. For example, Carter *et al.* synthesized a *tert*-butyl ketone precursor that under UV irradiation produced 5,6-dihydro-2'-deoxyuridine-6-yl (see Scheme I-6), a lesion thought to be important in γ-radiolysis of DNA *(48)*. This lesion led to the minor but unexpected formation of deoxyribonolactone. The authors proposed a pathway involving intramolecular hydrogen atom abstraction by a 6'-uracil peroxyl radical *(48)*. Shaw *et al.* observed the formation of deoxyribonolactone induced by γ-irradiation of 2'-deoxycytidine in frozen aqueous solutions as determined by HPLC and ^{1}H-NMR *(49)*.

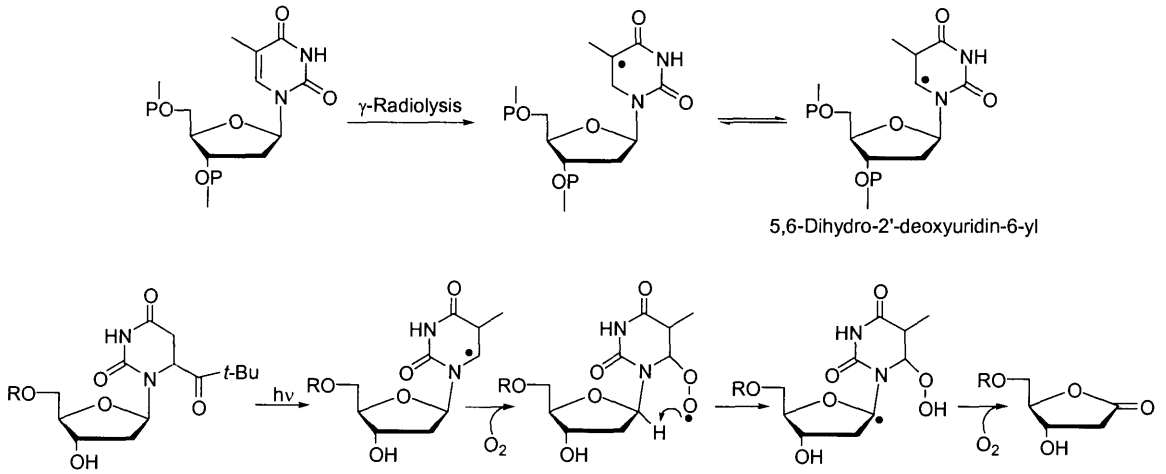

Scheme I-6. Formation of a deoxythymidine radical by γ-radiation *(48)*.

3.6 Enediynes. All of the enediynes isolated to date are products of the eubacteria Actinomycetales *(50)*. They are potent cytotoxic agents due to their ability to cleave DNA *(50, 51)*. The enediyne antitumor antibiotics, neocarzinostatin, calicheamicin γ_1^I, and esperamicin A1, induce DNA cleavage by deoxyribose oxidation in DNA during a reaction involving drug-centered carbon radicals *(52, 53)* (see Figure I-7).

In the case of neocarzinostatin, the enediyne-containing chromophore undergoes nucleophilic attack by a thiol to generate a diradical species *(56)*, while thiol mediated reduction of the methyltrisulfide in calicheamicin and esperamicin A1 leads to the formation of the diradical (see Scheme I-7). When bound in the minor groove, the diradical causes deoxyribose hydrogen atom abstraction on both strands leading to sequence-dependent bistranded DNA lesions.

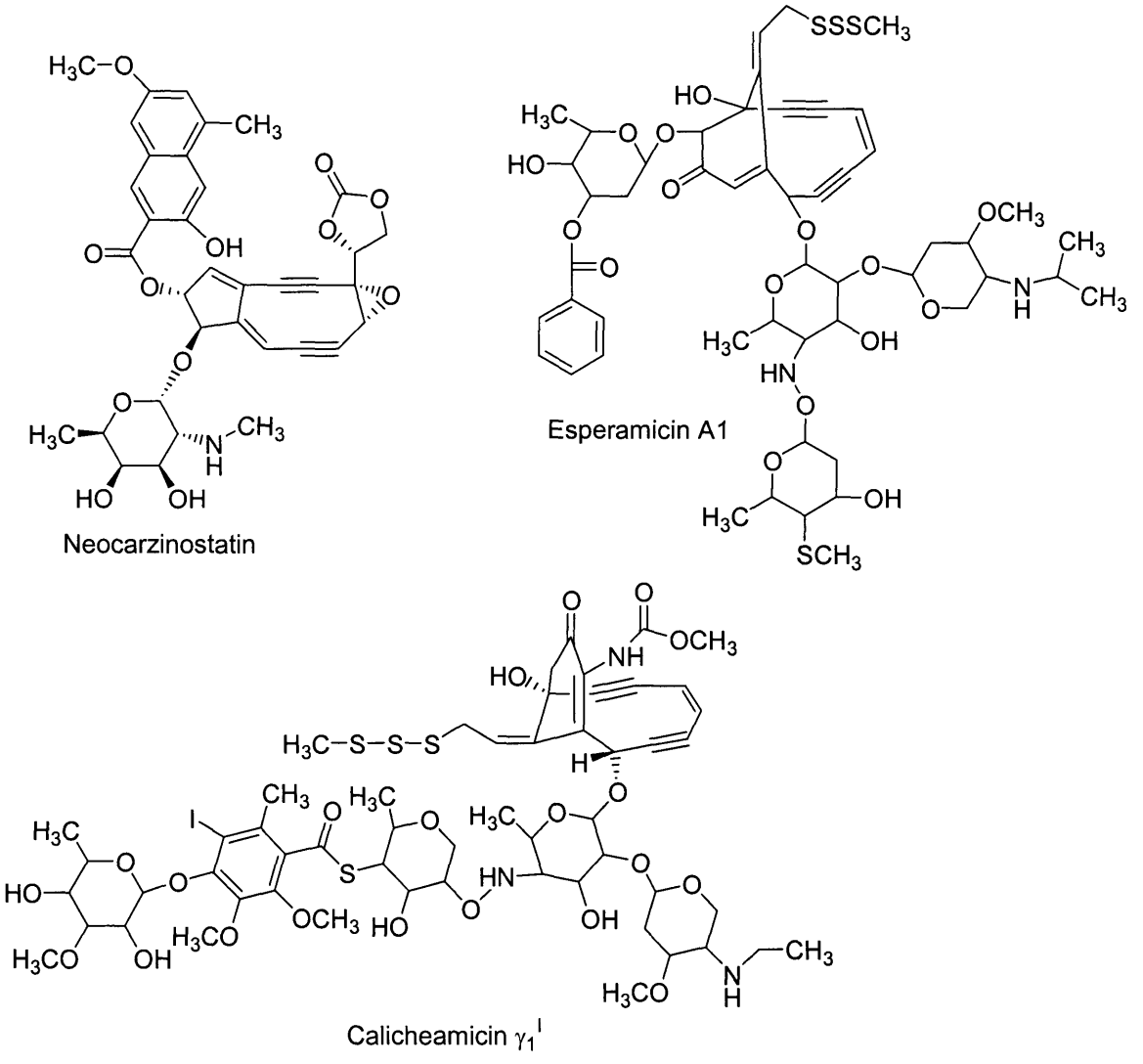

Figure I-7: The structures of neocarzinostatin *(54)*, esperamicin A1 *(55)* and calicheamicin γ_1^I *(52)*.

For neocarzinostatin, these lesions consist of strand breaks and abasic sites predominantly at AG<u>C</u>·GC<u>T</u> and AG<u>T</u>·AC<u>T</u> sequences *(56)*. This involves mainly C1' chemistry at the <u>C</u> of AG<u>C</u>, C4' chemistry at the <u>T</u> of AG<u>T</u>, and C5' chemistry at the <u>T</u> residues on the complementary strands *(56)*. Other factors such as the structure and the reducing potential of the activating thiol also have been found to affect the ratio of

neocarzinostatin induced lesions, and to alter the partitioning of the C4' abstraction products (*vide infra*) *(56)*. DNA mismatches and other structural changes of DNA, such as elimination of the 2-amino group of guanine, have also been shown to influence the extent of lesions *(56)*. Deoxyribonolactone was characterized as a product of neocarzinostatin induced release of cytosine using GC/MS by Kappen *et al. (57)*, while involvement of the C1' position with esperamicin A1 was demonstrated in tritium labeling studies *(58)*.

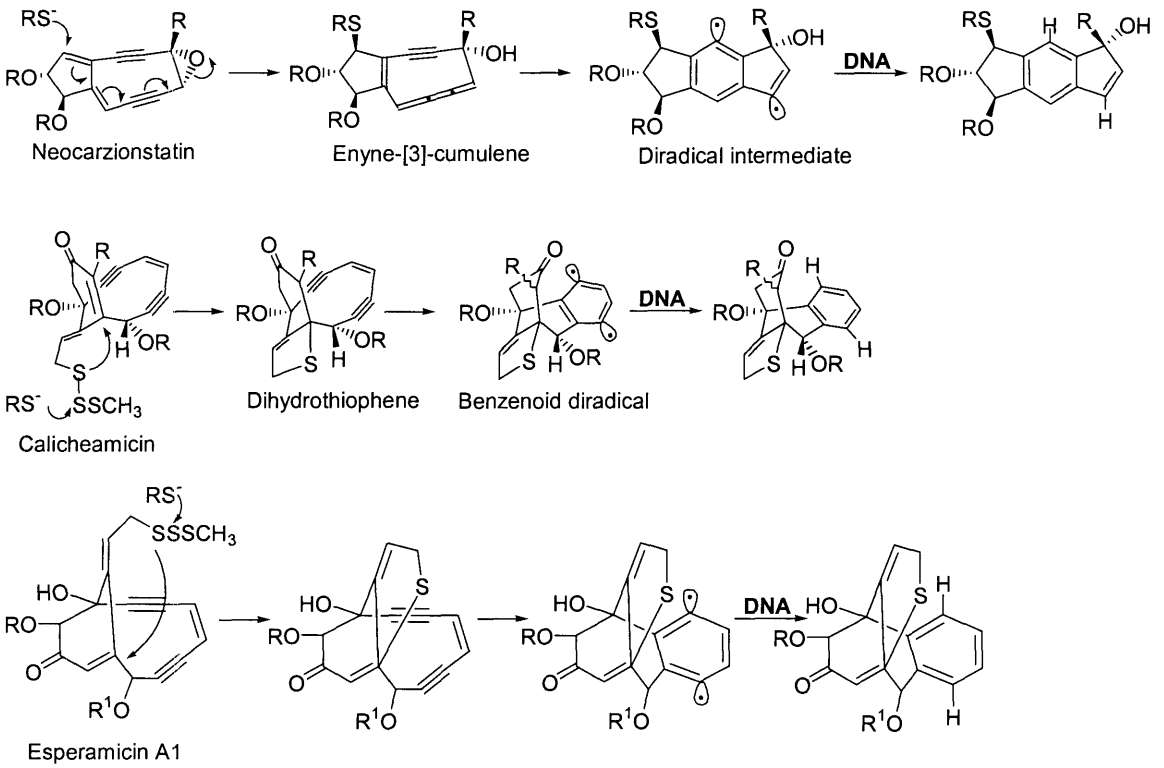

Scheme I-7. Activation of neocarzinostatin, calicheamicin and esperamicin A1 *(52, 53, 59)*.

Esperamicin A1 is an exception in the enediyne family, as it mainly induces single-strand breaks *(59)*. The activated esperamicin diradical binds to DNA by an intercalation-like mechanism mediated by its anthranilate moiety *(60)*. About 25% of double-stranded DNA damage induced by esperamicin A1 consists of a deoxyribonolactone abasic site opposite a strand break produced by C5' oxidation *(60)*.

3.7 UV irradiation of 5-bromouracil (BrdU)-containing oligodeoxynucleotides. Replacement of thymine in DNA by 5-bromouracil, a non-natural base analog, has long been known to enhance photosensitivity with respect to DNA-protein crosslinking *(61)*, single- and double-strand breaks and creation of alkali labile sites *(62)*. Efficient formation of deoxyribonolactone was observed by Sugiyama *et al.* in duplex hexamers containing d(ApBrdU) in the middle of the hexamer, with release of the adenine base *(63)*. The authors suggest that the formation of deoxyribonolactone is due to the C1' hydrogen atom abstraction at dA by the adjacent uracilyl-5-yl radical formed from BrdU *(63)*.

3.8 Peroxyl radicals. Peroxyl radicals are products of lipid peroxidation and generate abasic sites, among other lesions, when interacting with DNA *(64)*. Treatment of DNA with 2,2'azo-bis(2-amidinopropane) hydrochloride, a peroxyl radical generator, leads to a C1' oxidized site as judged differential reactivity exonuclease III and T4 endonuclease V *(64)*. T4 endonuclease V incises DNA at "regular" and C4' oxidized abasic sites, whereas exonuclease III recognizes "regular" and C1' oxidized sites *(64)*. Harkin *et al.* suggest that the C1' radical induced by peroxyl radicals is identical to the

products induced by *bis*(1,10-phenanthroline)copper(I) *(64)*, but so far no definitive chemical analysis has been done to ascertain the identity of this deoxyribose oxidation product.

4. C2' OXIDATION

The C2' position features two prochiral hydrogen atoms that have not been implicated significantly in deoxyribose oxidation possibly due to low solvent accessibility or low reactivity of these C-H bonds *(8)*. *Ab initio* calculations of the deoxyribose radical energies indicate that the C2' radical is less favorable by 3-4 kcal/mol in comparison to C1', C3' and C4' positions *(28)*. Consequently, it is not surprising that only very reactive DNA damaging agents, such as hydroxyl radicals, react at this site *(5)*.

So far, only the erythrose abasic site has been shown to be a product of C2' deoxyribose oxidation (see Scheme I-8). Besides ionizing radiation *(65)*, photo activation of 5-bromouracil containing oligodeoxynucleotides have been observed to induce C2' oxidation *(66, 67)* (see Scheme I-9). Upon heating under alkaline conditions, the erythrose abasic site containing DNA has been shown to undergo retroaldol reaction to give two fragments, both having phosphoglycolaldehyde termini in high yield *(66)* (see Scheme I-8).

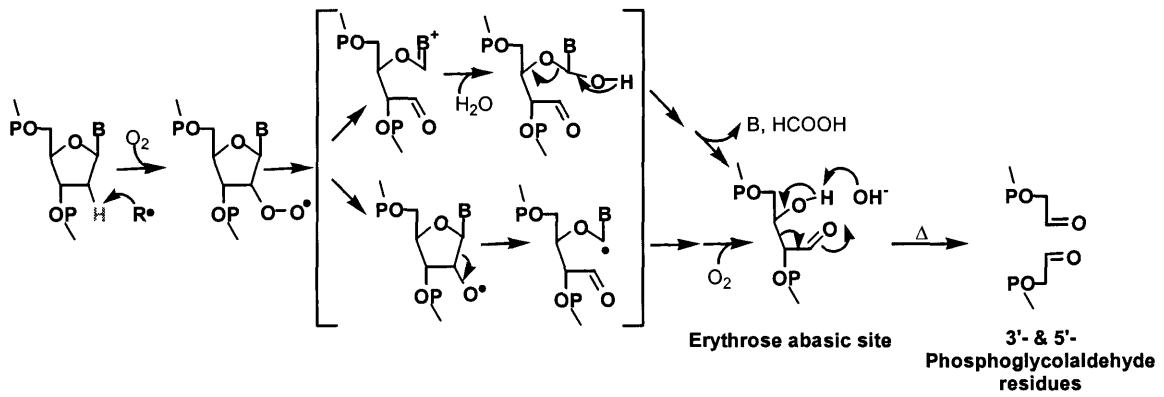

Scheme I-8. Oxidation of the C2' position in deoxyribose *(65, 66, 68)*.

4.1 γ-Radiation. The erythrose abasic site was first characterized in γ-irradiated DNA by Dizdaroglu *et al.* using GC-MS *(65)*. The free hydroxyl group next to the phosphate ester causes this site to be alkali-labile *(65)* (see Scheme I-8). Due to the use of alkaline phosphatase in their experiments, the authors had to reduce the aldehyde group with $NaBD_4$ to avoid cleavage of the site during the dephosphorylation reaction *(65)*.

4.2 Photolysis of 5-halouracils. The incorporation of mutagenic 5-halouracils into DNA has been shown to cause DNA strand breaks, DNA-protein crosslinking, and creation of alkali-labile sites following irradiation with UV-light *(66)*. Incorporation of 5-iodouracil (IdU) and 5-bromouracil (BrdU) into oligodeoxynucleotides leads to C1' and C2' oxidation and the associated erythrose abasic site *(66, 67)* (see Scheme I-9).

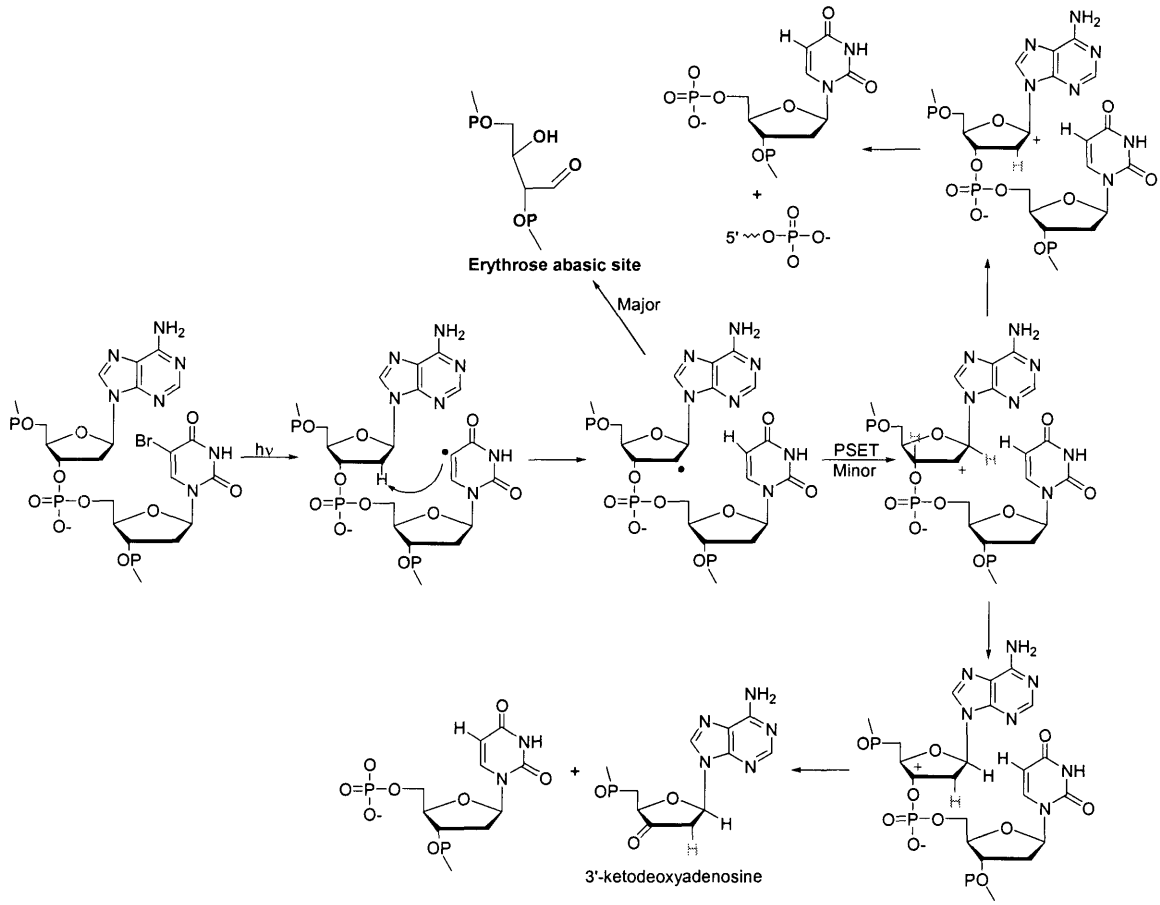

Scheme I-9. Proposed mechanism of C2' radical formation produced upon UV-irradiation of 5-halouracil *(69)*.

Sugiyama *et al.* demonstrated the formation of the erythrose abasic site in UV-irradiated 13-mers containing IdU, using an approach involving enzyme digestion, alkaline hydrolysis and $NaBH_4$ treatment followed by HPLC separation *(66)*. Stereospecifically deuterated 5-halouracil-containing oligodeoxynucleotides (designated 2'α-D and 2'β-D) showed a substantial kinetic isotope effect on the yield of the erythrose abasic site for the 2'α-D oligodeoxynucleotide, whereas 2'β-D produced the same amount of the erythrose abasic site as an unlabeled oligodeoxynucleotide *(67)*. The

authors concluded that the formation of the erythrose abasic site occurs *via* rate-limiting abstraction of 2'α-hydrogen atom from deoxyribose by the uracilyl-5-yl radical *(67)*. The 2'α-hydrogen is closer to the C5' position of adjacent uracil, suggesting that the distance and facility of hydrogen atom abstraction controls the ratio of competitive C1' and C2' oxidation in B-DNA *(67)*. Cook *et al.* exploited kinetic isotope effects to show that a greater proportion of C2' hydrogen atom abstraction occurs in double- *versus* single-stranded DNA *(69)*. They also used tritium transfer experiments to show that, after C2' radical oxidation, 1,2-hydride rearrangements take place to form DNA strand breaks containing either 3'-phosphates (C1' hydride shift) or a 3'-keto-2'-deoxynucleotide (C3' hydride shift) as a minor pathway *(69)*. The efficiencies of these two mechanisms were shown to be oxygen-dependent *(69)*.

5. C4' OXIDATION

The C4' hydrogen atom is very solvent accessible and resides on the outer edge of the minor groove in B-DNA *(19, 28)*. Solvent accessibility and relatively low bond dissociation energy of the carbon-hydrogen bond makes the C4' position a major target of minor groove-binding oxidants *(29)*. C4' oxidation leads to strand breaks containing either a 3'-phosphoglycolate residue and a base propenal (or malondialdehyde and a free base) or a 4'-keto-1'-aldehyde abasic site (see Scheme I-10) *(16, 70-72)*. The 3'-phosphoglycolate residue often serves as a signature for C4' oxidation *(73)*. The labile base propenals are mainly detected with the non-specific thiobarbituric acid assay that reacts with both malondialdehyde and base propenal or with co-elution of standards using

HPLC *(16, 21, 72)*. The 4'-keto-1'-aldehyde abasic site is alkali labile (see Scheme I-10) and can be trapped using hydrazine *(74)*. Although bleomycin is the most well studied molecule that damages DNA by abstracting the C4' hydrogen atom, many other oxidants have been shown to oxidize this site, including enediynes (*vide infra*).

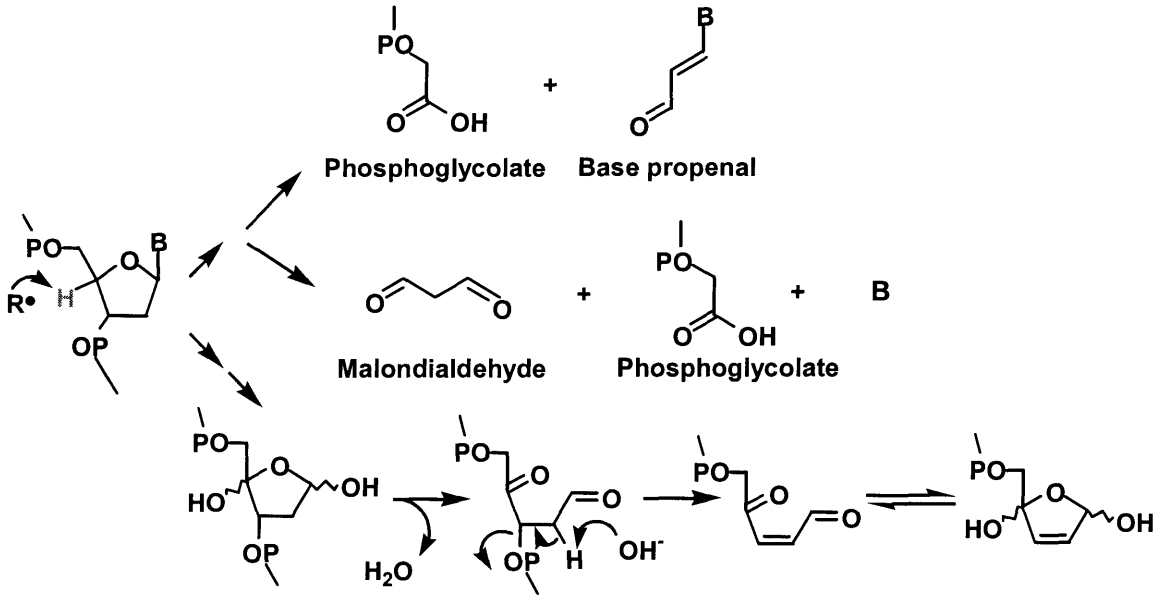

Scheme I-10. Oxidation of the C4' position in deoxyribose.

Overall, C4' oxidation has important biological effects. The 4'-keto-1'-aldehyde abasic site has been shown to be readily excised by the Apel protein, the major human AP endonuclease, while phosphoglycolate is a relatively poor substrate for Apel excision thus diminishing probability of repair of the lesion in DNA *(75)*. Greenberg *et al.* have shown *in vitro* that the 4'-keto-1'-aldehyde abasic site is a blocking lesion for Klenow exo^+/exo^- fragments and the bypass polymerases pol II, pol IV and pol V in the presence of Rec A were compromised in their ability to extend past the lesion with preferential thymidine incorporation by polymerase II exo^- thus possibly resulting mutagenicity *(76)*.

The presence of base-propenals was shown to inhibit DNA synthesis in HeLa cells as well as the function of thymidine kinase and DNA polymerase α *(77)*. In addition, base-propenals have been shown to form the mutagenic DNA adduct M_1G, the pyrimidopurinone of deoxyguanosine *(11, 78)*. Taken together, these findings demonstrate the potential for negative biological effects of C4' oxidation *in vivo*.

5.1 Quinobenzoxazine magnesium complexes. Quinobenzoxazines (see Figure I-8) are mammalian toposiomerase II inhibitors that have demonstrated promising anticancer activity in mice *(79)*. The intercalation complex of the quinobenzoxazines with double-stranded DNA has been proposed to involve a quinobenzoxazine dimer linked by two magnesium ions *(79)*. Photoactivation of quinobenzoxazine (S)-A-62176 bound to DNA was shown by gel-electrophoresis, to induce 3'-phosphoglycolate, 3'-phosphate, 5'-phosphate and a alkali-labile site *(79)*.

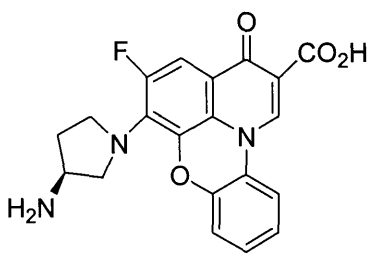

Figure I-8. The quinobenzoxazine (*S*)-1-(3-aminopyrrolidin-1-yl)-2-fluoro-4-oxo-4H-quino[2,3,4-ij][1,4]-benzoxazine-5-carbocylic acid, also known as (S)-A-62176 *(79)*.

5.2 Ni(II)·X-X-His. Metallopeptides of the general form Ni(II)·X-X-His (where X is any amino acid) can be activated by $KHSO_5$, magnesium monoperoxyphthalate or H_2O_2 to selectively degrade DNA *via* a minor groove-binding interaction *(80)*. The site selectivity exhibited by this class of compounds appears to be derived from the identity and chirality of the amino acids comprising the tripeptide. For example, Ni(II) Gly-D-Asn-His was found to modify 5'-CCT sites, while Ni(II) Lys/Arg-Gly-His was found to modify A/T rich regions *(80)*. The X-X-His ligand system can be chemically activated in the presence of Cu(II) or Ni(II) to oxidize DNA and proteins *(80)*. The Ni(II)·X-X-His peptides appear to operate *via* the formation of a non-diffusible, complex-centered oxidant *(80)*. The resulting deoxyribose oxidation produces both 3'-phosphoglycolate and the 4'-keto-1'-aldehyde abasic site varying in proportion depending on the identity of amino acids *(80)*.

5.3 *Bis*(2-ethyl-2-hydroxybutyrato)oxochromate(V). Oxidative DNA damage is considered to be an important mechanism in the genotoxicity and mutagenicity of chromate, Cr(VI) *(81)*. Reduction of Cr(VI) by intracellular constituents, such as ascorbate and glutathione, generates a mixture of high valent chromium species *(81)*. Bis(2-ethyl-2-hydroxybutyrato)oxochromate(V) (Cr(V)-EHBA) resembles the transient Cr(V)-ascorbate complex and undergoes stochiometric disproportionation through a Cr(IV) intermediate yielding Cr(VI) and Cr(III) at neutral pH without formation of ligand or O_2-based radicals *(81)*. Under oxygenated conditions, Cr(V)-EHBA induces sequence-independent formation of phosphoglycolate as determined by gel-electrophoresis *(81)*.

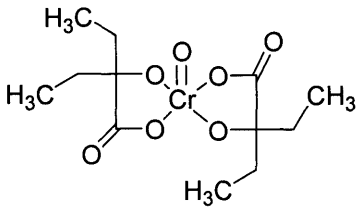

Figure I-9: Structure of *bis*(2-ethyl-2-hydroxybutyrato)oxochromate(V).

5.4 Bleomycin. The bleomycins represent a family of glycopeptide-derived antitumor antibiotics widely used in clinical settings to treat cancer (see Figure I-10). The interaction of several members of the bleomycin family, in particular bleomycin A1, with DNA and the resulting oxidation chemistry are very well studied and have been reviewed by Stubbe *et al. (2)* and Burger *(82)*.

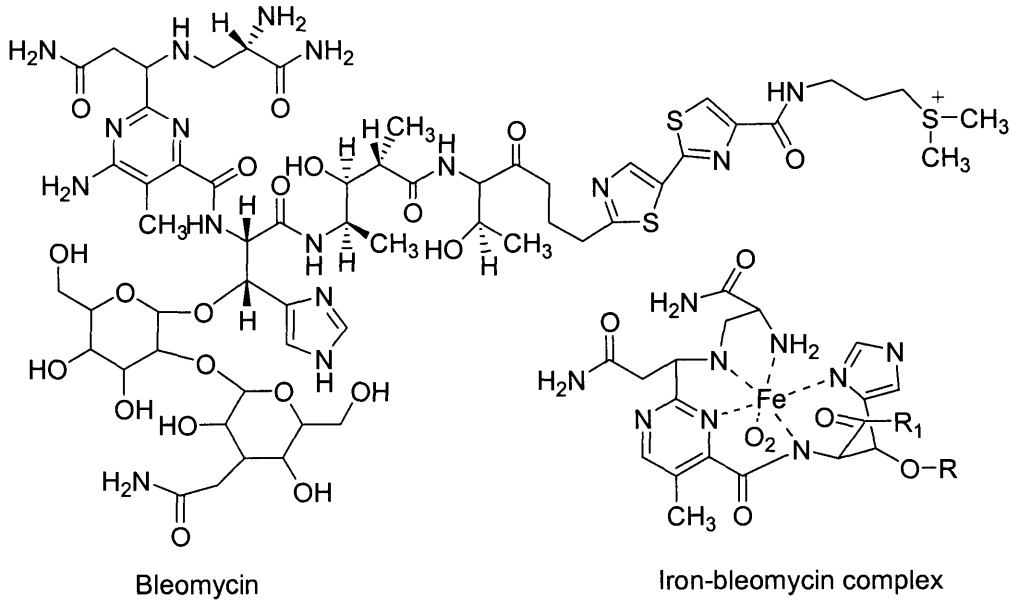

Bleomycin

Iron-bleomycin complex

Figure I-10: Structure of bleomycin A2 and the iron-bleomycin complex *(2, 53)*.

The attack of DNA by the bleomycin-Fe(II) complex requires a sequence of preliminary steps, including activation *(53)*. The drug binds to DNA in the minor groove and is activated by molecular oxygen and one electron or by hydrogen peroxide *(82)*. It is thought that the reactive form of bleomycin is the complex bleomycin$(Fe,O)^{3+}$ which is probably formed from the activated bleomycin species bleomycin(Fe^{3+},HO_2^{1-}) *(83)*. By measuring kinetic isotope effects in tritium labeled deoxyribose Stubbe and co-workers established that abstraction of the C4' hydrogen atom is the rate-limiting step in bleomycin-induced DNA degradation *(2)*. Bleomycin causes the formation of cytosine-, thymine-, and adenine-propenals and phosphoglycolate *(16, 70)* and the 4'-keto-1'-aldehyde abasic site accounts for 40% of bleomycin-induced DNA oxidation products *(2, 84)*.

5.5 Radiation. In contrast to other C4' oxidants, γ-radiation causes C4'-oxidation to form malondialdehyde and not base-propenals *(16)*. The formation of malondialdehyde in irradiated DNA follows a linear dose-dependence *(16)* and is accompanied by formation of 3'-phosphoglycolate, as was shown by Henner *et al.* using gel electrophoresis *(73)*. Rashid *et al.* proposed that the lack of base-propenal formation in γ-irradiated DNA *versus* bleomycin treatment was due to a difference in mechanism leading to ultimate C4' oxidation products *(16)*. While bleomycin stays bound to the C4' radical after hydrogen atom abstraction and influences the formation of end products, γ-radiation leads to the formation of a C4' peroxyl radical that will decompose to malondialdehyde, 3'-phosphoglycolate and a free base, rather than base-propenal, under physiological conditions *(16)*.

X-irradiation of single crystals of deoxycytidine hydrochloride has been shown by Hole *et al.* to form C4' radicals using electron paramagnetic resonance *(47)*. The authors suggest that the hydrogen atom abstraction resulted from initial one electron oxidation of the deoxycytidine base followed by intramolecular oxidation of the C4'-position.

5.6 Enediynes. As discussed in section 3.6 enediyne antibiotics are natural products and are characterized by the presence of an enediyne unit that can form a diradical (see Figure I-7 and Scheme I-7). In addition to neocarzinostatin, calicheamicin, and esperamicin this group of antibiotics includes maduropeptin and dynemicin *(8)*. Calicheamicin undergoes reductive activation and causes only bistranded lesions consisting of C4' oxidation on one strand and C5' oxidation on the opposite strand resulting in 3'-phosphoglycolate and to a major extent, the 4'-keto-1'-aldehyde abasic site *(85)*.

As has been shown for neocarzinostatin *(7)*, the structure and charge of activating thiols influences the partitioning of calicheamicin-induced deoxyribose C4' oxidation products *(85)*. Negatively charged thiols do not affect the proportions of the C4' deoxyribose oxidation products *(85)*, but neutral and, to an even greater extent, positively charged thiols inhibit the formation of 3-phosphoglycolate with a proportional increase in the formation of 4'-keto-1'-aldehyde abasic site *(85)*. Lopez-Laarraza *et al.* explain these findings with the involvement of thiols in a reaction with oxygen-derived intermediates at a critical point of the partitioning of the C4' oxidation reaction (see Scheme I-10). Under anaerobic conditions, the nitroaromatic radiation sensitizer, misonidazole, substitutes for

oxygen and causes an enhanced formation 3'-phosphoglycolate due to the formation of an oxyl radical intermediate at the C4' position in neocarzinostatin treated DNA *(7, 86)*. This suggests that thiols are able to reduce the oxyl radical to produce the 4'-keto-1'-aldehyde abasic site, with limited access of negatively charged thiols thus allowing the formation of increased levels of 3'-phosphoglycolate *(85)*.

The esperamicins are also activated by an intramolecular conjugate addition of thiolate derived by reduction of an intrinsic trisulfide to give a reactive *bis* radical, 1,4-benzyne. The diradical binds in the minor groove of DNA and causes double-strand scission by synchronous homolytic hydrogen atom abstraction from deoxyribose on opposing strands *(59)*. Esperamicins C-E induce DNA cleavage by 4'-hydrogen abstraction in conjunction with C5' hydrogen atom abstraction to form 3-phosphoglycolate and nucleoside-5'-aldehyde, whereas esperamicin A1 does not induce C4' hydrogen atom abstraction *(59)*.

As discussed earlier for C1' chemistry in section 3.6 in this chapter, neocarzinostatin is capable of oxidizing the C4' position in a sequence dependent manner resulting in 4'-keto-1'aldehyde abasic site and appears to be a function of the thiol used as an activator *(7, 87)*. Neocarzinostatin also forms phosphoglycolate to a lesser extent *(7, 87)*.

5.7 Copper complexes. As discussed in section 3.1, *bis*(1,10-phenanthroline)copper(I) and the 3-Clip-Phen copper complex produce 3'-phosphoglycolate *via* C4' abstraction as a minor pathway, the amount of which varies as a function of DNA sequence *(39, 40, 88)*. Copper(II) complexes with benzothiazolesulfonamide, also discussed in section 3.1, exhibit a minor C4' oxidation pathway producing 3'-phosphoglycolate and malondialdehyde, but not base propenals *(41)*. This is an interesting finding taken in context with γ-radiation, that exhibits the same C4' oxidation products *(16)*. This may indicate that γ-radiation and copper(II) benzothiazolesulfonamide complexes share a common C4' oxidation mechanism, which differs for other C4' oxidants.

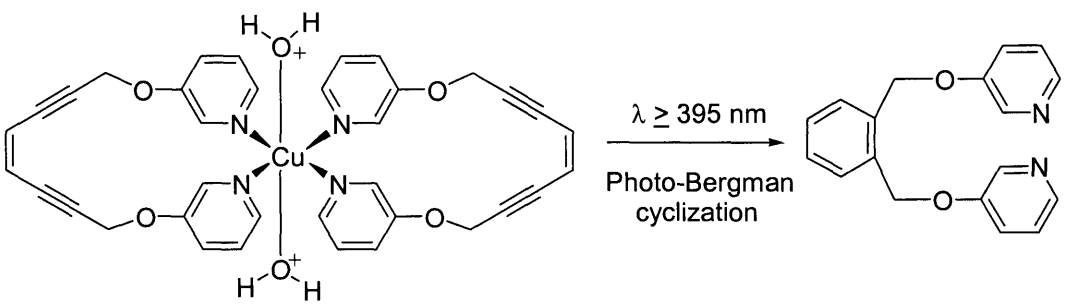

Scheme I-11: Photo-Bergman cyclization of *Bis*[*cis*-1,8-bis(pyridine-3-oxy)-oct-4-ene-2,6-diyne]copper(II) *(89, 90)*

Synthetic enediynes can undergo cyclization induced by photolysis while coordinated to copper. *Bis*[*cis*-1,8-bis(pyridine-3-oxy)-oct-4-ene-2,6-diyne]-copper(II)$(NO_3)_2$ exhibits a photoelectronic Bergman cyclization upon irradiation with wavelengths ≥ 395 nm (see Scheme I-11). A photochemical intermediate, proposed to be

a 1,4-phenyl diradical, reacts with DNA *via* C4' hydrogen atom abstraction producing 3'-phosphoglycolate *(90)*.

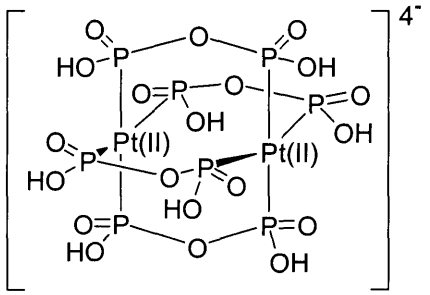

Figure I-11: Structure of $Pt_2(P_2O_5H_2)_4^{4-}$ *(91)*.

5.8 $Pt_2(P_2O_5H_2)_4^{4-}$. This tetraanionic platinum complex (see Figure I-11) abstracts hydrogen atoms from organic substrates upon exposure to 367 nm light without hydroxyl radicals as the putative reactive intermediates *(91)*. The cleavage reaction obtained using this complex on double-stranded DNA is similar to that of Fe(II)/EDTA and is dependent on the presence of molecular oxygen *(91)*. Gel electrophoresis was employed to show that 3'-phosphoglycolate and nucleoside-5'-aldehydes are the major products of DNA oxidation induced by this platinum complex *(91)*.

5.9 Methidumpropyl-EDTA/Fe(II) (MPE). MPE contains the metal chelator EDTA tethered to the DNA intercalator methidium and cleaves DNA efficiently and with little sequence selectivity, in a reaction dependent on Fe(II) ions and molecular oxygen *(92)*. No base propenal was detected in MPE-oxidized DNA, but 3'-phosphoglycolate was determined by gel electrophoresis as a major MPE-induced product *(92)*.

5.10 Peroxynitrite. The formation, biological relevance and chemistry of peroxynitrite is discussed in detail in Chapter V. Briefly, Yermilov *et al.* used thin layer chromatography to measure the dose dependent formation of thymine-propenal in peroxynitrite-treated thymidine *(93)*. The formation of thymine-propenal is increasingly suppressed by sodium bicarbonate, where peroxynitrite is converted to nitrosoperoxycarbonate, suggesting that only peroxynitrite but not nitrosoperoxycarbonate can induce the formation of basepropenals *(93)*.

6. C5' OXIDATION

The C5' position of deoxyribose has two prochiral hydrogen atoms, H5' and H5", that are highly solvent accessible in the minor groove of a B-DNA helix, with one atom pointing away from the groove toward solvent (see Figure I-2) *(8, 18, 29)*. The two C5' hydrogens have been shown to have the greatest surface accessibility of all deoxyribose hydrogen atoms *(19)*. Variations in the DNA sequence influence the accessibility of the minor groove and therefore of the H4' and H5" atoms, but not the H5' atom *(94, 95)*.

As with C4' oxidation, the products of C5' oxidation partition to form either a strand break containing a 3'-formylphosphate residue and a 2'-phosphoryl-1,4-dioxobutane moiety or a nucleoside-5'-aldehyde (see Scheme I-12). The Dedon group has recently shown that the 2'-phosphoryl-1,4-dioxobutane residue undergoes β-elimination to form *trans*-1,4-dioxo-2-butene (manuscript submitted). The C5' radical, for example the 2'deoxyadenosin-5'-yl, has also been shown to form a base-sugar linkage

producing 5',8-cyclopurine-2'-deoxynucleosides (see Scheme I-12) *(96, 97)*. This lesion is repaired by the nucleotide-excision repair pathway albeit with poor efficiency but not by base excision repair. It has also been found to be a strong block to mammalian gene expression and, therefore, has been proposed to be cytotoxic *(98)*.

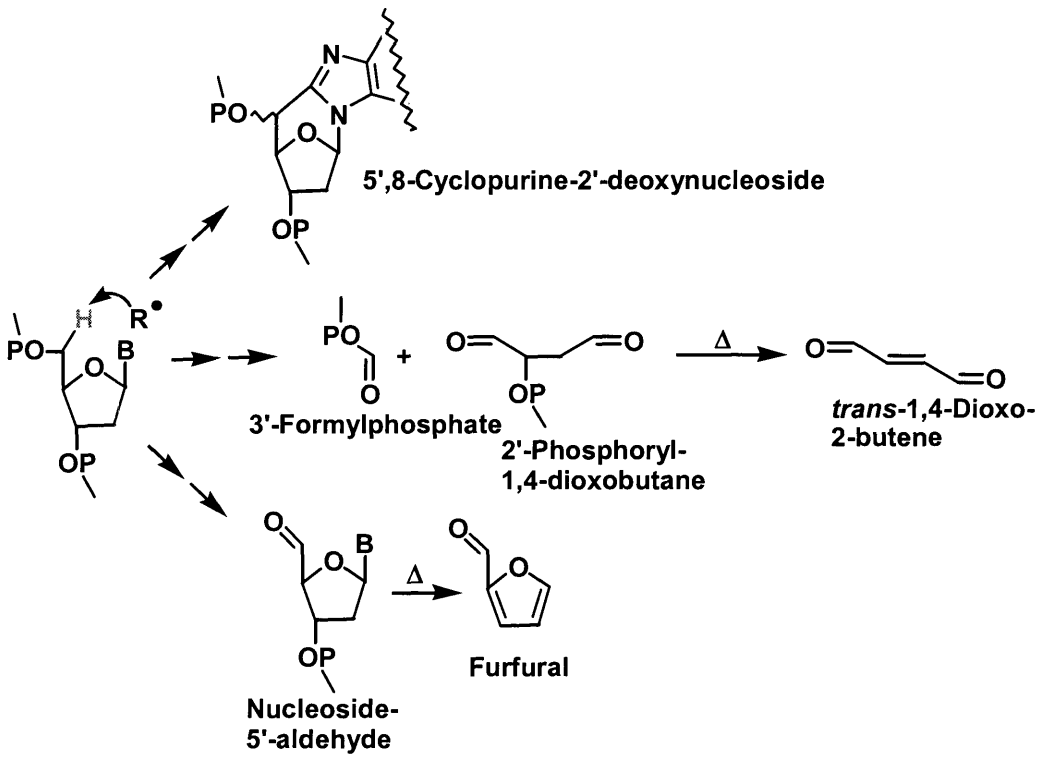

Scheme I-12. Oxidation of the C5' position in deoxyribose.

6.1 Enediynes. As discussed in section 3.6 of this chapter, neocarzinostatin is capable of oxidizing the C5' position in a sequence-dependent manner resulting in strand breaks *(99)*. Neocarzinostatin attack at the AG<u>C</u>·GC<u>T</u> sequence results in the formation of a bistranded lesion consisting of a C1'-mediated deoxyribonolactone abasic site at <u>C</u> and a strand break at <u>T</u> containing thymidine-5'-aldehyde *(99, 100)*. On the opposing strand, attack at the AG<u>T</u>·AC<u>T</u> sequence causes a bistranded lesion consisting of either a

strand break or an abasic site due to C4' oxidation at the T residue of the GT step and a strand break with thymidine-5'-aldehyde or 3'-formylphosphate and 2'-phosphoryl-1,4-dioxobutane residues *(53)*. Bulge structures in duplex DNA can be effectively cleaved by neocarzinostatin at the 3'-side of the bulge, and is entirely due to C5' hydrogen atom abstraction *(101)*.

Calicheamicin cleaves double-stranded DNA with strong sequence selectivity for TCCT and related sequences *(102)* (see also section 5.6 in this Chapter). Zein *et al.* proposed that calicheamicin abstracts the C5' hydrogen atom leading to the formation of a nucleoside-5'-aldehyde and on the opposing DNA strand cleavage was seen three bases in the 3' direction *(102)*. Hangeland *et al.* showed that calicheamicin shows a preference for the 5'(S) deoxyribose hydrogen atom *(103)*.

The formation of nucleoside-5'-aldehyde by esperamicins A1 is discussed in section 5.6 in this chapter.

6.2 Copper complexes. Bis(1,10-phenanthroline)copper complexes have recently been shown to induce nucleoside-5'-aldehyde-containing strand breaks in DNA *(88)*. In addition, the 3-clip-bis(1,10-phenanthroline)copper(I) (3-clip-phen) complex has been shown to produce furfural upon heating of treated DNA, as characterized by GC/MS *(40)*. This reactivity reflects the ability of 3-clip-phen to react not only in the floor of the minor groove in DNA, leading to the major pathway of C1' oxidation, but also to the edge of the minor groove, generating C4' and C5' oxidation *(40)*.

As a minor pathway, copper(II) complexes with benzothiazolesulfonamide induce C5' oxidation and generate furfural and free bases after heating oxidized DNA *(41)*.

6.3 Manganese(III)-*bis-aqua-meso*-tetrakis(4-N-methylpyridiniumyl)-porphyrin (Mn-TMPyP). Mn-TMPyP is also discussed in section 3.2. C5' oxidation is a minor pathway in Mn-TMPyP induced DNA degradation. After activation with potassium monopersulfate, Mn-TMPyP produces nucleoside-5'-aldehyde that is released as furfural after heating oxidized calf thymus DNA *(42)*. The molar ratio of furfural to the C1' oxidation product 5-MF was estimated to be ~0.15 *(42)*. The nucleoside-5'-aldehyde was quantified after derivatization to an O-carboxymethyl oxime derivative using HPLC/ESI/MS *(104)*. Mn-TMPyP has been suggested to induce DNA cleavage by hydroxylation of deoxyribose carbons, as opposed to radical mediated hydrogen atom abstraction, as shown in Scheme I-5 for $Cu(OP)_2$ *(42)*.

In certain sequences, Mn-TMPyP has been found to induce only C5' oxidation and no C1' oxidation. After binding to an AT sequence, the interaction of Mn-TMPyP induces specific cleavage at the 3' side of a GC or CG base pair *(105)*. In this case, the resulting strand break is formed by C5' deoxyribose oxidation, and no C1' oxidation was detected *(105)*.

6.4 γ-Radiation. Langfinger *et al.* irradiated deoxyguanosine under aerobic conditions and isolated 2'-deoxyguanosine-5'-aldehyde as a major oxidation product using HPLC followed by NMR characterization *(106)*. The authors suggested that the

major primary precursor for the 2'-deoxyguanosine-5'-aldehyde is not a C5' radical, but a base radical *(106)*. This was concluded from their observation that under anoxic conditions in the presence of tetranitromethane the yield of 2'-deoxyguanosine-5'-aldehyde decreased which led to the hypothesis that the attacking species is hot the hydroxyl radical but an as of yet unidentified base radical *(106)*.

DNA oxidized by γ-radiation (at a dose range between 0 and 80 Gy) produces 5',8-cyclopurine-2'-deoxyadenosine in a linear dose response with a yield of about 0.7 lesions per Gray per 10^6 nt as quantified by GC/MS and LC/MS *(96)*. The ratio of 5'-*R* diastereomer to the 5'-*S* diastereomer is about two *(96)*, which has biological consequences since the 5'-*R* diastereomers are repaired more efficiently *(98)*. 5',8-Cyclopurine-2'-deoxyguanosine has been shown to occur in irradiated human cells *(107)*. In single-stranded DNA, 5',8-cyclopurine-2'-deoxyadenosine and 5',8-cyclopurine-2'-deoxyguanosine are formed in roughly equal quantities *(108)*. The fact that 5',8-cyclopurine-2'-deoxyadenosine predominates over 5',8-cyclopurine-2'-deoxyguanosine in double stranded DNA was explained by Dirksen *et al.* by the presence of AT-rich regions in DNA which undergo structural breathing at a higher rate than GC regions *(108)*.

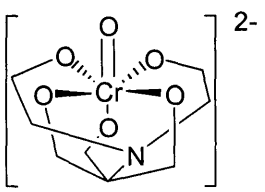

Figure I-12: Structure of *bis*[(hydroxyethyl)-amino-tris(hydroxymethyl)methane]-oxochromate(V) *(109)*.

6.5 Chromium(V) complexes. The two complexes (2-ethyl-2-hydroxybutyrato)oxochromate(V), also discussed in section 5.3 in this chapter, and *bis*[(hydroxyethyl)-amino-tris(hydroxymethyl)methane]oxochromate(V) (shown in Figure I-12) have been found to cause the formation of furfural as the major product, and 5-MF and base propenals as minor products *(109)*. The formation of furfural and 5-MF were attributed to two electron oxidation of the C1' and C5' positions of deoxyribose to the oxo-chromium(V) center *(109)*. The formation of furfural as the major product was suggested to be caused by the ease of abstraction from the C5' in comparison to the C1' position within a Cr(V)-DNA intermediate in which the metal center is bound to the phosphate diester moiety in DNA *(109)*.

7. BIOLOGICAL CONSEQUENCES OF DEOXYRIBOSE OXIDATION

The biological consequences of each oxidative deoxyribose lesion are discussed in sections 2 to section 6 in this chapter. This is a summary of the material presented in those sections. The deoxyribonolactone abasic site arising from C1'-oxidation of deoxyribose causes the formation of protein-DNA cross-links in abortive attempts at repair by polymerase β *(9)* and endonuclease III *(10)*. Furthermore, the deoxyribonolactone was found to induce DNA polymerase-mediated mutagenesis *in vitro (32)*. The half-life of deoxyribonolactone in DNA under physiological conditions (pH 7.4, 37 °C) has been estimated to range from 20 to 54 h and is dependent on the sequence context of the lesion *(33)*.

Removal of 3'-terminal blocking groups, such as phosphoglycolate, has been shown to be rate-limiting during DNA repair with a reduction of the rate of repair by 25-fold in comparison to an AP site *(27)*. Phosphoglycolate is removed in *E. coli* by exonuclease I and IX *(110, 111)*. The 4'-keto-1'-aldehyde abasic site is readily excised by the Ape1 protein, the major human AP endonuclease, while phosphoglycolate is a relatively poor substrate for Ape1 excision thus diminishing probability of repair of the lesion in DNA *(75)*. Greenberg *et al.* have shown *in vitro* that the 4'-keto-1'-aldehyde abasic site is a blocking lesion for Klenow exo^+/exo^- fragments and the bypass polymerases pol II, pol IV and pol V in the presence of Rec A were compromised in their ability to extend past the lesion with preferential thymidine incorporation by polymerase II exo^- thus possibly resulting mutagenicity *(76)*. The presence of base-propenals inhibits DNA synthesis in HeLa cells as well as the function of thymidine kinase and DNA polymerase α *(77)*. The electrophilic products of deoxyribose oxidation also have the potential to react with DNA bases to form mutagenic adducts. The first example of this phenomenon entails the reaction of base propenals, which arise from 4'-oxidation of deoxyribose, with dG to form the mutagenic pyrimidopurinone adduct, M_1G *(11)* (see Scheme I-1).

The C5' radical can form a base-sugar linkage producing 5',8-cyclopurine-2'-deoxynucleosides (see Scheme I-12) *(96, 97)*. This lesion is repaired by the nucleotide-excision repair pathway, albeit with poor efficiency, but not by base excision repair. 5',8-cyclopurine-2'-deoxynucleosides are a strong block to mammalian gene expression and, therefore, have been proposed to be cytotoxic *(98)*.

7.1 Biological consequences of PGA formation. Awada *et al.* have demonstrated the formation of glyoxal and the mutagenic 1,N^2-glyoxal adducts of dG *(12, 13)* in reactions of DNA with phosphoglycolaldehyde under physiological conditions *(14)* (see Scheme I-2). This decomposition has a half-life of about 30 days *in vitro* and in combination with the rarity of the PGA lesion makes the formation of measurable quantities of glyoxal adducts in oxidized DNA due to PGA extremely unlikely. It is more likely that PGA is repaired or that the reactive aldehyde moiety forms a secondary lesion, before it can decompose to form glyoxal.

However, if glyoxal is being formed *in vivo*, this could lead to the formation of mutation with 65% of all mutations in mammalian cells consisting of single-base substitutions. Most of these single base substitutions (83%) occur at G:C base pairs, which causes predominantly G:C → T:A transversions, followed by G:C → C:G transversions and G:C → A:T transitions *(112, 113). In vitro* studies have shown that glyoxal can form cross-links between bases *(12)*.

So far, the repair of PGA has received very little attention and has only been studied *in vitro* using cell extracts. In *E. coli*, PGA is hydrolyzed efficiently by exonuclease III and endonuclease IV *(114)*. In human cells, Ape1 catalyzes the incision of hydrolytic abasic sites, but hydrolyzes 3'-phosphoglycolates about 25-fold more slowly *(75)*. The similarities between 3'-phosphoglycolate and PGA could support the conclusion that Ape1 is part of the repair pathway for PGA in human cells, however, the presence of a reactive aldehyde might complicate the repair of this lesion. Therefore, the

repair of PGA in human cells remains an open question. If not repaired, PGA has been shown to block DNA synthesis *in vitro (26)*. So far, nothing is known about the consequences of PGA formation *in vivo* and about the half-life of PGA residues in cells. It is also not known whether PGA will form mutations in cells and if so, what kind of mutations and at what frequency. This represents an area of future research.

7.2 Measuring DNA oxidation in cells. Several analytical techniques are available to study oxidative DNA modification in cells. Strand breaks can be measured using the comet assay *(115)* or alkaline elution *(116)*. These assays provide only estimates of deoxyribose oxidation, due to the fact that not all deoxyribose oxidation events lead to strand break formation. These studies also do not provide information about the chemical identity and quantity of the deoxyribose oxidation products responsible for the strand break. Therefore, the total of deoxyribose oxidation is underestimated using these assays. Combining the comet assay with repair enzymes for base lesions has been used to quantify base lesions in addition to deoxyribose oxidation *(115)*, but as is the case for deoxyribose oxidation, no specific information about identity and quantity of individual base lesions can be obtained. Another tool that measures the total quantity of deoxyribose oxidation is the so called aldehyde reactive probe (ARP) *(117-119)*. This probe uses hydroxylamine chemistry as is used for our technique, as described in Chapter 2, in combination with an avidin—biotin horseradish peroxidase based Enzyme Linked ImmunoSorbent Assay (ELISA) assay. Similar to alkaline elution and the comet assay, this assay can only measure the total quantity of ketone and aldehyde containing deoxyribose oxidation products, with no knowledge gained about the

identities of lesions. This also leads to an underestimation of the total deoxyribose oxidation due to lesions that do not react with the hydroxylamine moiety, such as deoxyribonolactone and phosphoglycolate.

Methods that can measure specific DNA oxidation products in cells include ^{32}P-postlabeling, HPLC/MS/MS, and immunological detection *(120)*. However, the use of antibodies targeted against specific DNA lesions (for review see *121, 122*) is limited due to cross reactivity with unmodified DNA bases *(123)*. ^{32}P-postlabeling consists of enzymatic hydrolysis of DNA, followed by the introduction of a radioactive phosphate on the 5'-OH end of the digested nucleoside 3'-monophosphates. The modified and normal nucleotides are then separated by either thin-layer chromatography, gel electrophoresis, or reverse phase HPLC prior to quantification *(124, 125)*. This method often exhibits a high background because of artefactual oxidation induced by radioactivity *(123)* and definitive chemical identification of the resulting lesions is only ascertained by co-chromatography of standards. This method leads to underestimation of the lesions formed due to less than 100% efficiency of the several enzymatic steps involved in this assay.

Table I-1: Oxidative DNA lesions measured in cells induced by γ-radiation.

Lesion	lesions/10^6 nt/Gy	Reference
thymine glycol	0.09	*(120)*
5,6-dihydroxy-5,6-dihydrothymidine	0.097	*(126)*
5-(hydroxymethyl)-2'-deoxyuridine	0.029	*(126)*
5-formyl-2'-deoxyuridine	0.022	*(126)*
8-oxo-dG	0.020	*(126)*
8-oxo-dG *	0.044	*(115)*
8-oxo-7,8-dihydro-2'-adenosine	0.003	*(126)*
4,6-diamino-5-formamidopyrimidine	0.005	*(126)*
2,6-diamino-4-hydroxy-5-formamidopyrimidine	0.039	*(126)*
5-hydroxy-2'deoxyuridine	< 0.0002	*(126)*
PGA **	0.0024	See Chapter VI

All lesions measured using HPLC/MS/MS unless otherwise indicated; * measured using HPLC/ECD; ** measured using GC/MS as described in Chapter III.

HPLC coupled to electrochemical detection has been employed for the measurement of several DNA base lesions such as 8-oxo-7,8-dihydro-2'-deoxyguanosine (8-oxo-G) *(127-129)*. This method, although very sensitive, is limited to electrochemically active lesions. A highly sensitive and specific method that combines HPLC separation with electrospray ionization tandem mass spectrometry has been used to assess DNA adducts of bulky chemicals such as benzo[a]pyrene *(130)* and UV-induced pyrimidine dimer photoproducts *(131)* and other modified DNA bases such as 8-oxo-G in cells *(123)*. Table I-1 is a summary of oxidative DNA lesions measured in cells using several of the methods mentioned above induced by γ-radiation.

7.3 Radiation-induced mutations. The deleterious effects of exposure to high, acute doses of ionizing radiation are well documented (see for example *132*). The mutagenic potential of ionizing radiation has been well studied especially for the *HPRT* (hypoxanthine-guanine phosphoribosyl transferase) gene (see Table 2) (see for example *(133, 134)*). Radiation induces point mutations and deletions, the latter predominating in mice *(135)* and sometimes including entire genes *(136)*. Large scale events involving loss of heterozygosity were found to be the most frequent ones *(137, 138)*, which was often the result of a simple deletion, and only sometimes the result of recombinational processes *(139, 140)*. There is no evidence for site specificity for mutations induced by radiation *(141)*. The spectrum of molecular, structural changes associated with direct radiation-induced mutations differs markedly from that for spontaneous mutations, where point mutations predominate *(141)*. For γ-radiation, base substitutions were the results of ≈2/3 of all induced point mutations with every possible type of base substitution *(142)*. The remainder of point mutations caused frame shifts and small deletions *(142)*. Table I-2 illustrates that mutations induced by radiation of differing quality are very similar in the mutational profile for the *HPRT* locus in Chinese hamster cells. However, the presented data does not indicate mutation frequencies, which are shown in Table I-3, and it does not show the size of deletions. Schwartz *et al.* have observed that deletions induced by α-particles are larger than for γ-radiation in the same cell system and gene locus *(143)*.

Table I-2: Molecular structure of γ-radiation-induced *HPRT* mutations.

Treatment	Dose (Gy)	Number of mutants	Deletions		Point mutations	
			total	percentage	total	percentage
Control	0	169	36	21%	133	79%
X-rays	8	137	31	23%	106	77%
α-Particles	2	141	27	19%	114	81%

The data in the table is derived from Chinese hamster ovary cells at the *HPRT* locus in clonal subpopulations derived from single cells surviving irradiation. The number of mutants referred to in the table represents the number of mutants examined. Data adapted from Little *et al. (134)*.

The differences and similarities of radiation effects of radiation with differing LET are illustrated in Table I-3. Low LET radiation represents γ-radiation and x-rays, and high LET radiation represents α-particles. The PGA results for γ-radiation were calculated for the TK6 cell genome. For α-particles, it was assumed that cells exhibit a 1000-fold quenching effect as has been seen for γ-irradiated TK6 cells in comparison to *in vitro* results (see Chapter VI). However, it is not known whether the same quenching effect is observed for α-particles, which is an area for future studies. Overall, α-particles are in general more cytotoxic, clastogenic and mutagenic than γ-radiation (see for example *144, 145*).

Table I-3. Average yield of damage in a single mammalian cell after 1 Gy of radiation (adapted from *(146)* and references therein).

Radiation	Low LET	High LET
Tracks in nucleus	1000	2
Base damage	10^4	10^4
DNA SSB	850	450
8-oxo-dG	700	-
Chromosome aberration	0.3	2.5
HPRT mutation	10^{-6}	10^{-5}
Lethal lesion	0.5	2.6
Cell inactivation	30%	85%
PGA yield	16*	0.9**

SSB, single-strand break, HPRT, hypoxanthine-guanine phosphoribosyl transferase; * from acute high-dose irradiation of TK6 cells (see Chapter IV); ** calculated for TK6 cells using the *in vitro* result of 0.13 PGA molecules/10^6 nt/Gy (see Chapter III) assuming a 1000 fold quenching effect *in vivo* (as experienced for γ-radiation; see Chapter VI).

The effects of exposure to low doses, such as clinically relevant doses of radiation, are less well known and the effects of chronic, low-dose rate exposures, important for radiation workers, are essentially untested. To assess detrimental health effects, such as cancer, resulting from low level and/or chronic exposures are extrapolated downward from models of high, acute exposure-induced effects in a linear fashion. This mathematical approach neglects a dose-response threshold (see for review *147*) and assumes equivalent effects regardless of the rate of dose administration *(148)*. Although this provides a means by which to assign risk, these expectations have been invalidated (see for example *149, 150*). Recent studies investigating the genetic effects of

acute, low-dose exposure, generally defined as <20 cGy, have revealed a variety of responses not typically observed in high, acute-dose studies (for review see *148*).

Schwartz *et al.* have observed dose-dependent changes in mutational spectra in γ-irradiated Chinese hamster ovary cells at the *HPRT* locus *(151)*. At low doses, the principal radiation-induced mutations were point mutations. With increasing dose, multibase deletions became the predominant mutation type by 6 Gy *(151)*. Evans and co-workers observed a decrease in mutant frequency with decreased dose rates of X-irradiation *(152)*. While acute, high-dose exposures induce a significant increase in easily detectable chromosomal aberrations as well as point mutations, the spectrum of induced genetic effects resulting from acute, low doses does not include chromosomal aberrations *(148)*. In fact, responses to these low doses have ranged from a significant increase in point mutations and mutation frequencies *(153)* to a significant decrease of point mutations *(154)* or an inverse dose-response relationship *(155, 156)*.

Neoplasia in cells exposed acutely to low radiation doses was found to be decreased in comparison to high doses *(148)*. The validity of a non-threshold linearity with respect to exposure and effects based on acute, low-dose research is questionable and actually appears to support the concept of an adaptive response *(148, 157-159)*. Transcriptional responses in cells may serve to modulate oxidative stress by either increasing the cellular capacity to scavenge free radicals and/or the ability to repair damaged DNA *(148, 157, 160)*. This would essentially serve to maintain both the spontaneous frequency of mutants and spectrum of mutations. In fact, there was no

significant difference between the mutational spectra of mice exposed to chronic, low-dose rate exposures of 3 Gy of γ-radiation and unexposed mice *(148)* and neither of these groups differed significantly from the spontaneous mutational spectrum *(161)*. This might be explained by adaptive response, which was tested by exposing cells to very low doses of radiation and subsequently to a high dose. In these cells, fewer chromosome aberrations than in cells that have not been pre-exposed to low doses of radiation *(160)* and fewer gene mutations have been observed (for review, see *158*). Repair of radiation-induced lesions may also explain the non-linear results at chronic low-dose exposures.

7.4 The role of oxidative DNA damage in cancer. Oxidative mechanisms have been proposed to posses a role in the initiation, promotion and malignant conversion (progression) stages of carcinogenesis (for reviews see *162-167*). Due to the fact that cancer risk increases with age and is associated with an accumulation of DNA damage, research has been focused on DNA damage as a cause for carcinogenesis. Lesions such as 8-oxo-dG are established biomarkers of oxidative stress *(168)*. Since 8-oxo-dG can lead to mutations (G:C → T:A transversions), this has led to the proposed potential as a marker for a disease endpoint such as cancer *(163, 169, 170)*.

Numerous studies have attempted to establish a relationship between levels of oxidative DNA damage and cancer (see for reviews *141, 170, 171*). Elevated levels of damage are purported to arise as a consequence of an environment in the tumor low in antioxidant enzymes and high in ROS generation *(163)*. It has been argued that the mere presence of 8-oxo-dG in DNA is unlikely to be necessary or sufficient to cause tumor

formation *(162)*. There are many pathological conditions in which levels of oxidative DNA damage are elevated with no increased incidence of carcinogenesis (see for extensive review *162*). Therefore, oxidative DNA damage may be an epiphenomenon to an on-going pathophysiological process, and elevated levels do not have a role in carcinogenesis. Elevated levels of oxidative DNA damage may occur as a result of well-established characteristics of tumors such as increased metabolism and cell turnover. It also has been hypothesized that cancer cells themselves produce ROS, which is believed to play a role in activation of proto-oncogenes and transcription factors, genomic instability, invasion and metastasis *(163)*. In case of radiation induced cancers, multiple unbalanced chromosomal rearrangements have been shown, but few show specific translocations and deletions associated with the activation of known oncogenes and tumor suppressor genes *(141)*.

It has been proposed that the most likely mutational event in the initiation of radiationoncogenesis involves loss of heterozygocity of a tumor suppressor gene *(141)*. In general, for DNA mutations to induce cancer, the nuclei of undifferentiated, proliferating stem cells must be affected. Given that tissue samples from tumors that have been used to study oxidative DNA damage are a heterogeneous mixture of differentiated and undifferentiated cells (with the former predominating), current analytical methods will not reflect the level of oxidative lesions in stem cells. Furthermore, in order to be carcinogenic, a lesion must occur within the coding region of DNA, decreasing the probability of any mutation induced by oxidative DNA damage to lead to cancer

induction. Therefore the extent to which oxidative DNA damage contributes to carcinogenesis is not well defined and requires much further study.

8. SUMMARY

Pathways for the oxidation of the deoxyribose moiety in DNA and the oxidizing species were discussed in this chapter. Although all seven hydrogen atoms (shown in Figure I-2) have been found to be abstracted by individual oxidizing species, it is clear that each oxidizing species generates a unique spectrum of deoxyribose oxidation products. There are hydrogen atoms in the deoxyribose that show a preferential abstraction, such as the C4' position, due to solvent accessibility and bond dissociation energy issues. Of particular interest are species that show differences in partitioning of damage pathways. One such example is the partitioning of the C4' chemistry to form either base propenals (or malondialdehyde) and 3'-phosphoglycolate, or the 4'-keto-1'-aldehyde abasic site (see Scheme I-10). The mechanisms of damage formation and partitioning are responsible for the ultimate oxidation products which, in case of bleomycin, lead to the formation of base propenals whereas γ-radiation leads to the formation of malondialdehyde. The C3' position, of particular interest here, may also involve partitioning between the formation of 3'-phosphoglycolaldehyde and base propenoate on the one hand and the abasic site leading to 2-methylene-3(2*H*)-furanone on the other. So far, C3' oxidation in deoxyribose has only been shown for rhodium(III) complexes *(23)*. 2-Methylene-3(2*H*)-furanone has been proposed to exist by Stubbe *et al.* but remains to be chemically proven *(2)*. Ongoing collaborative studies with Professor

Amanda Bryant-Friedrich and the use of her C3'-radical generating system will help to resolve these issues *(24)*. Due to the lack of knowledge about C3' oxidation, we decided to develop a sensitive analytical method to positively identify and quantify phosphoglycolaldehyde. This method was applied to quantify 3'-phosphoglycolaldehyde residues produced by various oxidizing species *in vitro* and in cells, which enhances overall knowledge about the reactivity of deoxyribose in DNA.

8. REFERENCES

(1) Beckman, K.B., Ames, B.N. (1998). The free radical theory of aging matures. *Physiological reviews.* ***78(2)***, 547-581.

(2) Stubbe, J., Kozarich, J.W. (1987). Mechanisms of Bleomycin-Induced DNA Degradation. *Chem Rev* ***87***, 1107-1136.

(3) Grisham, M.B., Jourd'heuil, D., Wink, D.A. (2000). Review article: chronic inflammation and reactive oxygen and nitrogen metabolism--implications in DNA damage and mutagenesis. *Aliment Pharmacol Ther* ***14 Suppl 1***, 3-9.

(4) Dedon, P.C., Tannenbaum, S.R. (2004). Reactive nitrogen species in the chemical biology of inflammation. *Archives of biochemistry and biophysics.* ***423***, 12-22.

(5) Greenberg, M.M. (1999). Chemistry of DNA Damage. In Comprehensive Natural Products Chemistry, **7**, E.T. Kool, ed. (Amsterdam: Elsevier Science B. V.), 372-425.

(6) Greenberg, M.M. (1998). Investigating nucleic acid damage processes via independent generation of reactive intermediates. *Chemical research in toxicology.* ***11(11)***, 1235-1248.

(7) Dedon, P.C., Jiang, Z.W., Goldberg, I.H. (1992). Neocarzinostatin-mediated DNA damage in a model AGT.ACT site: mechanistic studies of thiol-sensitive partitioning of C4' DNA damage products. *Biochemistry* ***31***, 1917-1927.

(8) Pogozelski, W.K., Tullius, T.D. (1998). Oxidative strand scission of nucleic acids: routes initiated by hydrogen abstraction from the sugar moiety. *Chem. Rev.* ***98***, 1089-1107.

(9) DeMott, M.S., Beyret, E., Wong, D., Bales, B.C., Hwang, J.T., Greenberg, M.M., Demple, B. (2002). Covalent trapping of human DNA polymerase beta by the oxidative DNA lesion 2-deoxyribonolactone. *J. Biol. Chem.* ***277***, 7637-7640.

(10) Hashimoto, M., Greenberg, M.M., Kow, Y.W., Hwang, J.T., Cunningham, R.P. (2001). The 2-deoxyribonolactone lesion produced in DNA by neocarzinostatin and other damaging agents forms cross-links with the base-excision repair enzyme endonuclease III. *J. Am. Chem. Soc.* ***123***, 3161-3162.

(11) Dedon, P.C., Plastaras, J.P., Rouzer, C.A., Marnett, L.J. (1998). Indirect mutagenesis by oxidative DNA damage: formation of the pyrimidopurinone adduct of deoxyguanosine by base propenal. *Proc. Natl. Acad. Sci. USA* ***95***, 11113-11116.

(12) Kasai, H., Iwamoto-Tanaka, N., Fukada, S. (1998). DNA modifications by the mutagen glyoxal: adduction to G and C, deamination of C and GC and GA cross-linking. *Carcinogenesis.* ***19(8)***, 1459-1465.

(13) Loeppky, R.N., Cui, W., Goelzer, P., Park, M., Ye, Q. (1999). Glyoxal-guanine DNA adducts: detection, stability and formation in vivo from nitrosamines. *IARC scientific publications.*

(14) Awada, M., Dedon, P.C. (2001). Formation of the 1,N2-glyoxal adduct of deoxyguanosine by phosphoglycolaldehyde, a product of 3'-deoxyribose oxidation in DNA. *Chem. Res. Toxicol.* ***14***, 1247-1253.

(15) Kennedy, L.J., Moore Jr., K., Caulfield, J.L., Tannenbaum, S.R., Dedon, P.C. (1997). Quantitation of 8-oxoguanine and strand breaks produced by four oxidizing agents. *Chem. Res. Toxicol.* ***10***, 386-392.

(16) Rashid, R., Langfinger, D., Wagner, R., Schuchmann, H.P., von Sonntag, C. (1999). Bleomycin versus OH-radical-induced malonaldehydic-product formation in DNA. *Int J Radiat Biol* ***75***, 101-109.

(17) Gao, X., Stassinopoulos, A., Rice, J.S., Goldberg, I.H. (1995). Structural basis for the sequence-specific DNA strand cleavage by the enediyne neocarzinostatin chromophore. Structure of the post-activated chromophore-DNA complex. *Biochemistry.* ***34(1)***, 40-49.

(18) Alden, C.J., Kim, S.H. (1979). Solvent-accessible surfaces of nucleic acids. *Journal of molecular biology.* ***132(3)***, 411-434.

(19) Balasubramanian, B., Pogozelski, W.K., Tullius, T.D. (1998). DNA strand breaking by the hydroxyl radical is governed by the accessible surface areas of the hydrogen atoms of the DNA backbone. *Proc. Natl. Acad. Sci. U S A* ***95***, 9738-9743.

(20) Aydogan, B., Marshall, D.T., Swarts, S.G., Turner, J.E., Boone, A.J., Richards, N.G., Bolch, W.E. (2002). Site-specific OH attack to the sugar moiety of DNA: a comparison of experimental data and computational simulation. *Radiation research.* ***157(1)***, 38-44.

(21) von Sonntag, C. (1987). The Chemical Basis of Radiation Biology (New York: Taylor & Francis).

(22) Breen, A.P., Murphy, J.A. (1995). Reactions of oxyl radicals with DNA. *Free radical biology & medicine.* ***18(6)***, 1033-1077.

(23) Sitlani, A., Long, E.C., Pyle, A.M., Barton, J.K. (1992). DNA Photocleavage by Phenanthrenequinone Diimine Complexes of Rhodium(III): Shape-Selective Recognition and Reaction. *J. Am. Chem. Soc* ***114***, 2303-2312.

(24) Koerner, S., Bryant-Friedrich, A., Giese, B. (1999). C-3'-branched thymidines as precursors for the selective generation of C-3'-nucleoside radicals. *J. Org. Chem.* ***64***, 1559-1564.

(25) Debije, M.G., Bernhard, W.A. (2001). Electron paramagnetic resonance evidence for a C3' sugar radical in crystalline d(CTCTCGAGAG) X-irradiated at 4 K. *Radiat Res* ***155***, 687-692.

(26) Johnson, A.W., Demple, B. (1988). Yeast DNA diesterase for 3'-fragments of deoxyribose: purification and physical properties of a repair enzyme for oxidative DNA damage. *The Journal of biological chemistry.* ***263(34)***, 18009-18016.

(27) Izumi, T., Hazra, T.K., Boldogh, I., Tomkinson, A.E., Park, M.S., Ikeda, S., Mitra, S. (2000). Requirement for human AP endonuclease 1 for repair of 3'-blocking damage at DNA single-strand breaks induced by reactive oxygen species. *Carcinogenesis.* ***21(7)***, 1329-1334.

(28) Miaskiewicz, K., Osman, R. (1994). Theoretical Study on the Deoxyribose Radicals formed by Hydrogen Abstraction. *J Am Chem Soc* ***116***, 232-238.

(29) Colson, A.O., Sevilla, M.D. (1995). Elucidation of primary radiation damage in DNA through application of ab initio molecular orbital theory. *International journal of radiation biology.* ***67(6)***, 627-645.

(30) Kroeger, K.M., Hashimoto, M., Kow, Y.W., Greenberg, M.M. (2003). Cross-linking of 2-deoxyribonolactone and its beta-elimination product by base excision repair enzymes. *Biochemistry.* ***42(8)***, 2449-2455.

(31) Xu, Y.J., DeMott, M.S., Hwang, J.T., Greenberg, M.M., Demple, B. (2003). Action of human apurinic endonuclease (Ape1) on C1'-oxidized deoxyribose damage in DNA. *DNA repair.* ***2(2)***, 175-185.

(32) Berthet, N., Roupioz, Y., Constant, J.F., Kotera, M., Lhomme, J. (2001). Translesional synthesis on DNA templates containing the 2'-deoxyribonolactone lesion. *Nucleic acids research.* ***29(13)***, 2725-2732.

(33) Zheng, Y., Sheppard, T.L. (2004). Half-life and DNA strand scission products of 2-deoxyribonolactone oxidative DNA damage lesions. *Chemical research in toxicology.* ***17(2)***, 197-207.

(34) Tronche, C., Goodman, B.K., Greenberg, M.M. (1998). DNA damage induced via independent generation of the radical resulting from formal hydrogen atom abstraction from the C1'-position of a nucleotide. *Chemistry & biology.* ***5(5)***, 263-271.

(35) Meijler, M.M., Zelenko, O., Sigman, D.S. (1997). Chemical Mechanism of DNA Scission by (1,10-Phenanthroline)copper. Carbonyl Oxygen of 5-Methylenefuranone Is Derived from Water. *J Am Chem Soc* ***119***, 1135-1136.

(36) Vialas, C., Pratviel, G., Meunier, B. (2000). Oxidative damage generated by an oxo-metalloporphyrin onto the human telomeric sequence. *Biochemistry* ***39***, 9514-9522.

(37) Sigman, D.S., Graham, D.R., D'Aurora, V., Stern, A.M. (1979). Oxygen-dependent cleavage of DNA by the 1,10-phenanthroline . cuprous complex. Inhibition of Escherichia coli DNA polymerase I. *The Journal of biological chemistry.* ***254(24)***, 12269-12272.

(38) Kuwabara, M., Yoon, C., Goyne, T., Thederahn, T., Sigman, D.S. (1986). Nuclease activity of 1,10-phenanthroline-copper ion: reaction with CGCGAATTCGCG and its complexes with netropsin and EcoRI. *Biochemistry.* ***25(23)***, 7401-7408.

(39) Goyne, T.E., Sigman, D.S. (1987). Nuclease activity of 1,10-phenanthroline-copper ion. Chemistry of deoxyribose oxidation. *J Am Chem Soc* ***109***, 2846-2848.

(40) Pitie, M., Burrows, C.J., Meunier, B. (2000). Mechanisms of DNA cleavage by copper complexes of 3-clip-phen and of its conjugate with a distamycin analogue. *Nucleic Acids Res* ***28***, 4856-4864.

(41) Gonzâalez-Alvarez, M., Alzuet, G., Borrâas, J., Pitiâe, M., Meunier, B. (2003). DNA cleavage studies of mononuclear and dinuclear copper(II) complexes with benzothiazolesulfonamide ligands. *Journal of biological inorganic chemistry : JBIC : a publication of the Society of Biological Inorganic Chemistry.* ***8(6)***, 644-652.

(42) Pratviel, G., Pitiâe, M., Bernadou, J., Meunier, B. (1991). Mechanism of DNA cleavage by cationic manganese porphyrins: hydroxylations at the 1'-carbon and 5'-carbon atoms of deoxyriboses as initial damages. *Nucleic acids research.* ***19(22)***, 6283-6288.

(43) Carter, P.J., Cheng, C.-C., Thorp, H.H. (1998). Oxidation of DNA and RNA by oxoruthenium(IV) metallointercalators: visualizing the recognition properties of dipyridophenanzine by high-resolution electrophoresis. *J Am Chem Soc* ***120***, 632-642.

(44) Neyhart, G.A., Cheng, C.-C., Thorp, H.H. (1995). Kinetics and mechanism of the oxidation of sugar and nucleotides by oxoruthenium(IV): model studies for predicting cleavage patterns in polymeric DNA and RNA. *J Am Chem Soc* ***117***, 1463-1471.

(45) Urata, H., Yamamoto, K., Akagi, M., Hiroaki, H., Uesugi, S. (1989). A 2-deoxyribonolactone-containing nucleotide: isolation and characterization of the alkali-sensitive photoproduct of the trideoxyribonucleotide d(ApCpA). *Biochemistry.* ***28(25)***, 9566-9569.

(46) Urata, H., Akagi, M. (1991). Photo-induced formation of the 2-deoxyribonolactone-containing nucleotide for d(ApCpA); effects of neighboring bases and modification of deoxycytidine. *Nucleic acids research.* ***19(8)***, 1773-1778.

(47) Hole, E.O., Sagstuen, E., Nelson, W.H., Close, D.M. (2000). Free radical formation in X-irradiated crystals of 2'-deoxycytidine hydrochloride. Electron magnetic resonance studies at 10 K. *Radiation research.* ***153(6)***, 823-834.

(48) Carter, K.N., Greenberg, M.M. (2003). Independent generation and study of 5,6-Dihydro-2'-deoxyuridin-6-yl, a member of the major family of reactive intermediates formed in DNA from the effects of gamma-radiolysis. *The Journal of organic chemistry.* ***68(11)***, 4275-4280.

(49) Shaw, A.A., Cadet, J. (1996). Direct effects of gamma-radiation on 2'-deoxycytidine in frozen aqueous solution. *International journal of radiation biology.* ***70(1)***, 1-6.

(50) Cosgrove, J.P., Dedon, P.C. (2002). Binding and reaction of calicheamicin and other enediyne antibiotics with DNA. In Interaction of Small Molecules with DNA and RNA: From Synthesis to Nucleic Acid Complexes, M. Demeunynck, C. Bailly, D. Wilson, eds. (New York: John Wiley and Sons).

(51) Nicolaou, K.C., Dai, W.-M. (1991). Chemistry and biology of the enediyne antibiotics. *Angewandte Chemie, Internationale Edition* ***30***, 1387-1530.

(52) Lee, M.D., Ellestad, G.A., Borders, D.B. (1991). Calicheamicins: Discovery, structure, chemistry, and interaction with DNA. ***24***, 235-243.

(53) Dedon, P.C., Goldberg, I.H. (1992). Free-radical mechanisms involved in the formation of sequence-dependent bistranded DNA lesions by the antitumor antibiotics bleomycin, neocarzinostatin, and calicheamicin. *Chemical research in toxicology.* ***5(3)***, 311-332.

(54) Meienhofer, J., Maeda, H., Glaser, C.B., Czombos, J., Kuromizu, K. (1972). Primary structure of neocarzinostatin, an antitumor protein. *Science* ***178***, 875-876.

(55) Golik, J., Dubay, G., Groenewold, G., Kawaguchi, H., Konishi, M., Krishnan, B., Ohkuma, H., Saitoh, K.-i., Doyle, T.W. (1987). Esperamicins, a novel class of potent antitumor antibiotics. 3. Structures of esperamicins A1, A2, and A1b. *J Am Chem Soc* ***109***, 3462-3464.

(56) Kappen, L.S., Goldberg, I.H. (1992). Neocarzinostatin acts as a sensitive probe of DNA microheterogeneity: switching of chemistry from C-1' to C-4' by a G.T mismatch 5' to the site of DNA damage. *Proc Natl Acad Sci U S A* ***89***, 6706-6710.

(57) Kappen, L.S., Goldberg, I.H. (1989). Identification of 2-deoxyribonolactone at the site of neocarzinostatin-induced cytosine release in the sequence d(AGC). *Biochemistry.* ***28(3)***, 1027-1032.

(58) Kappen, L.S., Chen, C.Q., Goldberg, I.H. (1988). Atypical abasic sites generated by neocarzinostatin at sequence- specific cytidylate residues in oligodeoxynucleotides. *Biochemistry* ***27***, 4331-4340.

(59) Christner, D.F., Frank, B.L., Kozarich, J.W., Stubbe, J., Golik, J., Doyle, T.W., Rosenberg, I.E., Krishnan, B. (1992). Unmasking the chemistry of DNA cleavage by the esperamicins: modulation of the 4'-hydrogen abstraction and bistranded damage by the fucose-anthranilate moiety. *J Am Chem Soc* ***114***, 8763-8767.

(60) Yu, L., Golik, J., Harrison, R., Dedon, P.C. (1994). The deoxyfucose-anthranilate of esperamicin A1 confers intercalative DNA binding and causes a switch in the chemistry of bistranded DNA lesions. *J Am Chem Soc* ***116***, 9733-9738.

(61) Saito, I., Matsuura, T. (1985). Chemical aspects of UV-induced cross-linking of proteins to nucleic acids. Photoreactions with lysine and tryptophan. *Acc. Chem. Res.* ***18***, 134-141.

(62) Ogata, R., Gilbert, W. (1977). Contacts between the lac repressor and the thymines in the lac operator. *Proceedings of the National Academy of Sciences of the United States of America.* ***74(11)***, 4973-4976.

(63) Sugiyama, H., Tsutsumi, Y., Saito, I. (1990). Highly sequence selective photoreaction of 5-bromouracil-containing deoxyhexanucleotides. *J Am Chem Soc* ***112***, 6720-6721.

(64) Harkin, L.A., Burcham, P.C. (1997). Formation of novel C1-oxidised abasic sites in alkylperoxyl radical-damaged plasmid DNA. *Biochemical and biophysical research communications.* ***237(1)***, 1-5.

(65) Dizdaroglu, M., Schulte-Frohlinde, D., von Sonntag, C. (1977). gamma-radiolyses of DNA in oxygenated aqueous solution. Structure of an alkali-labile site. *Z. Naturforsch.* ***32C***, 1021-1022.

(66) Sugiyama, H., Tsutsumi, Y., Fujimoto, K., Saito, I. (1993). Photoinduced deoxyribose-C2' oxidation in DNA: Alkali-dependent cleavage of erythrose-containing sites via a retroaldol reaction. *J. Am. Chem. Soc.* ***115***, 4443-4448.

(67) Sugiyama, H., Fujimoto, K., Saito, I. (1996). Evidence for the intrastrand C2' hydrogen abstraction in photoirradiation of 5'-halouracil-containing

oligonucleotides by using stereospecifically C2'-deuterated deoxyadenosine. *Tetrahedron Letters* ***37***, 1805-1808.

(68) Pratviel, G., Bernadou, J., Meunir, B. (1995). Carbon-hydrogen bonds of DNA sugar units as targets for chemical nucleases and drugs. *Angewandte Chemie, Internationale Edition* ***34***, 746-769.

(69) Cook, G.P., Chen, T., Koppisch, A.T., Greenberg, M.M. (1999). The effects of secondary structure and O2 on the formation of direct strand breaks upon UV irradiation of 5-bromodeoxyuridine-containing oligonucleotides. *Chemistry & Biology* ***6***, 451-459.

(70) Giloni, L., Takeshita, M., Johnson, F., Iden, C., Grollman, A.P. (1981). Bleomycin-induced strand-scission of DNA. Mechanism of deoxyribose cleavage. *J Biol Chem* ***256***, 8608-8615.

(71) Henner, W.D., Grunberg, S.M., Haseltine, W.A. (1983). Enzyme action at 3' termini of ionizing radiation-induced DNA strand breaks. *J Biol Chem* ***258***, 15198-15205.

(72) Janicek, M.F., Haseltine, W.A., Henner, W.D. (1985). Malondialdehyde precursors in gamma-irradiated DNA, deoxynucleotides and deoxynucleosides. *Nucleic Acids Res* ***13***, 9011-9029.

(73) Henner, W.D., Rodriguez, L.O., Hecht, S.M., Haseltine, W.A. (1983). gamma Ray induced deoxyribonucleic acid strand breaks. 3' Glycolate termini. *J Biol Chem* ***258***, 711-713.

(74) Saito, I., Kawabata, H., Fujiwara, T., Sugiyama, H., Matsuura, T. (1989). A novel ribose C-4' hydroxylation pathway in neocarzinostatin-mediated degradation of oligonucleotides. *J. Am. Chem. Soc.* ***111***, 8302-8303.

(75) Xu, Y.J., Kim, E.Y., Demple, B. (1998). Excision of C-4'-oxidized deoxyribose lesions from double-stranded DNA by human apurinic/apyrimidinic endonuclease (Ape1 protein) and DNA polymerase beta. *The Journal of biological chemistry.* ***273(44)***, 28837-28844.

(76) Greenberg, M.M., Weledji, Y.N., Kroeger, K.M., Kim, J., Goodman, M.F. (2004). In vitro effects of a C4'-oxidized abasic site on DNA polymerases. *Biochemistry.* ***43(9)***, 2656-2663.

(77) Grollman, A.P., Takeshita, M., Pillai, K.M., Johnson, F. (1985). Origin and cytotoxic properties of base propenals derived from DNA. *Cancer Res* ***45***, 1127-1131.

(78) Plastaras, J.P., Dedon, P.C., Marnett, L.J. (2002). Effects of DNA structure on oxopropenylation by the endogenous mutagens malondialdehyde and base propenal. *Biochemistry* ***41***, 5033-5042.

(79) Yu, H., Kwok, Y., Hurley, L.H., Kerwin, S.M. (2000). Efficient, Mg(2+)-dependent photochemical DNA cleavage by the antitumor quinobenzoxazine (S)-A-62176. *Biochemistry.* ***39(33)***, 10236-10246.

(80) Liang, Q., Ananias, D.C., Long, E.C. (1998). Ni(II)Xaa-Xaa-His induced DNA cleavage: deoxyribose modification by a common "activated' intermediate derived from KHSO5, MMPP, or H2O2. *J Am Chem Soc* ***120***, 248-257.

(81) Sugden, K.D. (1999). Formation of modified cleavage termini from the reaction of chromium(V) with DNA. *J Inorg Biochem 77*, 177-183.

(82) Burger, R.M. (1998). Cleavage of nucleic acids by bleomycin. *Chem. Rev.* ***98***, 1153-1169.

(83) Wu, Y.-D., Houk, K.N., Valentine, J.S., Nam, W. (1992). Is intramolecular hydrogen-bonding important for bleomycin reactivity? A molecular mechanics study. *Inorganic Chemistry* ***31***, 718-720.

(84) Wu, J.C., Stubbe, J., Kozarich, J.W. (1985). Mechanism of bleomycin: evidence for 4'-ketone formation in poly(dA-dU) associated exclusively with free base release. *Biochemistry* ***24***, 7569-7573.

(85) Lopez-Larraza, D.M., Moore, K., Jr.;, Dedon, P.C. (2001). Thiols alter the partitioning of calicheamicin-induced deoxyribose 4'-oxidation reactions in the absence of DNA radical repair. *Chemical research in toxicology.* ***14(5)***, 528-535.

(86) Kappen, L.S., Goldberg, I.H., Frank, B.L., Worth, L., Christner, D.F., Kozarich, J.W., Stubbe, J. (1991). Neocarzinostatin-induced hydrogen atom abstraction from C-4' and C-5' of the T residue at a d(GT) step in oligonucleotides: shuttling between deoxyribose attack sites based on isotope selection effects. *Biochemistry* ***30***, 2034-2042.

(87) Frank, B., Worth, L., Christner, D., Kozarich, J., Stubbe, J., Kappen, L., Goldberg, I. (1991). Isotope Effects on the Sequence-Specific Cleavage of DNA by Neocarzinostatin: Kinetic Partitioning between 4'- and 5'-Hydrogen Abstraction at Unique Thymidine Sites. *J Am Chem Soc* ***113***, 2271-2275.

(88) Oyoshi, T., Sugiyama, H. (2000). Mechanism of DNA strand scission induced by (1,10-phenanthroline) copper complex: major direct DNA strand cleavage is not through 1',2'-dehydronucleotide intermediate nor beta-elimination of forming ribonolactone. *J Am Chem Soc* ***122***, 6313-6314.

(89) Benites, P.J., Rawat, D.S., Zaleski, J.M. (2000). Metalloenediynes: ligand field control of thermal Bergman cyclization reactions. *J Am Chem Soc* ***122***, 7208-7217.

(90) Benites, P.J., Holmberg, R.C., Rawat, D.S., Kraft, B.J., Klein, L.J., Peters, D.G., Thorp, H.H., Zaleski, J.M. (2003). Metal-ligand charge-transfer-promoted photoelectronic Bergman cyclization of copper metalloenediynes: photochemical DNA cleavage via C-4' H-atom abstraction. *Journal of the American Chemical Society.* ***125(21)***, 6434-6446.

(91) Breiner, K.M., Daugherty, M.A., Oas, T.G., Thorp, H.H. (1995). An anionic diplatinum DNA photocleavage agent: chemical mechanism and footprinting of the lambda repressor. *J Am Chem Soc* ***117***, 11673-11679.

(92) Hertzberg, R.P., Dervan, P.B. (1984). Cleavage of DNA with methidiumpropyl-EDTA-iron(II): Reaction conditions and product analyses. *Biochemistry* ***23***, 3934-3945.

(93) Yermilov, V., Yoshie, Y., Rubio, J., Ohshima, H. (1996). Effects of carbon dioxide/bicarbonate on induction of DNA single-strand breaks and formation of 8-nitroguanine, 8-oxoguanine and base-propenal mediated by peroxynitrite. *FEBS letters.* ***399(1-2)***, 67-70.

(94) Barone, F., Belli, M., Mazzei, F. (1994). Influence of DNA conformation on radiation-induced single-strand breaks. *Radiat Environ Biophys* ***33***, 23-33.

(95) Sy, D., Savoye, C., Begusova, M., Michalik, V., Charlier, M., Spotheim-Maurizot, M. (1997). Sequence-dependent variations of DNA structure modulate radiation- induced strand breakage. *Int J Radiat Biol* ***72***, 147-155.

(96) Dizdaroglu, M., Jaruga, P., Rodriguez, H. (2001). Identification and quantification of 8,5'-cyclo-2'-deoxy-adenosine in DNA by liquid chromatography/ mass spectrometry. *Free radical biology & medicine.* ***30(7)***, 774-784.

(97) Chatgilialoglu, C., Guerra, M., Mulazzani, Q.G. (2003). Model studies of DNA C5' radicals. Selective generation and reactivity of 2'-deoxyadenosin-5'-yl radical. *Journal of the American Chemical Society.* ***125(13)***, 3839-3848.

(98) Brooks, P.J., Wise, D.S., Berry, D.A., Kosmoski, J.V., Smerdon, M.J., Somers, R.L., Mackie, H., Spoonde, A.Y., Ackerman, E.J., Coleman, K., Tarone, R.E., Robbins, J.H. (2000). The oxidative DNA lesion 8,5'-(S)-cyclo-2'-deoxyadenosine is repaired by the nucleotide excision repair pathway and blocks gene expression in mammalian cells. *The Journal of biological chemistry.* ***275(29)***, 22355-22362.

(99) Kappen, L.S., Goldberg, I.H. (1983). Deoxyribonucleic acid damage by neocarzinostatin chromophore: strand breaks generated by selective oxidation of C-5' of deoxyribose. *Biochemistry* ***22***, 4872-4878.

(100) Meschwitz, S.M., Goldberg, I.H. (1991). Selective abstraction of 2H from C-5' of thymidylate in an oligodeoxynucleotide by the radical center at C-6 of the diradical species of neocarzinostatin: chemical evidence for the structure of the activated drug-DNA complex. *Proc Natl Acad Sci U S A* ***88***, 3047-3051.

(101) Gu, F., Xi, Z., Goldberg, I.H. (2000). DNA damage by thiol-activated neocarzinostatin chromophore at bulged sites. *Biochemistry* ***39***, 4881-4891.

(102) Zein, N., Sinha, A.M., McGahren, W.J., Ellestad, G.A. (1988). Calicheamicin gamma 1I: an antitumor antibiotic that cleaves double-stranded DNA site specifically. *Science* ***240***, 1198-1201.

(103) Hangeland, J.J., De Voss, J.J., Heath, J.A., Townsend, C.A. (1992). Specific abstraction of the 5'(S) - and 4'-deoxyribosyl hydrogen atoms from DNA by Calicheamicin. *J Am Chem Soc* ***114***, 9200-9202.

(104) Angeloff, A., Dubey, I., Pratviel, G., Bernadou, J., Meunier, B. (2001). Characterization of a 5'-aldehyde terminus resulting from the oxidative attack at C5' of a 2-deoxyribose on DNA. *Chemical research in toxicology.* ***14(10)***, 1413-1420.

(105) Pitie, M., Pratviel, G., Bernadou, J., Meunier, B. (1992). Preferential hydroxylation by the chemical nuclease meso-tetrakis-(4-N-methylpyridiniumyl)porphyrinatomanganeseIII pentaacetate/KHSO5 at the 5' carbon of deoxyriboses on both 3' sides of three contiguous A.T base pairs in short double-stranded oligonucleotides. *Proceedings of the National Academy of Sciences of the United States of America.* ***89(9)***, 3967-3971.

(106) Langfinger, D., von Sonntag, C. (1985). Gamma-Radiolysis of 2'-Deoxyguanosine: The Structure of the Malondialdehyde-Like Product. *Zeitschrift fuer Naturforschung* ***40C***, 446-448.

(107) Dizdaroglu, M., Dirksen, M.L., Jiang, H.X., Robbins, J.H. (1987). Ionizing-radiation-induced damage in the DNA of cultured human cells. Identification of 8,5-cyclo-2-deoxyguanosine. *The Biochemical journal.* ***241(3)***, 929-932.

(108) Dirksen, M.L., Blakely, W.F., Holwitt, E., Dizdaroglu, M. (1988). Effect of DNA conformation on the hydroxyl radical-induced formation of 8,5'-cyclopurine 2'-deoxyribonucleoside residues in DNA. *International journal of radiation biology.* ***54(2)***, 195-204.

(109) Bose, R.N., Moghaddas, S., Mazzer, P.A., Dudones, L.P., Joudah, L., Stroup, D. (1999). Oxidative damage of DNA by chromium(V) complexes: relative importance of base versus sugar oxidation. *Nucleic acids research.* ***27(10)***, 2219-2226.

(110) Sandigursky, M., Franklin, W.A. (1993). Exonuclease I of Escherichia coli removes phosphoglycolate 3'-end groups from DNA. *Radiation research.* ***135(2)***, 229-233.

(111) Sandigursky, M., Franklin, W.A. (1998). Exonuclease IX of Escherichia coli removes 3' phosphoglycolate end groups from DNA. *Radiation research.* ***150(6)***, 609-611.

(112) Murata-Kamiya, N., Kamiya, H., Kaji, H., Kasai, H. (2000). Mutations induced by glyoxal and methylglyoxal in mammalian cells. *Nucleic acids symposium series* ***44***, 3-4.

(113) Murata-Kamiya, N., Kamiya, H., Kaji, H., Kasai, H. (1997). Glyoxal, a major product of DNA oxidation, induces mutations at G:C sites on a shuttle vector plasmid replicated in mammalian cells. *Nucleic Acids Res.* ***25***, 1897-1902.

(114) Demple, B., Johnson, A., Fung, D. (1986). Exonuclease III and endonuclease IV remove 3' blocks from DNA synthesis primers in H2O2-damaged Escherichia coli. *Proceedings of the National Academy of Sciences of the United States of America.* ***83(20)***, 7731-7735.

(115) Pouget, J.P., Ravanat, J.L., Douki, T., Richard, M.J., Cadet, J. (1999). Measurement of DNA base damage in cells exposed to low doses of gamma-radiation: comparison between the HPLC-EC and comet assays. *Int J Radiat Biol* ***75***, 51-58.

(116) Epe, B., Pflaum, M., Boiteux, S. (1993). DNA damage induced by photosensitizers in cellular and cell-free systems. *Mutation research.* ***299(3-4)***, 135-145.

(117) Ide, H., Akamatsu, K., Kimura, Y., Michiue, K., Makino, K., Asaeda, A., Takamori, Y., Kubo, K. (1993). Synthesis and damage specificity of a novel probe for the detection of abasic sites in DNA. *Biochemistry* ***32***, 8276-8283.

(118) Kubo, K., Ide, H., Wallace, S.S., Kow, Y.W. (1992). A novel, sensitive, and specific assay for abasic sites, the most commonly produced DNA lesion. *Biochemistry* ***31***, 3703-3708.

(119) Atamna, H., Cheung, I., Ames, B.N. (2000). A method for detecting abasic sites in living cells: age-dependent changes in base excision repair. *Proc Natl Acad Sci U S A* ***97***, 686-691.

(120) Le, X.C., Xing, J.Z., Lee, J., Leadon, S.A., Weinfeld, M. (1998). Inducible repair of thymine glycol detected by an ultrasensitive assay for DNA damage. *Science* ***280***, 1066-1069.

(121) Poirier, M.C. (1994). Human exposure monitoring, dosimetry, and cancer risk assessment: the use of antisera specific for carcinogen-DNA adducts and carcinogen-modified DNA. *Drug metabolism reviews* ***26***, 87-109.

(122) Poirier, M.C. (1993). Antisera specific for carcinogen-DNA adducts and carcinogen-modified DNA: applications for detection of xenobiotics in biological samples. *Mutation research.* ***288(1)***, 31-38.
(123) Frelon, S., Douki, T., Ravanat, J.L., Pouget, J.P., Tornabene, C., Cadet, J. (2000). High-performance liquid chromatography--tandem mass spectrometry measurement of radiation-induced base damage to isolated and cellular DNA. *Chemical research in toxicology.* ***13(10)***, 1002-1010.
(124) Weinfeld, M., Soderlind, K.J. (1991). 32P-postlabeling detection of radiation-induced DNA damage: identification and estimation of thymine glycols and phosphoglycolate termini. *Biochemistry* ***30***, 1091-1097.
(125) Weinfeld, M., Buchko, G.W. (1993). Postlabeling methods for the detection of apurinic sites and radiation- induced DNA damage. *IARC Sci Publ* ***124***, 95-103.
(126) Pouget, J.P., Frelon, S., Ravanat, J.L., Testard, I., Odin, F., Cadet, J. (2002). Formation of modified DNA bases in cells exposed either to gamma radiation or to high-LET particles. *Radiation research.* ***157(5)***, 589-595.
(127) Douki, T., Delatour, T., Paganon, F., Cadet, J. (1996). Measurement of oxidative damage at pyrimidine bases in gamma-irradiated DNA. *Chemical research in toxicology.* ***9(7)***, 1145-1151.
(128) Berger, M., Anselmino, C., Mouret, J.-F., Cadet, J. (1990). High performance liquid chromatography-electrochemical assay for monitoring the formation of 8-oxo-7,8-dihydroadenine and its related 2'-deoxyribonucleoside. *Journal of liquid chromatography* ***13***, 929-940.
(129) Wagner, J.R., Hu, C.C., Ames, B.N. (1992). Endogenous oxidative damage of deoxycytidine in DNA. *Proceedings of the National Academy of Sciences of the United States of America.* ***89(8)***, 3380-3384.
(130) Fang, A.H., Smith, W.A., Vouros, P., Gupta, R.C. (2001). Identification and characterization of a novel benzo[a]pyrene-derived DNA adduct. *Biochem Biophys Res Commun* ***281***, 383-389.
(131) Douki, T., Court, M., Sauvaigo, S., Odin, F., Cadet, J. (2000). Formation of the main UV-induced thymine dimeric lesions within isolated and cellular DNA as measured by high performance liquid chromatography-tandem mass spectrometry. *The Journal of biological chemistry.* ***275(16)***, 11678-11685.
(132) Hall, E.J. (1994). Radiobiology for the radiologist, 4th Edition (Philadelphia: J.B. Lippincott).
(133) Bao, C.Y., Ma, A.H., Evans, H.H., Horng, M.F., Mencl, J., Hui, T.E., Sedwick, W.D. (1995). Molecular analysis of hypoxanthine phosphoribosyltransferase gene deletions induced by alpha- and X-radiation in human lymphoblastoid cells. *Mutation research.* ***326(1)***, 1-15.
(134) Little, J.B., Nagasawa, H., Pfenning, T., Vetrovs, H. (1997). Radiation-induced genomic instability: delayed mutagenic and cytogenetic effects of X rays and alpha particles. *Radiat Res* ***148***, 299-307.
(135) Sankaranarayanan, K. (1991). Ionizing radiation and genetic risks. II. Nature of radiation-induced mutations in experimental mammalian in vivo systems. *Mutation research.* ***258(1)***, 51-73.
(136) Thacker, J. (1986). The nature of mutants induced by ionizing radiation in cultured hamster cells. III. Molecular characterization of HPRT-deficient mutants

induced by gamma-rays or alpha-particles showing that the majority have deletions of all or part of the hprt gene. *Mutation research.* ***160(3)***, 267-275.

(137) Yandell, D.W., Dryja, T.P., Little, J.B. (1986). Somatic mutations at a heterozygous autosomal locus in human cells occur more frequently by allele loss than by intragenic structural alterations. *Somatic cell and molecular genetics.* ***12(3)***, 255-263.

(138) Evans, H.H., Mencl, J., Ricanati, M., Horng, M.F., Chaudhry, M.A., Jiang, Q., Hozier, J., Liechty, M. (1996). Induction of multilocus mutations at the Tk1 locus after X irradiation of L5178Y cells at different times in the mitotic cycle. *Radiation research.* ***146(2)***, 131-138.

(139) Amundson, S.A., Xia, F., Wolfson, K., Liber, H.L. (1993). Different cytotoxic and mutagenic responses induced by X-rays in two human lymphoblastoid cell lines derived from a single donor. *Mutation research.* ***286(2)***, 233-241.

(140) Li, C.Y., Yandell, D.W., Little, J.B. (1992). Molecular mechanisms of spontaneous and induced loss of heterozygosity in human cells in vitro. *Somatic cell and molecular genetics.* ***18(1)***, 77-87.

(141) Little, J.B. (2000). Radiation carcinogenesis. *Carcinogenesis* ***21***, 397-404.

(142) Grosovsky, A.J., de Boer, J.G., de Jong, P.J., Drobetsky, E.A., Glickman, B.W. (1988). Base substitutions, frameshifts, and small deletions constitute ionizing radiation-induced point mutations in mammalian cells. *Proceedings of the National Academy of Sciences of the United States of America.* ***85(1)***, 185-188.

(143) Schwartz, J.L., Rotmensch, J., Sun, J., An, J., Xu, Z., Yu, Y., Hsie, A.W. (1994). Multiplex polymerase chain reaction-based deletion analysis of spontaneous, gamma ray- and alpha-induced hprt mutants of CHO-K1 cells. *Mutagenesis.* ***9(6)***, 537-540.

(144) Shadley, J.D., Whitlock, J.L., Rotmensch, J., Atcher, R.W., Tang, J., Schwartz, J.L. (1991). The effects of radon daughter alpha-particle irradiation in K1 and xrs-5 CHO cell lines. *Mutation research.* ***248(1)***, 73-83.

(145) Schwartz, J.L., Ashman, C.R., Atcher, R.W., Sedita, B.A., Shadley, J.D., Tang, J., Whitlock, J.L., Rotmensch, J. (1991). Differential locus sensitivity to mutation induction by ionizing radiations of different LETs in Chinese hamster ovary K1 cells. *Carcinogenesis.* ***12(9)***, 1721-1726.

(146) Nikjoo, H., Uehara, S., Wilson, W.E., Hoshi, M., Goodhead, D.T. (1998). Track structure in radiation biology: theory and applications. *International journal of radiation biology.* ***73(4)***, 355-364.

(147) Kondo, S. (1999). I. Evidence that there are threshold effects in risk of radiation. *Journal of nuclear science and technology* ***36***, 1-9.

(148) Wickliffe, J.K., Bickham, A.M., Rodgers, B.E., Chesser, R.K., Phillips, C.J., Gaschak, S.P., Goryanaya, J.A., Chizhevsky, I., Baker, R.J. (2003). Exposure to chronic, low-dose rate gamma-radiation at Chernobyl does not induce point mutations in Big Blue mice. *Environmental and molecular mutagenesis.* ***42(1)***.

(149) Kirsch-Volders, M., Aardema, M., Elhajouji, A. (2000). Concepts of threshold in mutagenesis and carcinogenesis. *Mutation research.* ***464(1)***, 3-11.

(150) Sinclair, W.K. (1998). The linear no-threshold response: Why not linearity? *Med. Phys.* ***25***, 285-290.

(151) Schwartz, J.L., Jordan, R., Sun, J., Ma, H., Hsieb, A.W. (2000). Dose-dependent changes in the spectrum of mutations induced by ionizing radiation. *Radiat Res **153***, 312-317.
(152) Evans, H.H., Nielsen, M., Mencl, J., Horng, M.F., Ricanati, M. (1990). The effect of dose rate on X-radiation-induced mutant frequency and the nature of DNA lesions in mouse lymphoma L5178Y cells. *Radiation research. **122(3)***, 316-325.
(153) Nagasawa, H., Little, J.B., Tsang, N.M., Saunders, E., Tesmer, J., Strniste, G.F. (1992). Effect of dose rate on the survival of irradiated human skin fibroblasts. *Radiation research. **132(3)***, 375-379.
(154) Huo, L., Nagasawa, H., Little, J.B. (2001). HPRT mutants induced in bystander cells by very low fluences of alpha particles result primarily from point mutations. *Radiation research. **156(5) Pt 1***, 521-525.
(155) Vilenchik, M.M., Knudson, A.G., Jr. (2000). Inverse radiation dose-rate effects on somatic and germ-line mutations and DNA damage rates. *Proceedings of the National Academy of Sciences of the United States of America. **97(10)***, 5381-5386.
(156) Amundson, S.A., Chen, D.J. (1996). Inverse dose-rate effect for mutation induction by gamma-rays in human lymphoblasts. *International journal of radiation biology. **69(5)***, 555-563.
(157) Bonner, W.M. (2003). Low-dose radiation: thresholds, bystander effects, and adaptive responses. *Proceedings of the National Academy of Sciences of the United States of America. **100(9)***, 4973-4975.
(158) Rigaud, O., Moustacchi, E. (1996). Radioadaptation for gene mutation and the possible molecular mechanisms of the adaptive response. *Mutation research. **358(2)***, 127-134.
(159) Sawant, S.G., Randers-Pehrson, G., Metting, N.F., Hall, E.J. (2001). Adaptive response and the bystander effect induced by radiation in c3h 10t(1/2) cells in culture. *Radiat Res **156***, 177-180.
(160) Wolff, S. (1996). Aspects of the adaptive response to very low doses of radiation and other agents. *Mutation research. **358(2)***, 135-142.
(161) de Boer, J.G., Erfle, H., Walsh, D., Holcroft, J., Provost, J.S., Rogers, B., Tindall, K.R., Glickman, B.W. (1997). Spectrum of spontaneous mutations in liver tissue of lacI transgenic mice. *Environmental and molecular mutagenesis. **30(3)***.
(162) Cooke, M.S., Evans, M.D., Dizdaroglu, M., Lunec, J. (2003). Oxidative DNA damage: mechanisms, mutation, and disease. *The FASEB journal : official publication of the Federation of American Societies for Experimental Biology. **17(10)***, 1195-1214.
(163) Toyokuni, S., Okamoto, K., Yodoi, J., Hiai, H. (1995). Persistent oxidative stress in cancer. *FEBS letters. **358(1)***, 1-3.
(164) Ohshima, H., Tatemichi, M., Sawa, T. (2003). Chemical basis of inflammation-induced carcinogenesis. *Archives of biochemistry and biophysics. **417(1)***, 3-11.
(165) Bjelland, S., Seeberg, E. (2003). Mutagenicity, toxicity and repair of DNA base damage induced by oxidation. *Mutation research. **531(1-2)***, 37-80.
(166) DeMarini, D.M., Brockman, H.E., de Serres, F.J., Evans, H.H., Stankowski, L.F., Jr.;, Hsie, A.W. (1989). Specific-locus mutations induced in eukaryotes

(especially mammalian cells) by radiation and chemicals: a perspective. *Mutation research.* ***220(1)***, 11-29.

(167) Clayson, D.B., Mehta, R., Iverson, F. (1994). International Commission for Protection Against Environmental Mutagens and Carcinogens. Oxidative DNA damage--the effects of certain genotoxic and operationally non-genotoxic carcinogens. *Mutation research.* ***317(1)***, 25-42.

(168) E.S.C.o.O.D.D. (2002). Comparative analysis of baseline 8-oxo-7,8-dihydroguanine in mammalian cell DNA, by different methods in different laboratories: an approach to consensus. *Carcinogenesis.* ***23(12)***, 2129-2133.

(169) Greenberg, M.M. (2004). In vitro and in vivo effects of oxidative damage to deoxyguanosine. *Biochemical Society Transactions* ***32***, 46-50.

(170) Olinski, R., Gackowski, D., Rozalski, R., Foksinski, M., Bialkowski, K. (2003). Oxidative DNA damage in cancer patients: a cause or a consequence of the disease development? *Mutation research.* ***531(1-2)***, 177-190.

(171) Marnett, L.J. (2000). Oxyradicals and DNA damage. *Carcinogenesis* ***21***, 361-370.

Chapter II

Development of a Method to Quantify 3'-Phosphoglycolaldehyde Residues in Oxidized DNA

1. ABSTRACT

Toward the goal of quantifying deoxyribose oxidation chemistry in cells, a method is reported for the quantification of 3'-phosphoglycolaldehyde (PGA) residues. The method exploits the aldehyde moiety in PGA by derivatization as a stable oxime with pentafluorobenzylhydroxylamine (PFBHA), followed by solvent extraction and gas chromatography/negative chemical ionization/mass spectrometry. A stable isotopically-labeled [$^{13}C_2$]-PGA is synthesized and used as an internal standard. The assay shows a linear response over the range of 30 fmol to 300 pmol and its precision is verified by analysis of a synthetic, PGA-containing oligodeoxynucleotide. The limit of detection in the presence of DNA is 30 fmol per sample, corresponding to 2 molecules of PGA in 10^6 nucleotides for 170 μg of DNA.

2. INTRODUCTION

As reviewed in Chapter I, oxidation of deoxyribose in DNA produces a variety of electrophilic products unique to each position in the sugar. However, the spectrum of lesions has not been fully defined nor have the various pathways been quantified fully *in vitro*, much less so in cells and tissues. It is important to define and quantify these lesions in cells not only to understand the chemistry relevant to the cellular environment, but also to define the mechanistic links between oxidative stress, DNA damage and the cellular responses. One of the goals of this thesis was to develop a general analytical approach to quantify deoxyribose oxidation products arising in isolated DNA and in cells. As both a proof of principle and a means to study a poorly characterized deoxyribose oxidation product, a GC/MS method was developed to quantify the phosphoglycolaldehyde residue arising from C3' oxidation of deoxyribose in DNA. This lesion has so far only been qualitatively detected using a rather unspecific gel shift assay *(1)*. Therefore, we decided to develop a technique for the specific detection and quantification of PGA, which is also capable of detecting all carbonyl containing dR oxidation products. The application of this method to quantify PGA caused by γ- and α-radiation, iron and peroxynitrite is presented in Chapters III-VI.

As shown in Figure II-1, the approach taken to develop an analytical method for deoxyribose oxidation products exploits the reaction of hydroxylamine compounds with carbonyl residues in the damage product to form stable oximes (see for example *2-6*). Oxyamines are a well known reagent to convert aldehyde and ketone carbonyl groups to

stable oximes that can be detected by GC/MS (see for example *(7)*). Carboxylic acids can also be derivatized by oxyamines after activation with carbodiimides *(8)*. The strategy is as follows: oxidized DNA is digested with nuclease P1, followed by derivatization of carbonyl groups using pentafluorobenzylhydroxylamine (PFBHA; *e.g.*, refs. *9-11*). The resulting oximes are selectively extracted into organic solvent under conditions of acidic pH in which the hydroxylamine nitrogen and phosphate oxygens are protonated. The phosphate oxygens are then silylated using *bis*(trimethylsilyl)trifluoroacetamide (BSTFA, $CF_3[=NSi(CH_3)_3]OSi(CH_3)_3$) and the products are quantified by isotope dilution mass spectrometry following resolution by gas chromatography.

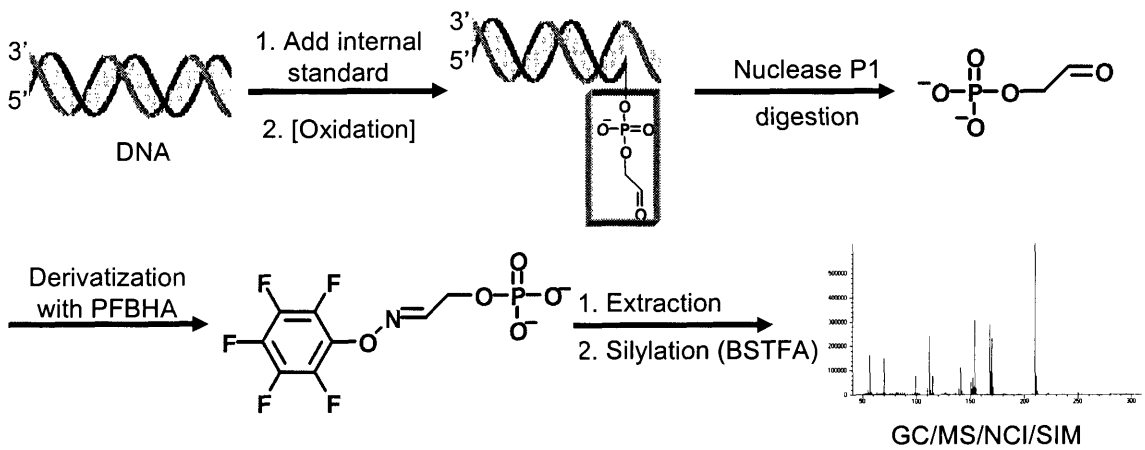

Figure II-1: General approach to quantify PGA and other deoxyribose oxidation products in DNA.

For PGA, the MS analysis is performed with negative chemical ionization, which was empirically determined to provide the strongest signal. The choice to leave the phosphate group on the glycolaldehyde residue was based on the ubiquitous presence of glycolaldehyde, glycolic acid and other analogs of deoxyribose oxidation as

contaminants. The development of this method was facilitated by synthesis of [$^{13}C_2$]-PGA for use as an internal standard and of a PGA-containing oligodeoxynucleotide as a positive control for method verification.

3. EXPERIMENTAL PROCEDURES

3.1 Materials. All chemicals and reagents were of the highest purity available and were used without further purification unless noted otherwise. Alkaline phosphatase, pentafluorobenzylhydroxylamine, *bis*(trimethylsilyl)trifluoroacetamide (containing 1% trimethylchlorosilane) and nuclease P1 were purchased from Sigma Chemical Co. (St. Louis, MO). Ethylacetate was purchased from Mallinckrodt Baker (Phillipsburg, NJ). Distilled and deionized water, further purified with a Milli-Q system (Millipore Corporation, Bedford, MA), was used in all experiments.

3.2 Instrumental Analyses. GC/MS analyses of derivatized PGA were performed with a HP6890 gas chromatograph (HP7673 auto-injector) coupled to a Hewlett Packard 5973N mass selective detector. UV spectra were obtained using a Beckman DU 640 UV-visible spectrophotometer. NMR studies of ^{1}H and ^{31}P were performed on a Varian 300 NMR spectrometer and of ^{13}C on a Varian Inova-500 NMR spectrometer. Scintillation counting was performed on a Beckman LS6000SC liquid scintillation counter.

3.3 Synthesis of PGA (performed by Dr. Mohammad Awada). PGA was synthesized as described elsewhere *(12)*. Briefly, D,L-glycerol phosphate was oxidized with sodium periodate at ambient temperature and pH 6 (HCl) for 1.5 h. Following consumption of unreacted periodate with ethylene glycol, the pH was readjusted to 7.0 with NaOH, $BaCl_2$ was added to precipitate iodate and the barium salt of 2-phosphoglycolaldehyde was precipitated with ethanol. Solvent was removed under vacuum and the barium ions were exchanged by passing the aqueous resuspension over a column of Dowex AG50X8 (H^+ form, BioRad). The pH of the solution was then readjusted to 7.0 with NaOH and the solution was stored at -80°C. ^1H NMR (D_2O): δ 5.18 (t, 1, H_1); 3.88 (m, 2, H_2); ^{13}C NMR: δ 90.7 (C-1), 68.2 (C-2), GC/MS/PCI: MH^+ 490.

3.4 Synthesis of [$^{13}C_2$]-PGA (performed by Dr. Mohammad Awada). [$^{13}C_2$]–Glycolaldehyde (Omicron; 1.6 mmol) was added to 10 mL of a solution of amidotriphosphate (1 M; prepared in the dark according to ref. *(13)*) and magnesium chloride (0.68 mM) with stirring to dissolve the salts. The reaction was allowed to proceed in the dark at ambient temperature and monitored every 24 h by thin layer chromatography (TLC; PGA as a standard; developed with 50:5:1 isopropanol/water/acetic acid and visualized with anisealdehyde solution). After 4 d, the product was purified by flash chromatography on a Silica Gel 60 column (2 x 15 cm) preconditioned with 200 ml of 50:5:1 isopropanol/water/acetic acid, washed after sample application with 500 ml of the same solvent, and eluted with 50:20:1 isopropanol/water/acetic acid. Fractions containing PGA (established by TLC) were

pooled and acetic acid removed by repeated drying of aqueous resuspensions under vacuum (five times). The dried product was taken up in 25 ml of water and the pH adjusted to 7 with NaOH. Unreacted amidotriphosphate was precipitated by addition of $BaCl_2$ to 0.3 M (-80 °C, 15 min) and centrifugation at 1100 x g for 1 min. The barium salt of PGA in the supernatant was precipitated with ethanol (4 volumes; -80 °C, 15 min). Following centrifugation (1100 x g, 5 min), the precipitate was dried, redissolved in water and Ba^{+2} removed with Dowex AG 50W X2 resin (0.4 g). The solution was filtered and neutralized with 1 N NaOH and the resulting disodium salt of PGA was dried and stored at –80 °C (20% yield). ^{1}H NMR (D_2O): δ 5.2 (t, 1, H_1), 3.2 (m, 2, H_2). ^{13}C NMR: δ 90.3 (d, 1, C-1), 67.7 (d, 1, C-2). ^{31}P NMR (D_2O): δ -21.

3.5 Synthesis of a 3'-PGA-containing oligodeoxynucleotide. A 16-mer oligodeoxynucleotide (TGACTAGGGCCCGCAG) containing a 3'-PGA residue was prepared from the corresponding 3'-phosphoglycerol-ended oligodeoxynucleotide (synthesized by Glen Research) by a published method *(14)*. Briefly, the 3'-phosphoglycerol-ended oligodeoxynucleotide was oxidized with $NaIO_4$ at 0 °C. The reaction was quenched with L-methionine and the oligodeoxynucleotide was purified on a NAP-25 Column (Amersham Biosciences). The final product was characterized by chemical sequencing and the presence of 3'-PGA was verified by sequencing gel analysis of the $NaBH_4$-reduced and NaClO-oxidized oligodeoxynucleotide as described elsewhere *(15)*. The product was stored at –80 °C.

3.6 Determination of the concentrations of PGA standards. The quantitative nature of these studies required rigorous determination of the absolute concentrations of PGA, [$^{13}C_2$]-PGA and the PGA-containing oligodeoxynucleotide. To this end, the concentrations of the PGA and [$^{13}C_2$]-PGA standards were determined by [^{1}H]-NMR spectroscopy relative to a known amount of dimethylsulfoxide. Independently, concentrations of phosphate in PGA and [$^{13}C_2$]-PGA stock solutions were determined by a modification of the chromogenic phosphate assay of Hergenrother and Martin *(16)*. Briefly, PGA (2.5 nmol) was treated with alkaline phosphatase (1.5 U) in 0.2 mL of buffer (10 mM Tris-HCl, 10 mM $MgCl_2$, 50 mM NaCl, 1 mM DTT, pH 7.9) for 1 h at 37 °C and the liberated phosphate was quantified adapting a chromogenic assay developed by Hergenrother *et al. (16)*. Phosphate was converted to a blue complex by reaction with ammonium molybdate in the presence of 10.5% ascorbic acid in 37% aqueous trichloroacetic acid; and sodium metaarsenite, in 2% trisodium citrate and 2% acetic acid. Solutions were prepared on the day of the assay. Phosphate was quantified using absorption measurements at 700 nm. Blanks contained no PGA but were treated identically. A calibration curve was obtained by using 0.1 – 10 nmol anhydrous monobasic potassium phosphate. Assays were performed in triplicate in two independent experiments.

The aldehyde content of the PGA-containing oligodeoxynucleotide was determined by oxime derivatization with [^{14}C]-labeled methoxylamine. Solutions containing oligodeoxynucleotide (4.4 nmol based on absorbance at 260 nm), 8 mM methoxylamine and 0.8 mM [^{14}C]-methoxylamine (0.55 Ci/mol; Moravek Biochemicals,

Brea, CA) in 50 mM potassium phosphate, 200 mM sodium borate buffer (pH 7.4) were incubated for 30 min at 37 °C. Unreacted methoxylamine was removed by two successive passages over G-25 Spin Columns (Pharmacia) and the concentration of the oligodeoxynucleotide was determined spectroscopically (260 nm). The quantity of [^{14}C]-label was determined by liquid scintillation counting. Assays were performed in triplicate including controls consisting of an oligodeoxynucleotide of identical sequence but lacking the 3'-PGA. It was determined that the aldehyde content of the oligodeoxynucleotide was 87%.

3.7 GC/MS analysis of PGA in the oligodeoxynucleotide. Following empirical optimization, the GC/MS method to quantify PGA in DNA was assessed with the PGA-containing oligodeoxynucleotide as follows. 500 µl samples were prepared that contained 1-100 pmol of PGA-containing oligodeoxynucleotide, 0-99 pmol of an oligodeoxynucleotide of identical sequence but lacking the PGA moiety (to produce a total of 100 pmol oligodeoxynucleotide), and 200 pmol of [$^{13}C_2$]-PGA as internal standard. The DNA was hydrolyzed with nuclease P1 (10 U; 16 µL of 2 mg/ml; 37 °C, 90 min) following addition of 55 µl of 1 M sodium acetate solution, pH 5.5 (0.1 M final concentration), 2 mM $ZnCl_2$ (0.2 mM final concentration) and 0.54 M HCl (to adjust pH to 5.5). Aldehyde and ketone moieties were converted to their oxime derivatives by addition of 50 µl of a freshly-prepared 80 mM PFBHA solution followed by adjustment of the pH to 3 with 5 µl of 6 N HCl and incubation at ambient temperature for 15 min. The pH was again adjusted to 0 by addition of 4 µl of 6 N HCl and the aqueous phase was extracted three times with 400 µl volumes of ethylacetate. The residue from the

pooled organic phases, dried under vacuum, was taken up in 30 µl of a 1:1 mixture of ethylacetate and BSTFA (containing 1% trimethylchlorosilane) and incubated at 70 °C for 1 h. After cooling at -80 °C for 10 min, samples were transferred to 2 ml screw-cap vials with 100 µl glass inserts and 1 µl was analyzed by GC/MS using negative chemical ionization (NCI) and selective ion monitoring (SIM) with the following conditions: 250 °C inlet (splitless mode); HP 19091S-433 HP-5MS 5% phenyl methyl siloxane column, 250 µm diameter, 30 m length and 0.25 µm film thickness; helium carrier purge: 7.63 psi, 50 ml/min flow, 2 min purge time; helium flow rate, 1 ml/min; oven temperature: initial 50 °C for 1.5 min, 10 °C/min ramp to 310 °C, 5 min hold at 310 °C. Data was acquired by selective ion monitoring (SIM) at *m/z* values of 241, 298 and 300, after a 16 min solvent delay. Quantities of PGA-PFBHA were determined from the ratio of peak areas of PGA-PFBHA peak to the [$^{13}C_2$]-PGA-PFBHA as related to a standard curve derived from samples containing 0-100 pmol of PGA plus 200 pmol of [$^{13}C_2$]-PGA and 100 pmol of an oligodeoxynucleotide lacking the PGA moiety. Calibration samples were carried through all steps of the method described above, prepared in parallel to all other samples, and subjected to identical conditions; all samples were analyzed on the same day.

4. RESULTS

4.1 Synthesis and quantification of PGA, [$^{13}C_2$]-PGA and the PGA-containing oligodeoxynucleotide. PGA was synthesized following the literature procedure of Lee *et al. (12)* (see Scheme II-1). The synthesis of [$^{13}C_2$]-PGA was based on a literature procedure published by Krishnamurthy *et al.* using commercially available [$^{13}C_2$]-glycolaldehyde as starting material *(13)* (see Scheme II-2). The purification procedure was optimized by Dr. Mohammad Awada in our laboratory using flash chromatography. The purity of both standards was established using ^{1}H-NMR, ^{13}C-NMR, ^{31}P-NMR and GC/MS. Both standards were stored as aqueous solutions at -80°C. PGA was observed to decompose during attempts to obtain dry material using rotary evaporation. Lyophilization proved to be the method of choice if water-free material was needed for analysis. The concentrations of both standards had to be determined in a rigorous approach due to the quantitative nature of our studies. Concentrations of PGA and [$^{13}C_2$]-PGA were determined using ^{1}H-NMR spectroscopy relative to a known amount of dimethylsulfoxide. As an independent method, we adapted a chromogenic assay developed by Hergenrother *et al.* to determine the phosphate content in our standards *(16)*. ^{31}P-NMR analysis of both standards excluded the presence of contaminating inorganic phosphate was excluded, which justified the use of an assay to determine phosphate as a measure of PGA standard concentrations. In order to verify the quantitative dephosphorylation by alkaline phosphatase as used by Hergenrother *et al.* the difference in retention time of the PGA-oxime and glycolaldehyde-oxime in high-

pressure liquid chromatography was exploited. Both quantification methods were in very good agreement; the ^{1}H-NMR spectroscopy method revealed a PGA concentration of 1.1 ± 0.1 mM and the chromogenic phosphate assay indicated a concentration of 1.0 ± 0.09 mM.

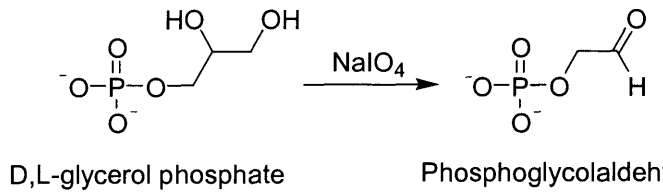

Scheme II-1: Synthesis of PGA as established by Lee *et al. (12)*.

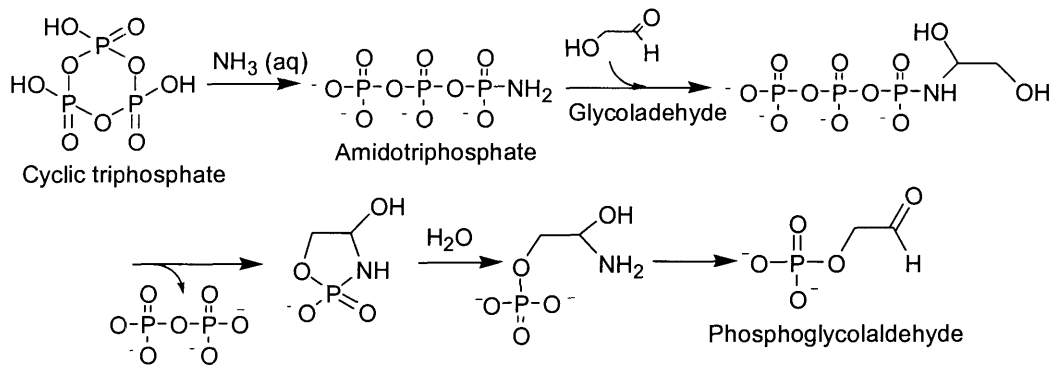

Scheme II-2: Synthesis of [$^{13}C_2$]-PGA as established by Krishnamurthy *et al. (12)*.

As a positive control and to prove the validity of our developed assay, an oligodeoxynucleotide containing a 3-phosphoglycolaldehyde residue was synthesized using a procedure developed by Junker *et al. (14)*. After synthesis of the 3'-phosphoglycerol-oligodeoxynucleotide, it was empirically determined that the oligodeoxynucleotide could not be dried by the commonly used method of speedvac concentration, due to decomposition of the glycerol moiety. As for the PGA standards,

lyophilization is the method of choice to dry the oligodeoxynucleotide. To determine the yield of PGA-containing oligodeoxynucleotide after sodium periodate cleavage of the 3'-phosphoglycerol-oligodeoxynucleotide, the resulting aldehyde was converted to an oxime using [^{14}C]-labeled methoxylamine. Scintillation counting of the purified oxime showed a yield of 83% of methoxylamine reactive material. To prove the presence of PGA in the oligodeoxynucleotide, Dr. Mohammad Awada used chemical sequencing *(15)*. The aldehyde was either oxidized with NaClO to glycolic acid or reduced with $NABH_4$ to a primary alcohol. The resulting oligodeoxynucleotides are shifted on a PAGE gel in comparison to the PGA-containing oligodeoxynucleotide and unmodified oligodeoxynucleotide. The oxidized oligodeoxynucleotide runs faster on the gel than PGA-containing oligodeoxynucleotide and the reduced oligodeoxynucleotide runs slower *(15)*.

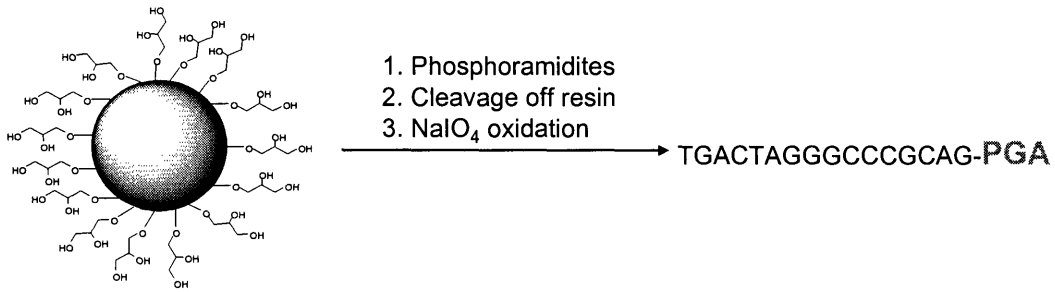

Scheme II-3: Synthesis of the PGA-containing oligodeoxynucleotide *(14)*.

4.2 Development and optimization of sample preparation steps. Given the potential for broad application of the assay for other deoxyribose oxidation products, particular attention was paid to optimizing the various steps involved in the PGA analytical method. The first step entails nuclease P1 digestion of the damaged DNA

which was taken from the published procedure from McGall *et al. (17)*. The PGA-containing oligodeoxynucleotide was used to demonstrate that the nuclease P1 treatment under the conditions used by McGall *et al.* went to completion *(17)*. Variations of incubation times and enzyme concentrations showed no difference in PGA recovery, therefore the original procedure of McGall was used in all experiments.

The next step was to optimize the oximation reaction. The optimal conditions for the oximation reaction with PFBHA were found to consist of a 15 min reaction at pH 2 at ambient temperature. No difference in yield was observed for temperatures up to 75 °C and for times ranging from 15 to 60 min, so a 15 min incubation at ambient temperature was chosen to minimize adventitious DNA oxidation and the slow conversion of phosphoglycolaldehyde to glyoxal *(18)*. The yield of the oximation reaction has been shown to be quantitative over the pH range of 2 to 7, with a decrease evident at pH 8 (*e.g.*, refs. *19, 20*). The choice of pH for our work was arbitrary.

The final optimization steps involved extraction and silylation of the PGA-oxime derivative. Solvent extraction to purify the PFBHA oxime was found to be more efficient and less problematic than HPLC pre-purification, with the latter complicated by sample carry-over in the injector. Extraction of the PFBHA oxime of PGA into ethyl acetate was carried out at pH 0 (to neutralize the negative charge on the phosphate in the derivative and to maximize the positive charge on the unreacted PFBHA). Quantitative recovery of PGA from the PGA-containing oligodeoxynucleotide under these conditions shows that the PGA-oxime is stable under these conditions. Subsequent drying of the extracts under vacuum was found to produce a lower background signal, in comparison to removing

traces of water in the ethyl acetate extracts with magnesium sulfate. Finally, the efficiency of silylation of the phosphate oxygens was found to proceed optimally in a 60 min reaction with ethyl acetate present (50% reduction in the absence of ethyl acetate) and at 70 °C (50% and 90% reductions at 50 °C and 90 °C, respectively).

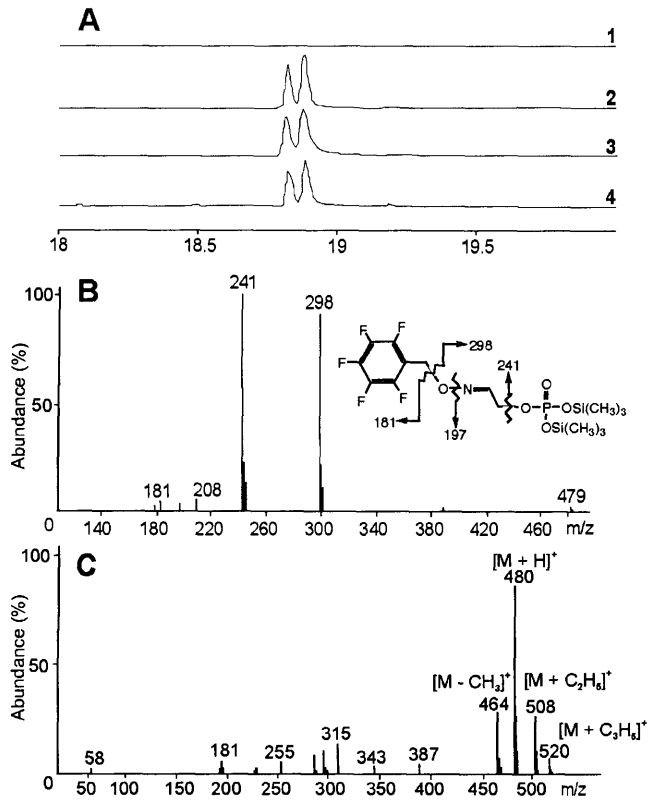

Figure II-2: Chromatographic and mass spectral data for the PGA-PFBHA oxime. **(A)** GC chromatograms of the *cis* and *trans* oxime isomers of **(1)** a blank sample containing calf thymus DNA, **(2)** synthetic PGA, **(3)** the oligodeoxynucleotide containing PGA and **(4)** a sample of calf-thymus DNA γ-irradiated with 107 Gy. All samples were subjected to the entire analytical method described in section 3.7 in this Chapter. **(B)** Mass spectrum of the silylated PGA-PFBHA oxime using negative chemical ionization and **(C)** positive chemical ionization.

4.3 Optimization of the GC/MS analysis of PGA. The reaction of PGA with PFBHA leads to *E*- and *Z*-isomers about the oxime bond (see Scheme II-4), isomers that produced two signals in the GC/MS chromatograms, as shown in Figure II-2A. Both species could be used to quantify the oxime in PCI mode. However, given the limited sensitivity achieved with PCI (5 pmol detection limit compared to 30 fmol with NCI; *vide infra*), NCI was selected in spite of the fact that it resulted in complete fragmentation of the second, later-eluting species with loss of the [^{13}C] labels.

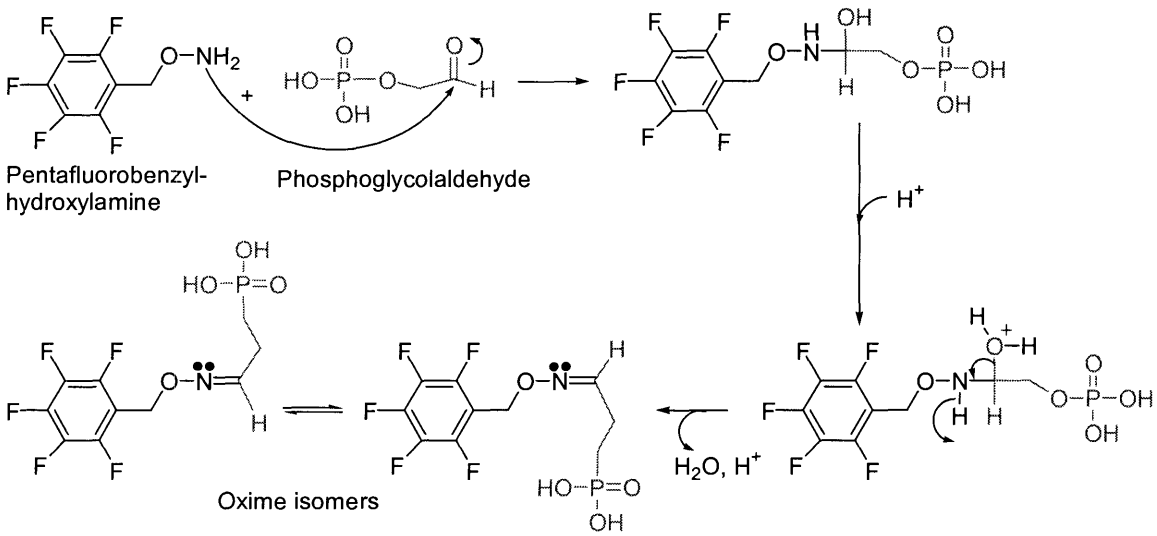

Scheme II-4: Reaction of PGA with PFBHA.

Because the internal standard and the analyte differ by only two mass units, we investigated the degree of signal carryover due to isotope natural abundance and fragmentation. The silylated PFBHA oxime of [$^{13}C_2$]-PGA was found to produce no M-2 ions, even at very high concentrations, while the M+2 signal arising from the same form of unlabeled PGA was found to contribute 9% of the analyte peak area to the internal standard. The latter result correlates very well with the calculated value of 9.1% using

known natural abundances of ^{13}C, ^{17}O, ^{18}O and ^{30}Si *(21)*. All data were corrected for the 9% M+2 contribution of the analyte to the internal standard.

As shown in Figure II-2C, the mass spectrum of silylated PGA-PFBHA in PCI mode exhibits the molecular ion *m/z* 480 ($M+H^+$), and characteristic PCI ions *m/z* 464 ($M-CH_3$), 508 ($M+C_2H_5$) and 520 ($M+C_3H_6$). The molecular anion *m/z* 479 (M^-) in the NCI mass spectrum is weakened as a result of fragmentation (Figure II-2B) and was insufficient for quantitative studies. However, the structurally important ion *m/z* 298 (M–pentafluorobenzyl), a signal characteristic of PFBHA oximes *(22)*, preserves the isotopic labels in the analyte and internal standard and can be used for quantitative purposes. Interestingly, this fragment ion was apparent only for the earlier eluting of the *E* and *Z* isomer peaks in the GC chromatogram, with the later eluting peak producing a prominent signal at *m/z* 241. We therefore used the earlier eluting peak for quantification of PGA. While the signals at *m/z* 241, 197 and 181 (all characteristic signals of PFBHA) did not contain structural features that distinguished between internal standard and analyte, the strong signal at *m/z* 241 served as a qualifying ion to ensure the identity of PGA. The isotope labeled standard had the same fragmentation pattern, with an additional two mass units for the *m/z* 298 (M–pentafluorobenzyl) ion due to the two ^{13}C labels.

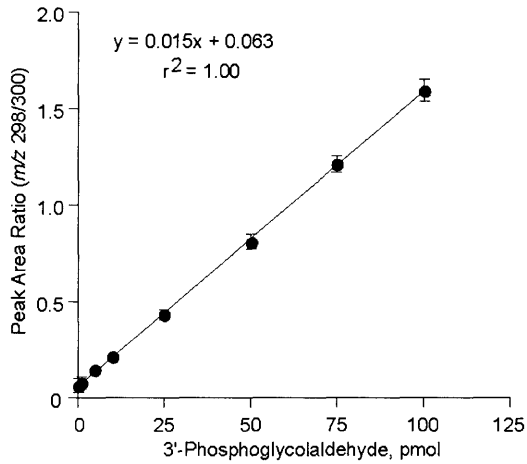

Figure II-3: Calibration curve for the GC/NCI/MS analysis of PGA. Samples containing 200 pmol of [$^{13}C_2$]-PGA, 0-100 pmol of PGA and 170 μg of calf thymus DNA were analyzed as described in Experimental Procedures. The data represent mean ± S.D. for five independent experiments; X-axis values represent PGA in the 30 μl resuspension of which 1 μl was used for analysis.

4.4 Calibration of the GC/MS assay. Figure II-3 shows the results from experiments in which known quantities of PGA (0–100 pmol) were added to a fixed amount of [$^{13}C_2$]-PGA (200 pmol) and 170 μg calf thymus DNA in a total volume of 500 μl (50 mM potassium phosphate buffer, pH 7.4). Following nuclease P1 digestion, the samples were subjected to PFBHA derivatization, extraction, silylation and GC/MS analysis in SIM (*m/z* 241, 298 and 300). Excellent linearity was observed (r^2 = 1.00) in the relationship between the quantity of PGA added and the ratio of the area of the PGA signal (*m/z* 298) to the area of the [$^{13}C_2$]-PGA signal (*m/z* 300). The calibration curve does not pass through the origin due to the presence of a contaminant(s) introduced during sample work up. The contaminant(s), with the same retention times as both of the PGA derivatives, was consistently observed for *m/z* 298 and produced a signal

corresponding to a peak area ratio of 0.0628. This is equivalent to 140 fmol of PGA in 170 μg of DNA or 8 PGA residues per 10^6 nt. The calf thymus DNA employed for these studies accounted for most of this signal, with a small portion of the contaminant (equivalent to ~ 0.1 PGA per 10^6 nt) traced to the potassium phosphate buffer and to HCl solutions. All PGA analyses were corrected for this background using the calibration curve.

Closer examination of Figure II-3 also unexpectedly revealed that the unlabeled PGA standard generates a stronger signal than [$^{13}C_2$]-labeled PGA. For example, a peak area ratio (*m/z* 298/300) of 1 in Figure II-3 corresponds to 0.0615 nmol of PGA and 0.2 nmol of [$^{13}C_2$]-PGA. There are several possible explanations for this phenomenon. The first involves incorrect determination of the concentrations of standards. This was ruled out by the fact that two independent approaches were used to define the concentrations (chromogenic phosphate assay and NMR), both of which were in excellent agreement (within 5%). Second, the oximation efficiency may differ for PGA and [$^{13}C_2$]-labeled PGA. Again, this seems unlikely in light of the fact that under the conditions chosen for present studies, the oximation is quantitative and the resulting oximes are stable.

The third and most likely explanation for the observed signal bias is an apparent difference in distribution of *E*- and *Z*-isomers formed during oximation of PGA and [$^{13}C_2$]-labeled PGA. While only one isomer is detected with SIM at *m/z* 298 or 300 as discussed above, both isomers are observed with SIM at *m/z* 241, with the earlier eluting peak corresponding to the signals detected in SIM at *m/z* 298 and 300. The peak area

ratios of the early-eluting isomer to the late-eluting isomer for *m/z* 241 were 0.43 (± 0.03) for unlabeled PGA analysis and 0.32 (± 0.01) for [$^{13}C_2$]-PGA. The distribution of oxime isomers for PGA was found to be concentration independent for all concentrations used in calibration. We do not know the basis for this phenomenon but there are several possible explanations, all involving ^{13}C isotope effects. These include a bias in the formation of the isomers; different ionization potentials for the oximes of PGA and [$^{13}C_2$]-PGA; different fragmentation patterns; or an instrument bias towards the detection of one mass versus the other. We do not know whether the observed distribution of isomers is the only contribution to the observed difference in signal intensity, which so far remains unresolved. However, this difference in signal strength between PGA and [$^{13}C_2$]-PGA is of no consequence for the validity of our quantitative results since we are using calibration curves to calculate the detected PGA concentration and the concentration of [$^{13}C_2$]-PGA is held constant for all analyses.

4.5 Assay precision, efficiency and detection limit. While the overall efficiency of PGA recovery could not be determined due to the lack of a [$^{13}C_2$]-PGA-PFBHA standard, the various steps in the assay were optimized as described earlier and control experiments with the PGA-containing oligodeoxynucleotide revealed the efficiency of the nuclease digestion step and the overall precision of the assay. As shown in Figure II-4, there was a strong correlation (97%) between the known and measured PGA levels in the oligodeoxynucleotide (slope = 0.97, r^2 = 1.0); this result also supports the quantification of the internal standard. Analysis of an oligodeoxynucleotide of the same sequence lacking a 3' modification showed no PGA signal above background (Figure II-

4). These findings reveal that the nuclease digestion step is virtually quantitative and that the assay is highly precise, at least for the DNA sequence of the oligodeoxynucleotide.

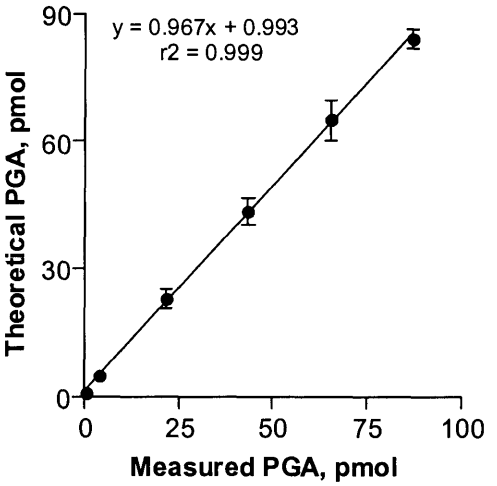

Figure II-4: Measured *versus* theoretical yields of PGA in a synthetic oligodeoxynucleotide. Varying amounts (1-100 pmol) of an oligodeoxynucleotide containing a 3'-PGA residue (or the same sequence lacking PGA) were subjected to PGA analysis as described in Experimental Procedures. Calculated PGA levels are based on the presence of 0.87 PGA residues per oligodeoxynucleotide molecule, as described in Experimental Procedures. The data represent mean ± SD for three independent experiments.

While the background signal accounted for 140 fmol of sample injected into the GC, we could reproducibly measure 30 fmol of PGA above this background, a level of PGA that resulted in at least a 3-fold signal-to-noise ratio. The determination of this detection limit was based on the measurement of the calibration sample with the lowest amount of PGA, which was 1 pmol. This constitutes a very conservative estimate, since 1 pmol of PGA was used for all analyses presented throughout Chapters II-VI. The

calibration sample has a total volume of 30 µl and only 1 µl of the sample is injected into the GC/MS, therefore resulting in a detection limit of 30 fmol. By definition, this calibration sample always contains 1 pmol of PGA, but the peak area ratio varies in this case by up to 40%. Injection reproducibility of the GC/MS autoinjector amounts to a variation of peak area of 10%, which is of no consequence due to the presence of the internal standard in the samples. It should be noted, that the reproducibility of peak areas and signal strength (meaning peak area) is strongly dependent on the buffer systems used. It was found that samples with high salt contents, such as the samples in bicarbonate buffer as discussed in Chapter V, exhibit increased peak area variation and a decrease in peak area of up to 3 orders of magnitude, when compared to samples in phosphate buffer.

5. DISCUSSION

In this thesis, we present a sensitive analytical method to quantify the lesion 3'-phosphoglycolaldehyde (PGA). The PGA residue is one of several that have been shown to have chemical and biological effects beyond the generation of a simple strand break, such as the reaction of base propenals to form the mutagenic M_1G adduct *(23, 24)* and the protein-DNA cross-linking at deoxyribonolactone lesions *(25, 26)*. In this case, phosphoglycolaldehyde residues give rise to the glyoxal adducts of dG in DNA *(18)*. PGA has been shown to form glyoxal by a novel radical-independent pathway and the glyoxal subsequently reacts with dG in DNA to form 1,N2- glyoxal adduct *(18)*.

The method presented here should be generally applicable to the various ketone and aldehyde residues arising from deoxyribose oxidation, the quantification of which would reveal the proportion of deoxyribose and base oxidation in cellular DNA as well as the spectrum of lesions arising in cells subjected to oxidative stress. PFBHA has been used by other groups to detect aldehydes and ketones in biological samples. For example, Loidl-Stahlhofen *et al.* used PFBHA derivatization to detect unknown hydroxyaldehydic lipid peroxidation products *(9)* and Tomita *et al.* used PFBHA to determine acetaldehyde levels in blood *(10)*. We optimized the oximation reaction with PFBHA for temperature, incubation time and optimal pH. Since there have been mixed reports about reproducibility issues with stored oximated samples *(27, 28)*, we performed the derivatization reactions and GC/MS analyses on the same day to minimize storage. Our GC/MS/NCI assay for PGA can reliably detect as little as 30 fmol and is linear up to 10 nmol, with the precision of the assay verified using a PGA-containing oligodeoxynucleotide. For the 170 μg DNA sample size used in these studies, the assay has a sensitivity of ~ 2 PGA per 10^6 nt, which can likely be increased by working with larger sample sizes.

The use of GC/MS for the measurement of oxidative DNA damage has undergone serious criticism due to previous overestimates of base damage caused by oxidation during silylation (*i.e.* references *29, 30*). As a result, it has been suggested that GC/MS is no longer useful for the accurate measurement of oxidative DNA damage unless HPLC prepurification is also used *(31)*. Dizdaroglu *et al.* discuss in detail the conditions of artifact formation and prevention in GC/MS and conclude that if care is taken to avoid

high temperatures during derivatization, GC/MS compares well with other methods, such as LC/MS/MS and HPLC/ECD, and offers greater sensitivity than LC/MS and LC/MS/MS *(32)*. Our procedure circumvents the problem of artifact formation by derivatizing the oxidative sugar damage to produce a stable oxime within 15 min at ambient temperature. As is apparent from the method validation that was undertaken using the PGA-containing oligodeoxynucleotide, artifact formation during the method described here can be excluded due to the strong correlation between PGA measured using the method and the known amount of PGA present in the oligodeoxynucleotide (see Figure II-4). The extraction step into ethylacetate serves as a prepurification and is faster than HPLC/GC-MS based methods. Another GC/MS method using a two step derivatization, including acetylation and pentafluorobenzylation, has been shown by Teixeira *et al.* to avoid artifactual oxidation *(33)*. Also, temperature has been shown to influence the amount of artifacts during silylation *(29)*, prompting us to use 70°C during our silylation procedure as opposed to 100°C as used by Douki *et al.* The possibility of introducing artifacts during enzymatic hydrolysis, which is currently used in GC/MS, HPLC-EC and HPLC-MS/MS methods, or the possibility of under-estimating the amount of DNA damage due to incomplete digestion, was ruled out by Douki *et al. (34)*.

REFFERENCES

(1) Sitlani, A., Long, E.C., Pyle, A.M., Barton, J.K. (1992). DNA Photocleavage by Phenanthrenequinone Diimine Complexes of Rhodium(III): Shape-Selective Recognition and Reaction. *J. Am. Chem. Soc* ***114***, 2303-2312.

(2) Coombs, M.M., Livingston, D.C. (1969). Reaction of apurinic acid with aldehyde reagents. *Biochim Biophys Acta* ***174***, 161-173.

(3) Kow, Y.W. (1989). Mechanism of action of Escherichia coli exonuclease III. *Biochemistry* ***28***, 3280-3287.

(4) Kow, Y.W., Dare, A. (2000). Detection of abasic sites and oxidative DNA base damage using an ELISA- like assay. *Methods* ***22***, 164-169.

(5) Hagen, S.R., Thompson, J.D., Snyder, D.S., Myers, K.R. (1997). Analysis of a monophosphoryl lipid A immunostimulant preparation from Salmonella minnesota R595 by high-performance liquid chromatography. *Journal of chromatography. A.* ***767(1-2)***, 53-61.

(6) Makrigiorgos, G.M., Chakrabarti, S., Mahmood, A. (1998). Fluorescent labeling of abasic sites: a novel methodology to detect closely-spaced damage sites in DNA. *Int J Radiat Biol* ***74***, 99-109.

(7) Hoffmann, G., Sweetman, L. (1987). O-(2,3,4,5,6-pentafluorobenzyl)oxime-trimethylsilyl ester derivatives for quantitative gas chromatographic and gas chromatographic-mass spectrometric studies of aldehydes, ketones and oxoacids. *J Chromatogr* ***421***, 336-343.

(8) Yasaka, Y., Tanaka, m. (1994). Labeling of free carboxyl groups. *Journal of Chromatography B* ***659***, 139-155.

(9) Loidl-Stahlhofen, A., Kern, W., Spiteller, G. (1995). Gas chromatographic-electron impact mass spectrometric screening procedure for unknown hydroxyaldehydic lipid peroxidation products after pentafluorobenzyloxime derivatization. *J. Chromatogr. B Biomed. Appl.* ***673***, 1-14.

(10) Tomita, M., Ijiri, I., Shimosato, K., Kawai, S. (1987). Simple and sensitive method for the determination of acetaldehyde in blood by gas chromatography. *J. Chromatogr.* ***414***, 454-459.

(11) Hsu, F.-F., Hazen, S.L., Giblin, D., Turk, J., Heineke, J.W., Gross, M.L. (1999). Mass Spectrometric Analysis of Pentafluorobenzyl Oxime Derivatives of Reactive Biological Aldehydes. *Intl. J. of Mass Spectrom.* ***185/186/187***, 795-812.

(12) Lee, L.V., Poyner, R.R., Vu, M.V., Cleland, W.W. (2000). Role of metal ions in the reaction catalyzed by L-ribulose-5-phosphate 4-epimerase. *Biochemistry* ***39***, 4821-4830.

(13) Krishnamurthy, R., Arrhenius, G., Eschenmoser, A. (1999). Formation of glycolaldehyde phosphate from glycolaldehyde in aqueous solution. *Orig. Life Evol. Biosph.* ***29***, 333-354.

(14) Junker, H.D., Hoehn, S.T., Bunt, R.C., Marathius, V., Chen, J., Turner, C.J., Stubbe, J. (2002). Synthesis, characterization and solution structure of tethered

oligonucleotides containing an internal 3'-phosphoglycolate, 5'- phosphate gapped lesion. *Nucleic Acids Res.* ***30***, 5497-5508.

(15) Awada, M., Dedon, P.C. (2001). Unit 10.8: Analysis of Oxidized DNA Fragments by Gel Electrophoresis. In Current Protocols in Nucleic Acid Chemistry, D. Bergstrom, ed. (New York: J. Wiley and Sons).

(16) Hergenrother, P.J., Martin, S.F. (1997). Determination of the kinetic parameters for phospholipase C (Bacillus cereus) on different phospholipid substrates using a chromogenic assay based on the quantitation of inorganic phosphate. *Anal. Biochem.* ***251***, 45-49.

(17) McGall, R., Lois E; , Ashley, G., Wu, S., Kozarich, J.W., Stubbe, J. (1992). New insight into the mechanism of base propenal formation during bleomycin-mediated DNA degradation. *J. Am. Chem. Soc.* ***114***, 4958-4967.

(18) Awada, M., Dedon, P.C. (2001). Formation of the 1,N2-glyoxal adduct of deoxyguanosine by phosphoglycolaldehyde, a product of 3'-deoxyribose oxidation in DNA. *Chem. Res. Toxicol.* ***14***, 1247-1253.

(19) Kobayashi, K., Tanaka, M., Kawai, S. (1980). Gas Chromatographic Determination of Low-Molecular-Weight Carbonyl Compounds in Aqueous Solution as Their O-(2,3,4,5,6-pentafluorobenzyl) Oximes. *J. Chrom.* ***187***, 413-417.

(20) Kobayashi, K., Fukui, E., Tanaka, M., Kawai, S. (1980). Gas Chromatographic Analysis of alpha-Keto Acids in Aqueous Solution as Theo-(2,3,4,5,6-pentafluorobenzyl)oximes of Their Methyl Esters. *J. Chrom.* ***202***, 93-98.

(21) Silverstein, R., Bassler, G., Morrill, T. (1974). Spectrometric Identification of Organic Compounds, 3rd Edition (New York: J Wiley & Sons).

(22) Thukkani, A.K., Hsu, F.F., Crowley, J.R., Wysolmerski, R.B., Albert, C.J., Ford, D.A. (2002). Reactive chlorinating species produced during neutrophil activation target tissue plasmalogens: production of the chemoattractant, 2-chlorohexadecanal. *J. Biol. Chem.* ***277***, 3842-3849.

(23) Dedon, P.C., Plastaras, J.P., Rouzer, C.A., Marnett, L.J. (1998). Indirect mutagenesis by oxidative DNA damage: formation of the pyrimidopurinone adduct of deoxyguanosine by base propenal. *Proc. Natl. Acad. Sci. USA* ***95***, 11113-11116.

(24) Plastaras, J.P., Dedon, P.C., Marnett, L.J. (2002). Effects of DNA structure on oxopropenylation by the endogenous mutagens malondialdehyde and base propenal. *Biochemistry* ***41***, 5033-5042.

(25) DeMott, M.S., Beyret, E., Wong, D., Bales, B.C., Hwang, J.T., Greenberg, M.M., Demple, B. (2002). Covalent trapping of human DNA polymerase beta by the oxidative DNA lesion 2-deoxyribonolactone. *J. Biol. Chem.* ***277***, 7637-7640.

(26) Hashimoto, M., Greenberg, M.M., Kow, Y.W., Hwang, J.T., Cunningham, R.P. (2001). The 2-deoxyribonolactone lesion produced in DNA by neocarzinostatin and other damaging agents forms cross-links with the base-excision repair enzyme endonuclease III. *J. Am. Chem. Soc.* ***123***, 3161-3162.

(27) Spaulding, R.S., Charles, M.J. (2002). Comparison of methods for extraction, storage, and silylation of pentafluorobenzyl derivatives of carbonyl compounds and multi-functional carbonyl compounds. *Anal. Bioanal. Chem.* ***372***, 808-816.

(28) Urbansky, E.T., Bashe, W.J. (2000). Comparative methodology in the determination of alpha-oxocarboxylates in aqueous solution ion chromatography versus gas chromatography after oximation, extraction and esterification. *J. Chromatogr. A* ***867***, 143-149.

(29) Douki, T., Delatour, T., Bianchini, F., Cadet, J. (1996). Observation and prevention of an artefactual formation of oxidized DNA bases and nucleosides in the GC-EIMS method. *Carcinogenesis.* ***17(2)***, 347-353.

(30) Ravanat, J.L., Turesky, R.J., Gremaud, E., Trudel, L.J., Stadler, R.H. (1995). Determination of 8-oxoguanine in DNA by gas chromatography--mass spectrometry and HPLC--electrochemical detection: overestimation of the background level of the oxidized base by the gas chromatography--mass spectrometry assay. *Chemical research in toxicology.* ***8(8)***, 1039-1045.

(31) Cadet, J., D'Ham, C., Douki, T., Pouget, J.P., Ravanat, J.L., Sauvaigo, S. (1998). Facts and artifacts in the measurement of oxidative base damage to DNA. *Free radical research.* ***29(6)***, 541-550.

(32) Dizdaroglu, M., Jaruga, P., Birincioglu, M., Rodriguez, H. (2002). Free radical-induced damage to DNA: mechanisms and measurement. *Free radical biology & medicine.* ***32(11)***, 1102-1115.

(33) Teixeira, A.J., Gommers-Ampt, J.H., Van de Werken, G., Westra, J.G., Stavenuiter, J.F., de Jong, A.P. (1993). Method for the analysis of oxidized nucleosides by gas chromatography/mass spectrometry. *Analytical biochemistry.* ***214(2)***, 474-483.

(34) Douki, T., Martini, R., Ravanat, J.L., Turesky, R.J., Cadet, J. (1997). Measurement of 2,6-diamino-4-hydroxy-5-formamidopyrimidine and 8-oxo-7,8-dihydroguanine in isolated DNA exposed to gamma radiation in aqueous solution. *Carcinogenesis.* ***18(12)***, 2385-2391.

Chapter III

Production of 3'-Phosphoglycolaldehyde Residues in DNA Exposed to γ- and α-Radiation

1. ABSTRACT

Deoxyribose oxidation in DNA represents a biologically important facet of oxidative DNA damage that gives rise to protein-DNA cross-links and base adducts. Toward the goal of quantifying deoxyribose oxidation chemistry in cells, we report here the quantification of 3'-phosphoglycolaldehyde (PGA) residues, which likely arise from C3'-oxidation of deoxyribose in DNA, induced by γ-radiation and α-particles. Samples were exposed to 0-100 Gy of ^{60}Co γ-radiation, which resulted in a linear dose-response of 1.5 PGA residues per 10^6 nucleotides per Gy and a radiation chemical yield (G-value) of 0.0016 μmol/J. When compared to the total quantity of deoxyribose oxidation (experiments performed by Mr. Xinfeng Zhou) occurring under the same conditions (141 oxidation events per 10^6 nucleotides per Gy; determined by plasmid topoisomer analysis), PGA formation occurs in 1% ± 0.02 of deoxyribose oxidation events. This small fraction is consistent with current models of limited solvent accessibility of the C3'-position of

deoxyribose, though partitioning of C3'-chemistry could lead to other damage products that would increase the fraction of oxidation at this site in deoxyribose. For α-particles, we found that the efficiency of PGA formation was 7% ± 0.5. This may indicate that direct radiation damage is more efficient at producing PGA lesions.

2. INTRODUCTION

Both the toxic and therapeutic effects of ionizing radiation likely involve damage to cellular proteins, lipids, carbohydrates, and, of particular interest here, nucleic acids *(1) (2)*. Cell killing, radiation mutagenesis, radiation carcinogenesis (see Chapter 1, sections 7.3 and 7.4) and genome instability are biological effects associated with radiation-induced DNA damage *(1)*. The therapeutic effect of radiation in cancer treatment is also believed to involve DNA damage *(2)*. Given the unspecific nature of the biological oxidation produced by ionizing radiation, both the nucleobases and deoxyribose moieties of DNA are subjected to oxidation. Toward the goal of defining the spectrum of DNA lesions produced by ionizing radiation, we have applied the PGA assay to DNA subjected to γ- and α-irradiation.

Radiation-induced deoxyribose damage generates a variety of diffusible electrophiles, covalently bound fragments and oxidized abasic sites, with a unique spectrum of products derived from each position in the sugar as discussed in Chapter I *(3, 4)*. γ-Radiation has been shown to induce oxidation at almost all deoxyribose positions with a variety of deoxyribose oxidation products as discussed in Chapter I. Briefly, γ-

radiation forms deoxyribonolactone (C1' oxidation) *(5, 6)*, the erythrose abasic site (C2' oxidation) *(7)*, malondialdehyde and phosphoglycolate (C4' oxidation) *(8, 9)*, 5',8-cyclopurine-2'-deoxyadenosine *(10)* and nucleoside-5'-aldehydes (C5' oxidation) *(11)*. So far the only evidence for C3' oxidation induced by radiation was produced by Debije *et al.*, who used electron paramagnetic resonance to prove the presence of a C3' radical in a crystalline duplex 11-mer oligodeoxynucleotide subjected to X-rays at 4 K *(12)*. Therefore the presence of PGA in γ-irradiated DNA is possible, if the partitioning of the C3' position in this case does not involve the sole formation of 2-methylene-3(2*H*)-furanone (see Scheme I-3). That partitioning can be a concern for γ-radiation is illustrated by the fact that γ-radiation does not cause the formation of base propenals at C4' oxidation as most other oxidizing agents discussed in Chapter I.

There are some factors that clearly distinguish ionizing radiation from other DNA-damaging agents. Of central importance is that radiation insult is always in the form of highly structured tracks that contain a diversity of microscopic features *(13, 14)*. For γ-radiation, most energy is deposited in the form of single, isolated sparse ionizations or excitations *(14)*. The ionizing density of tracks created by α-particles, however, is far higher than γ-radiation and hence α-particles are more efficient at the same absorbed dose in creating cytotoxicity, mutagenesis and genomic instability *(1, 14)*. These cellular effects have been attributed to a higher complexity of the resulting DNA damage *(15)*, even though the yield of strand breaks is constant with increasing linear energy transfer (LET) of radiation *(16)*. This difference in damage induction by high *versus* low LET radiation has also been attributed to direct *versus* indirect interaction of radiation with

DNA. Indirect interaction takes place when ionizing radiation reacts with water to produce hydroxyl radicals, hydrated electrons, and hydrogen atoms by homolysis of oxygen-hydrogen bonds *(17)*, which in turn react with DNA. This has been suggested to be the primary route of γ-radiation-induced damage *(17)* as opposed to α-particles that are believed to introduce damage mainly via direct interaction with DNA.

The analytical method described in Chapter II was applied to the quantification of PGA residues in DNA subjected to γ-and α-radiation, with the results providing direct chemical evidence for the formation of PGA in oxidized DNA. Furthermore, by coupling the assay results with a method for quantifying total deoxyribose oxidation in DNA (experiments performed by Mr. Xinfeng Zhou), we were able to establish the fraction of deoxyribose oxidation events that resulted in the formation of PGA residues as the first step in testing models of oxidative DNA damage chemistry.

3. MATERIALS AND METHODS

3.1 Materials. All chemicals and reagents were of highest purity available and were used without further purification unless noted otherwise. Calf thymus DNA, alkaline phosphatase, *bis*(trimethylsilyl)trifluoroacetamide (containing 1% trimethylchlorosilane), pentafluorobenzylhydroxylamine and nuclease P1 were purchased from Sigma Chemical Co. (St. Louis, MO). Ethylacetate was purchased from Mallinckrodt Baker (Phillipsburg, NJ). Distilled and deionized water was further purified with a Milli-Q system (Millipore Corporation, Bedford, MA) and was used in all experiments.

3.2 Instrumental Analyses. GC/MS analyses of derivatized PGA were performed with a HP6890 gas chromatograph (HP7673 auto-injector) coupled to a Hewlett Packard 5973N mass selective detector. UV spectra were obtained using a Beckman DU 640 UV-visible spectrophotometer.

3.3 γ-Irradiation of DNA. Samples were irradiated at ambient temperature in a Gammacell-220 (Atomic Energy of Canada, Ltd.) with an annular ^{60}Co source. On the date of calibration (02/01/1973), the sealed source contained 7,314 Ci of ^{60}Co and delivered γ-radiation at a rate of 2 Gy/min at the time of conducting our experiments.

3.4 α-Irradiation of DNA. Irradiations were carried out at ambient temperature using a ^{241}Americium source calibrated to deliver 13.5 Gy/min (construction and calibration of the source was performed in the laboratory of Professor Jeffrey A. Coderre). Samples were irradiated in circular dishes of 3.9 cm diameter with a mylar bottom (3.7 μm thickness) with rapid stirring. The radiation doses delivered to samples containing DNA (1 mM nt) in a total volume of 1 ml were calculated to be 0.39 Gy/min assuming instantaneous mixing and a α-particle penetration depth of 25 μm. Samples were irradiated for 0, 30, 60, 120 and 240 min. A control sample was stirred under identical conditions without irradiation for 240 min to eliminate mechanical factors in PGA induction. After irradiation, a 500 μl aliquot was used for the quantification of PGA. The DNA content of each sample was determined using absorption at 260 nm.

3.5 Quantification of PGA in oxidized DNA. Calf thymus DNA (170 μg at 1 mg/ml in Chelex-treated 50 mM potassium phosphate buffer, pH 7.4; dialyzed four times against 4 L of phosphate buffer) was mixed with 200 pmol of [$^{13}C_2$]–PGA (internal standard) in a total volume of 500 μl. Immediately after damage induction, the DNA was hydrolyzed with nuclease P1 (10 U; 16 μL of 2 mg/ml; 37 °C, 90 min) following addition of 55 μl of 1 M sodium acetate solution, pH 5.5 (0.1 M final concentration), 2 mM $ZnCl_2$ (0.2 mM final concentration) and 0.54 M HCl (to adjust pH to 5.5). Aldehyde and ketone moieties were converted to their oxime derivatives by addition of 50 μl of a freshly-prepared 80 mM PFBHA solution followed by adjustment of the pH to 3 with 5 μl of 6 N HCl and incubation at ambient temperature for 15 min. The pH was again adjusted to 0 by addition of 4 μl of 6 N HCl and the aqueous phase was extracted three times with 400

μl volumes of ethylacetate. The residue from the pooled organic phases, dried under vacuum, was taken up in 30 μl of a 1:1 mixture of ethylacetate and BSTFA (containing 1% trimethylchlorosilane) and incubated at 70 °C for 1 h. After cooling at -80 °C for 10 min, samples were transferred to 2 ml screw-cap vials with 100 μl glass inserts and 1 μl was analyzed by GC/MS using negative chemical ionization (NCI) and selective ion monitoring (SIM) with the following conditions: 250 °C inlet (splitless mode); HP 19091S-433 HP-5MS 5% phenyl methyl siloxane column, 250 μm diameter, 30 m length and 0.25 μm film thickness; helium carrier purge: 7.63 psi, 50 ml/min flow, 2 min purge time; helium flow rate, 1 ml/min; oven temperature: initial 50 °C for 1.5 min, 10 °C/min ramp to 310 °C, 5 min hold at 310 °C. Data was acquired by selective ion monitoring (SIM) at *m/z* values of 241, 298 and 300, after a 16 min solvent delay. Quantities of PGA-PFBHA were determined from the ratio of peak areas of PGA-PFBHA peak to the [$^{13}C_2$]-PGA-PFBHA- as related to a standard curve derived from samples containing 0-100 pmol of PGA plus 200 pmol of [$^{13}C_2$]-PGA and 170 μg of calf thymus DNA and carried through all steps of the method described above except for irradiation. Samples for calibration were prepared in parallel to all oxidized samples and subjected to identical conditions; all samples were analyzed on the same day.

3.6 Quantification of total deoxyribose oxidation (performed by Mr. Xinfeng Zhou). As an index of total deoxyribose oxidation, plasmid topoisomer analysis was employed to quantify DNA strand breaks and abasic sites produced by γ-radiation. The experiments were performed by irradiating (0-0.4 Gy) a solution of negatively supercoiled plasmid pUC19 (2686 bp; 300 μg/ml) in Chelex-treated 50 mM potassium

phosphate buffer, pH 7.4. Following the irradiation, one-tenth volume of 1 M putrescine dihydrochloride was added and the solution was incubated at 37 °C for 30 min to cleave all abasic sites (*e.g.*, ref. *18*). The plasmid topoisomers present in the DNA sample (0.4 μg) were resolved on a 1% agarose gel at 2.5 V/cm for 1.5 h in Tris-borate-EDTA buffer *(19)*. The gel was stained in a 0.5 μg/ml ethidium bromide solution for 1 h and then destained for 30 min in water, followed by acquisition of a digital image of the fluorescent DNA bands in the gel subjected to UV illumination (315 nm). The quantity of strand breaks caused by γ-radiation was calculated from the net increase in the percentage of nicked, form II plasmid, with a correction factor of 1.4 applied to the signal from the supercoiled, form I plasmid due to its lower affinity for ethidium bromide *(20)*.

4. RESULTS

4.1 Quantification of PGA in γ-irradiated calf thymus DNA. Samples containing 170 μg calf thymus DNA (1 mM nts) and [^{13}C]-labeled internal standard in potassium phosphate buffer (50 mM, pH 7.4) were subjected to γ-radiation over the range of 0 to 107 Gy. The samples were processed for GC/MS analysis of PGA and the results are shown in Figure III-1. Over the dose range studied, the data show excellent linearity (r^2=1.0), with a slope of 1.5 PGA residues per 10^6 nts per Gy.

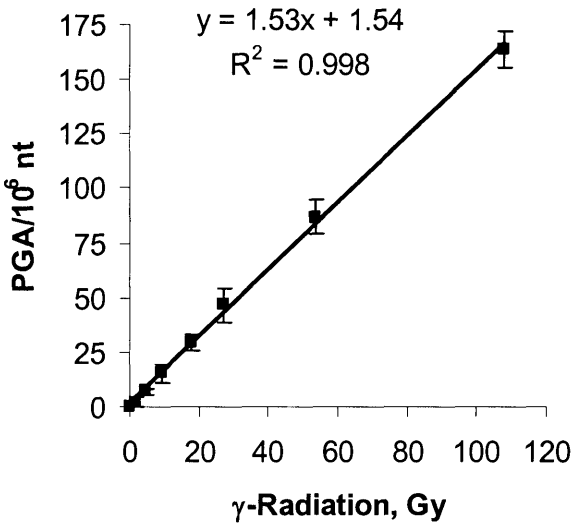

Figure III-1: PGA levels in γ-irradiated calf-thymus DNA. DNA subjected to 0-107 Gy of γ-radiation in a ^{60}Co source and processed for GC/MS analysis as described in Experimental Procedures. The data represent mean ± SD for five independent experiments.

4.2 Quantification of PGA in DNA oxidized by α-particles. The next objective was to assess the role of the LET characteristic of ionizing radiation in the efficiency of PGA formation by comparing the low LET γ-radiation to the high LET α-particles. Samples containing 170 μg calf thymus DNA (1 mM nts) and [^{13}C]-PGA, as internal standard, in potassium phosphate buffer (50 mM, pH 7.4) were subjected to α-particle irradiation at ambient temperature over the range of 0 to 93 Gy. The samples were processed for GC/MS analysis of PGA and the results are shown in Figure III-2. Over the dose range studied, the formation of PGA was linear (r^2=0.99), with a slope of 0.13 PGA residues per 10^6 nt per Gy.

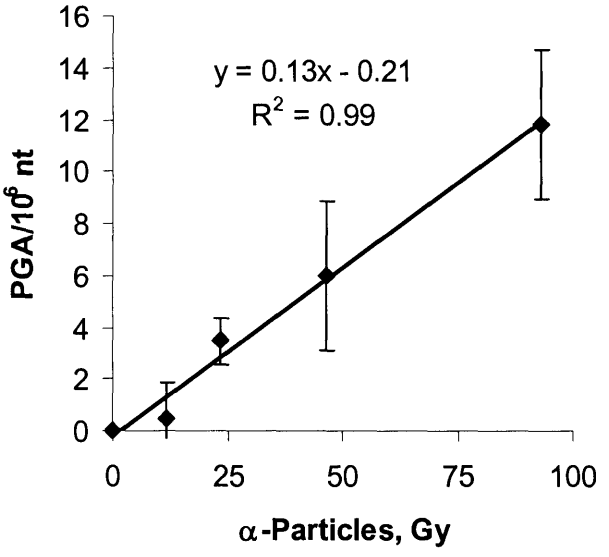

Figure III-2: PGA levels in calf thymus DNA treated with α-particles. DNA was subjected to 0 – 93 Gy of α-irradiation using a ^{241}Am source and processed for GC/MS analysis as described in the Experimental Procedures. The data represents the mean ± SD of three independent experiments.

4.3 Correlation of PGA levels with total deoxyribose oxidation. A major hurdle to comparative studies of oxidative DNA damage is determination of the total quantity of damage that occurs. To define the efficiency of formation of PGA, a deoxyribose oxidation product, produced by ionizing irradiation, the fraction of deoxyribose oxidation events that produced a PGA residue was estimated by topoisomer analysis of γ-irradiated plasmid DNA (experiments performed by Mr. Xinfeng Zhou).

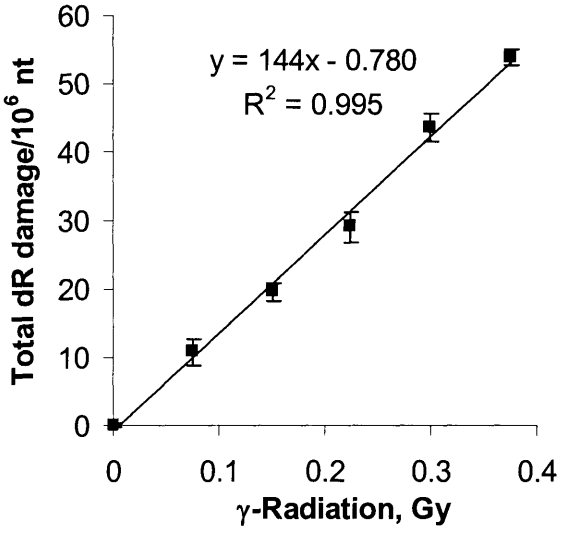

Figure III-3: Total deoxyribose oxidation events in DNA as a function of γ-radiation dose. Experiments performed by Mr. Xinfeng Zhou. Supercoiled pUC19 DNA was exposed to 0-0.4 Gy of γ-radiation and then treated with putrescine to convert abasic sites to strand breaks. The proportion of nicked, circular plasmid (*i.e.*, strand breaks + abasic sites) closely approximates the total number of deoxyribose oxidation events. The data represent mean ± S.D. for three independent experiments.

This assay exploits the change in electrophoretic migration of plasmid DNA when a strand break relieves the negative supercoiling of a substrate plasmid molecule. The plasmid pUC19 DNA used for these studies was subjected to γ- and α-irradiation under buffer and temperature conditions identical to those used in the GC/MS analyses of PGA. Abasic sites created by deoxyribose oxidation were converted to strand breaks by treatment of the irradiated DNA with putrescine dihydrochloride, which has been shown to cleave all types of oxidized abasic sites *(19, 21-23)* without apparent conversion of base lesions to strand breaks *(22, 23)*. The contribution of abasic sites to the total number

of damage events was minimal, with less than a 5% increase in strand breaks following putrescine treatment of plasmid DNA exposed to either γ- or α-radiation (data not shown).

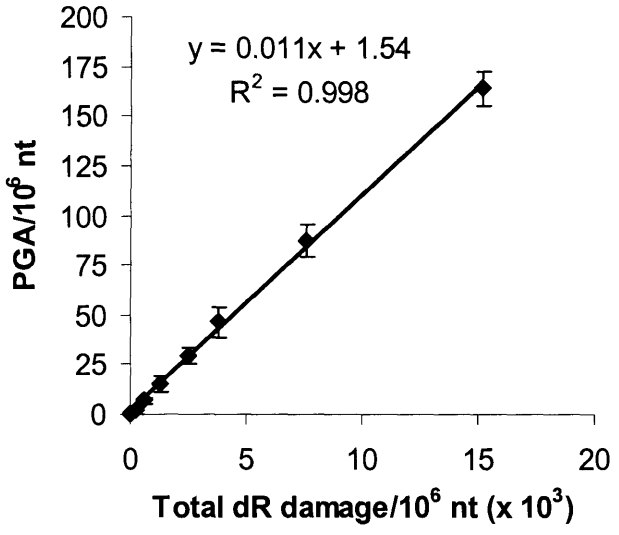

Figure III-4: Plot of PGA formation as a function of total deoxyribose oxidation events at different doses of γ–radiation. The slope of the line was calculated to be 0.011 by linear regression.

A critical feature of these plasmid topoisomer studies is the requirement to limit total deoxyribose oxidation events to one event or fewer per plasmid molecule, which avoids underestimation of damage events when two strand break events occur in a single plasmid molecule. This entails controlling total damage such that ≤ 30% of the plasmid molecules sustain an oxidation event, according to a Poisson distribution. The proportion of nicked, circular DNA (no linear DNA was observed) was used to calculate the total of direct strand breaks and abasic sites per Gy of γ-radiation, which amounted to 141 strand breaks per 10^6 nts per Gy (Figure III-3). As shown in Figure III-4, a plot of the number

of deoxyribose oxidation events *versus* the quantity of PGA residues produced at various doses of yields a slope of 0.011 PGA molecules per strand break corresponding to the presence of PGA in 1% ± 0.02 of all deoxyribose oxidation events. The induction of deoxyribose oxidation by α-particles, as shown in Figure III-5, is relatively low in comparison to γ-radiation induced deoxyribose oxidation (see Figure III-4). However, Figure III-6 reveals a relatively high yield of 7% ± 0.5 of PGA formed due to α-particle irradiation.

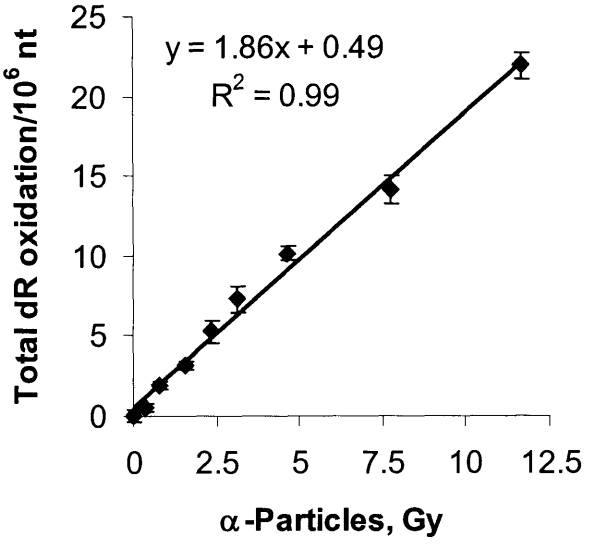

Figure III-5: Total deoxyribose oxidation events in plasmid DNA as a function of α-particle dose. Experiments performed by Mr. Xinfeng Zhou. Supercoiled pUC19 DNA was exposed to 0 – 12 Gy of α-particles and then treated with putrescine to convert abasic sites to strand breaks. The data represents the mean ± SD for three independent experiments.

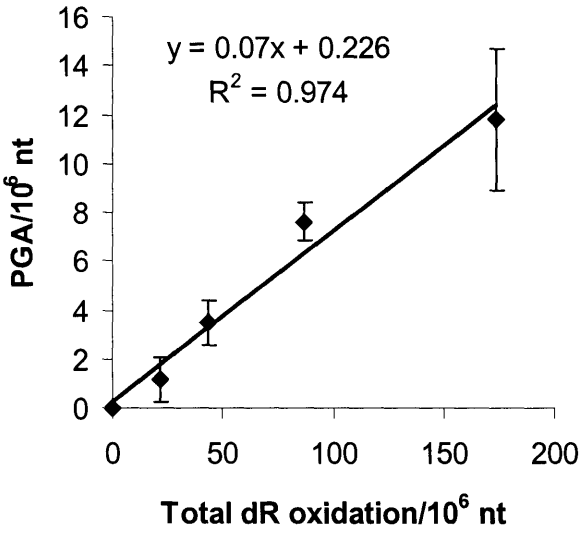

Figure III-6: Plot of PGA formation as a function of total deoxyribose oxidation events at different doses of α-irradiation. The slope of the line was calculated to be 0.07 by linear regression.

5. DISCUSSION

The oxidation of deoxyribose in DNA produces a variety of products as discussed in Chapter I. Several of these deoxyribose oxidation products have been shown to be responsible for blocking DNA synthesis (see for example *24*), the formation of covalent adducts with DNA repair proteins responsible for the removal of AP sites *(25-28)* and mutagenesis (see for example *29*). PGA has so far only been observed by gel shift assays in DNA degraded by rhodium(III) complexes *(30)* and in iron(II)/EDTA-damaged DNA *(31)*. As shown in Scheme I-2, PGA can decompose to form glyoxal, which in turn forms mutagenic glyoxal nucleobase adducts *(23, 32, 33)*. It has been reported that glyoxal adducts could not be observed in γ-irradiated 2'-deoxyribonucleosides analyzed by

reversed phase HPLC *(34)* indicating the absence of PGA formation in γ-irradiated DNA. However, Debije *et al.* proved the presence of C3' radical in a crystalline oligodeoxynucleotide subjected to X-rays using electron paramagnetic resonance *(12)*.

In this Chapter, we applied the analytical method for the quantification of PGA developed in Chapter II to the analysis of PGA produced by different forms of ionizing radiation. The studies presented here provide firm chemical evidence for the formation of PGA residues in DNA oxidized by radiation. This confirms the tentative identification of PGA by Sitlani *et al.* and Breiner *et al.* using gel shift assays *(30, 31)*. Such sequencing gel mobility studies have been used by many researchers to study deoxyribose oxidation. However, the approach does not provide rigorous chemical identification of the lesion and is poorly quantitative.

Although unlikely, we cannot rule out that the PGA observed here is a product of C2'-oxidation. Saito and coworkers studied the C2' oxidation product erythrose abasic site in UV-irradiated oligodeoxynucleotides containing IdU (discussed in Chapter I, section 4.2) *(35)*. Upon heating under alkaline conditions, the erythrose abasic site was been shown to undergo a retroaldol reaction to give two fragments in high yield, both possessing phosphoglycolaldehyde termini (see Scheme I-7) *(35)*. In our assay, such conditions are not used, but the possibility that the observed PGA at least in part is due to C2' oxidation cannot be totally discounted.

The inability of Murata-Kamiya *et al.* to detect glyoxal adducts in γ-irradiated DNA in combination with our observation that PGA residues arise in ~1% of the strand breaks and abasic sites produced by γ-radiation in DNA (1.5 PGA for every 140 strand breaks) has to be taken into context by the 10^4 hr half-time of glyoxal formation from PGA *(23)*. This indicates that the UV detection method used by Murata-Kamiya *et al. (34)* may not have been sensitive enough to detect the glyoxal or the glyoxal adducts formed by degradation of radiation-induced PGA.

The γ-radiation chemical yield (G–value) for PGA was found to be independent of the dose of radiation used and was calculated from the data presented in Figure III-1 as 1.6 nmol/J. This value is lower than the G–value for 3'-phosphoglycolate, a major product of radiation-induced oxidation of the 4'-position of deoxyribose, determined by Weinfeld *et al.* as 10.5 nmol/J *(36)*. Using the data presented in the paper of Weinfeld *et al.*, the amount of 3'-phosphoglycolate residues induced by 50 Gy of γ-radiation can be calculated as 351 residues per 10^6 nt. This compares to 87 PGA residues per 10^6 nt at 54 Gy. A lower yield of 3'-oxidation products than 4'-oxidation products has been claimed for Fe^{+2}/EDTA-induced damage *(37)*. These results are consistent with the model of Balasubramanian *et al.* that the greater solvent exposure of the 4'-position as opposed to the 3'-position leads to greater abstraction of the C4' hydrogen atom by the hydroxyl radical *(37)*.

However, the pathway leading to PGA may not be the only pathway involved in the degradation of the 3'-carbon radical in deoxyribose. Stubbe and Kozarich have

proposed that 3'-chemistry partitions to form a strand break with either a PGA residue or an alternative five-carbon fragment *(38)*. This partitioning is common with oxidation of the other positions in deoxyribose (see Chapter I), such as the two sets of products arising from 5'-oxidation: a nucleoside-5'-aldehyde residue or the 3'-formylphosphate and 2-phosphoryl-1,4-dioxobutane residues *(3)*. The latter accounts for only 10% of the 5'-chemistry produced by the enediyne antibiotic neocarzinostatin *(3)* so it is possible that the PGA residue is a minor lesion and that 3'-oxidation occurs more frequently than predicted by the solvent exposure model for deoxyribose oxidation in DNA *(37)*.

Little is known about the chemical nature of DNA lesions induced by high LET radiation, such as α-particles. Biological effects such as the induction of single-and double-strand breaks, cell death, damage repair and mutagenesis have been studied to some extent *(39-45)*. In comparison to γ-radiation, the high LET α-particles are more efficient at the same absorbed dose in creating cytotoxicity, mutagenesis and genomic instability *(1, 14)*. Hoglund *et al.* studied double-strand break induction and repair in human cells and found that with increasing LET rejoining of double-strand breaks was slower *(46)*. These cellular effects have been attributed to a higher complexity of DNA damage *(15)* which remains to be shown on a molecular basis.

In our comparison of α- and γ-radiation, we found that α-particles were more efficient than γ-radiation in inducing PGA, with 7% ± 0.5 of all deoxyribose oxidation products exhibited PGA. This stands in contrast to 1% ± 0.02 PGA formation efficiency associated with γ-radiation. Pouget *et al.* found in their cell exposure experiments that the

efficiency of base damage formation is on average two-fold lower for high LET radiation *(47)*, but our findings support the hypothesis that PGA is preferentially produced by direct radiation damage, as is more likely with α-particles. Jones *et al.* studied the induction of thymine glycol and the C4' deoxyribose oxidation product phosphoglycolate in isolated DNA *(48)*. This, to our knowledge, is the only other study of a specific deoxyribose oxidation product induced by α-particles. Jones *et al.* found no qualitative difference between the damage spectrum of γ- and α-irradiated DNA, but unfortunately did not provide any quantitative measurements *(48)*. Their work was focused on studying the effect of scavengers on the damage profile and not on establishing the quantity of phosphoglycolate in α-irradiated DNA. Taken together, these few finding show that the precise chemical nature of high LET radiation induced DNA damage in combination with cellular response remains a relatively unexplored field.

REFERENCES

(1) O'Neill, P. (2001). Radiation-induced damage in DNA. In Radiation chemistry: present status and future trends, **87**, 1 Edition, C.D. Jonah, B.S.M. Rao, eds. (Elsevier Science), 585-622.

(2) Greenberg, M.M. (1999). Chemistry of DNA Damage. In Comprehensive Natural Products Chemistry, **7**, E.T. Kool, ed. (Amsterdam: Elsevier Science B. V.), 372-425.

(3) Dedon, P.C., Jiang, Z.W., Goldberg, I.H. (1992). Neocarzinostatin-mediated DNA damage in a model AGT.ACT site: mechanistic studies of thiol-sensitive partitioning of C4' DNA damage products. *Biochemistry **31***, 1917-1927.

(4) Pogozelski, W.K., Tullius, T.D. (1998). Oxidative strand scission of nucleic acids: routes initiated by hydrogen abstraction from the sugar moiety. *Chem. Rev. **98***, 1089-1107.

(5) Carter, K.N., Greenberg, M.M. (2003). Independent generation and study of 5,6-Dihydro-2'-deoxyuridin-6-yl, a member of the major family of reactive intermediates formed in DNA from the effects of gamma-radiolysis. *The Journal of organic chemistry. **68(11)***, 4275-4280.

(6) Shaw, A.A., Cadet, J. (1996). Direct effects of gamma-radiation on 2'-deoxycytidine in frozen aqueous solution. *International journal of radiation biology.* ***70(1)***, 1-6.

(7) Dizdaroglu, M., Schulte-Frohlinde, D., von Sonntag, C. (1977). gamma-radiolyses of DNA in oxygenated aqueous solution. Structure of an alkali-labile site. *Z. Naturforsch.* ***32C***, 1021-1022.

(8) Rashid, R., Langfinger, D., Wagner, R., Schuchmann, H.P., von Sonntag, C. (1999). Bleomycin versus OH-radical-induced malonaldehydic-product formation in DNA. *Int J Radiat Biol* ***75***, 101-109.

(9) Henner, W.D., Rodriguez, L.O., Hecht, S.M., Haseltine, W.A. (1983). gamma Ray induced deoxyribonucleic acid strand breaks. 3' Glycolate termini. *J Biol Chem* ***258***, 711-713.

(10) Dizdaroglu, M., Jaruga, P., Rodriguez, H. (2001). Identification and quantification of 8,5'-cyclo-2'-deoxy-adenosine in DNA by liquid chromatography/ mass spectrometry. *Free radical biology & medicine.* ***30(7)***, 774-784.

(11) Langfinger, D., von Sonntag, C. (1985). Gamma-Radiolysis of 2'-Deoxyguanosine: The Structure of the Malondialdehyde-Like Product. *Zeitschrift fuer Naturforschung* ***40C***, 446-448.

(12) Debije, M.G., Bernhard, W.A. (2001). Electron paramagnetic resonance evidence for a C3' sugar radical in crystalline d(CTCTCGAGAG) X-irradiated at 4 K. *Radiat Res* ***155***, 687-692.

(13) Nikjoo, H., O'Neill, P., Terrissol, M., Goodhead, D.T. (1999). Quantitative modeling of DNA damage using Monte Carlo track structure method. *Radiat Environ Biophys* ***38***, 31-38.

(14) Goodhead, D.T. (1989). The initial physical damage produced by ionizing radiations. *International journal of radiation biology.* ***56(5)***, 623-634.

(15) Ward, J.F. (1994). The complexity of DNA damage: relevance to biological consequences. *Int J Radiat Biol* ***66***, 427-432.

(16) Nikjoo, H., Uehara, S., Wilson, W.E., Hoshi, M., Goodhead, D.T. (1998). Track structure in radiation biology: theory and applications. *International journal of radiation biology.* ***73(4)***, 355-364.

(17) von Sonntag, C. (1987). The Chemical Basis of Radiation Biology (New York: Taylor & Francis).

(18) Dedon, P.C., Salzberg, A.A., Xu, J. (1993). Exclusive production of bistranded DNA damage by calicheamicin. *Biochemistry* ***32***, 3617-3622.

(19) Ausubel, F.M., Brent, R., Kingston, R.E., Moore, D.D., Seidman, J.G., Smith, J.A., Struhl, K. (1989). Current Protocols in Molecular Biology (New York: John Wiley and Sons).

(20) Milligan, J.R., Aguilera, J.A., Ward, J.F. (1993). Variation of single-strand break yield with scavenger concentration for plasmid DNA irradiated in aqueous solution. *Radiat. Res.* ***133***, 151-157.

(21) Dedon, P.C., Plastaras, J.P., Rouzer, C.A., Marnett, L.J. (1998). Indirect mutagenesis by oxidative DNA damage: formation of the pyrimidopurinone adduct of deoxyguanosine by base propenal. *Proc. Natl. Acad. Sci. USA* ***95***, 11113-11116.

(22) Plastaras, J.P., Dedon, P.C., Marnett, L.J. (2002). Effects of DNA structure on oxopropenylation by the endogenous mutagens malondialdehyde and base propenal. *Biochemistry* ***41***, 5033-5042.

(23) Awada, M., Dedon, P.C. (2001). Formation of the 1,N2-glyoxal adduct of deoxyguanosine by phosphoglycolaldehyde, a product of 3'-deoxyribose oxidation in DNA. *Chem. Res. Toxicol.* ***14***, 1247-1253.

(24) Johnson, A.W., Demple, B. (1988). Yeast DNA diesterase for 3'-fragments of deoxyribose: purification and physical properties of a repair enzyme for oxidative DNA damage. *The Journal of biological chemistry.* ***263(34)***, 18009-18016.

(25) DeMott, M.S., Beyret, E., Wong, D., Bales, B.C., Hwang, J.T., Greenberg, M.M., Demple, B. (2002). Covalent trapping of human DNA polymerase beta by the oxidative DNA lesion 2-deoxyribonolactone. *J. Biol. Chem.* ***277***, 7637-7640.

(26) Hashimoto, M., Greenberg, M.M., Kow, Y.W., Hwang, J.T., Cunningham, R.P. (2001). The 2-deoxyribonolactone lesion produced in DNA by neocarzinostatin and other damaging agents forms cross-links with the base-excision repair enzyme endonuclease III. *J. Am. Chem. Soc.* ***123***, 3161-3162.

(27) Kroeger, K.M., Hashimoto, M., Kow, Y.W., Greenberg, M.M. (2003). Cross-linking of 2-deoxyribonolactone and its beta-elimination product by base excision repair enzymes. *Biochemistry.* ***42(8)***, 2449-2455.

(28) Xu, Y.J., DeMott, M.S., Hwang, J.T., Greenberg, M.M., Demple, B. (2003). Action of human apurinic endonuclease (Ape1) on C1'-oxidized deoxyribose damage in DNA. *DNA repair.* ***2(2)***, 175-185.

(29) Berthet, N., Roupioz, Y., Constant, J.F., Kotera, M., Lhomme, J. (2001). Translesional synthesis on DNA templates containing the 2'-deoxyribonolactone lesion. *Nucleic acids research.* ***29(13)***, 2725-2732.

(30) Sitlani, A., Long, E.C., Pyle, A.M., Barton, J.K. (1992). DNA Photocleavage by Phenanthrenequinone Diimine Complexes of Rhodium(III): Shape-Selective Recognition and Reaction. *J. Am. Chem. Soc* ***114***, 2303-2312.

(31) Breiner, K.M., Daugherty, M.A., Oas, T.G., Thorp, H.H. (1995). An anionic diplatinum DNA photocleavage agent: chemical mechanism and footprinting of the lambda repressor. *J Am Chem Soc* ***117***, 11673-11679.

(32) Kasai, H., Iwamoto-Tanaka, N., Fukada, S. (1998). DNA modifications by the mutagen glyoxal: adduction to G and C, deamination of C and GC and GA cross-linking. *Carcinogenesis.* ***19(8)***, 1459-1465.

(33) Loeppky, R.N., Cui, W., Goelzer, P., Park, M., Ye, Q. (1999). Glyoxal-guanine DNA adducts: detection, stability and formation in vivo from nitrosamines. *IARC scientific publications.*

(34) Murata-Kamiya, N., Kamiya, H., Muraoka, M., Kaji, H., Kasai, H. (1997). Comparison of oxidation products from DNA components by gamma- irradiation and Fenton-type reactions. *J. Radiat. Res. (Tokyo)* ***38***, 121-131.

(35) Sugiyama, H., Tsutsumi, Y., Fujimoto, K., Saito, I. (1993). Photoinduced deoxyribose-C2' oxidation in DNA: Alkali-dependent cleavage of erythrose-containing sites via a retroaldol reaction. *J. Am. Chem. Soc.* ***115***, 4443-4448.

(36) Weinfeld, M., Soderlind, K.J. (1991). 32P-postlabeling detection of radiation-induced DNA damage: identification and estimation of thymine glycols and phosphoglycolate termini. *Biochemistry* ***30***, 1091-1097.

(37) Balasubramanian, B., Pogozelski, W.K., Tullius, T.D. (1998). DNA strand breaking by the hydroxyl radical is governed by the accessible surface areas of the hydrogen atoms of the DNA backbone. *Proc. Natl. Acad. Sci. U S A* ***95***, 9738-9743.

(38) Stubbe, J., Kozarich, J.W. (1987). Mechanisms of Bleomycin-Induced DNA Degradation. *Chem Rev* ***87***, 1107-1136.

(39) Takatsuji, T., Yoshikawa, I., Sasaki, M.S. (1999). Generalized concept of the LET-RBE relationship of radiation-induced chromosome aberration and cell death. *J Radiat Res (Tokyo)* ***40***, 59-69.

(40) Prise, K.M., Ahnstrom, G., Belli, M., Carlsson, J., Frankenberg, D., Kiefer, J., Lobrich, M., Michael, B.D., Nygren, J., Simone, G., Stenerlow, B. (1998). A review of dsb induction data for varying quality radiations. *Int J Radiat Biol* ***74***, 173-184.

(41) Prise, K.M. (1994). Use of radiation quality as a probe for DNA lesion complexity. *Int J Radiat Biol* ***65***, 43-48.

(42) Prise, K.M., Pullar, C.H., Michael, B.D. (1999). A study of endonuclease III-sensitive sites in irradiated DNA: detection of alpha-particle-induced oxidative damage. *Carcinogenesis* ***20***, 905-909.

(43) Newman, H.C., Prise, K.M., Michael, B.D. (2000). The role of higher-order chromatin structure in the yield and distribution of DNA double-strand breaks in cells irradiated with X- rays or alpha-particles. *Int J Radiat Biol* ***76***, 1085-1093.

(44) Azzam, E.I., de Toledo, S.M., Waker, A.J., Little, J.B. (2000). High and low fluences of alpha-particles induce a G1 checkpoint in human diploid fibroblasts. *Cancer research.* ***60(10)***, 2623-2631.

(45) Wu, L.J., Randers-Pehrson, G., Xu, A., Waldren, C.A., Geard, C.R., Yu, Z., Hei, T.K. (1999). Targeted cytoplasmic irradiation with alpha particles induces mutations in mammalian cells. *Proceedings of the National Academy of Sciences of the United States of America.* ***96(9)***, 4959-4964.

(46) Hoglund, H., Stenerlow, B. (2001). Induction and rejoining of DNA double-strand breaks in normal human skin fibroblasts after exposure to radiation of different linear energy transfer: possible roles of track structure and chromatin organization. *Radiat Res* ***155***, 818-825.

(47) Pouget, J.P., Frelon, S., Ravanat, J.L., Testard, I., Odin, F., Cadet, J. (2002). Formation of modified DNA bases in cells exposed either to gamma radiation or to high-LET particles. *Radiation research.* ***157(5)***, 589-595.

(48) Jones, G.D., Boswell, T.V., Lee, J., Milligan, J.R., Ward, J.F., Weinfeld, M. (1994). A comparison of DNA damages produced under conditions of direct and indirect action of radiation. *Int J Radiat Biol* ***66***, 441-445.

Chapter IV

3-Phosphoglycolaldehyde and the Fenton Reaction

1. ABSTRACT

Reactive oxygen species (ROS), produced endogenously or by exposure to environmental chemicals, induce a wide variety of DNA lesions. The variety of chemistries associated with different oxidants suggests that each has the potential to produce a unique spectrum of DNA damage products. To extend our efforts to relate genotoxic chemistry to DNA deoxyribose oxidation damage, we measured total deoxyribose oxidation and 3'-phosphoglycolaldehyde (PGA) formation in DNA after exposure to Fe(II), Fe(II)/EDTA and Fe(II)/EDTA/H_2O_2. We found that the proportion of deoxyribose oxidation events containing PGA varies for each of the studied iron oxidizing systems. In the case of Fe(II) and Fe(II)/EDTA/H_2O_2, the yield of PGA per deoxyribose oxidation event was nonlinear and depended on the concentration of the oxidizing agent. Fe(II)/EDTA, however, produced a linear response for both PGA and total deoxyribose oxidation with PGA lesions arising in 5% ± 0.2 PGA of deoxyribose oxidation events. The differences in efficiency of PGA formation for these oxidizing agents, which traditionally have been thought to induce damage *via* hydroxyl radical

formation, show that either the proximity of hydroxyl radical formation to DNA components influences the yield of PGA or that the nature of ROS formation is more complicated than previously appreciated.

2. INTRODUCTION

The Fenton reaction has long been invoked as a common source of oxidative DNA damage in cells (*i.e.* reviewed in reference *1*). The reaction entails the reduction of hydrogen peroxide by a redox active metal to produce a hydroxyl radical capable of oxidizing DNA. Though iron (Fe) is the most abundant redox active metal in cells, little is known about the spectrum of deoxyribose oxidation products generated by Fe-mediated Fenton chemistry nor about the effect of the various chemical forms of Fe on the DNA damage. To this end, we have investigated the formation of PGA by Fe(II), Fe(II)/EDTA and Fe(II)/EDTA/H_2O_2.

Each oxidizing agent studied here produces DNA damage by a distinct mechanism. For example, it is known that in the presence of oxygen, Fe(II) and Fe(II)/EDTA introduce single- and double- strand breaks in DNA *(2)* presumably *via* the Fenton reaction:

$[Fe(EDTA)]^{2-} + O_2 \rightarrow [Fe(EDTA)]^{3-} + O_2^{\bullet-}$ **(1)** $6 \times 10^2\ M^{-1}\ s^{-1}$ *(3)*

$[Fe(EDTA)]^{2-} + O_2^{\bullet-} + 2\ H^+ \rightarrow [Fe(EDTA)]^{3-} + H_2O_2$ **(2)** *(4)*

$[Fe(EDTA)]^{2-} + H_2O_2 \rightarrow [Fe(EDTA)]^{3-} + {\bullet}OH + OH^-$ **(3)** $7.1 \times 10^3\ M^{-1}\ s^{-1}$ *(1)*

In the Fe(II) and Fe(II)/EDTA systems, the presence of molecular oxygen in solution is required for DNA damage to occur. Air-equilibrated aqueous solutions contain an oxygen concentration between 0.2 and 0.25 mM *(4)*, which is close to the maximum concentration of iron used in our experiments (0.3 mM). The reaction of O_2 with Fe(II) produces superoxide radical anions ($O_2^{\bullet-}$), a species that is not sufficiently reactive to modify DNA, but can undergo a conversion to more reactive species such as H_2O_2 *(1)*. The involvement of H_2O_2 in Fe(II)-mediated DNA damage has been studied by Svoboda *et al.* who found a greater than 90% decrease in 8-oxo-dG formation in calf thymus DNA in the presence of catalase *(5)*, an enzyme that catalyzes the disproportionation of H_2O_2 to H_2O and O_2. Superoxide anions can also undergo a disproportionation reaction catalyzed by Fe(II) and Fe(III) to produce hydroxyl radicals, the so called Haber-Weiss reaction *(1)*:

$$O_2^{\bullet-} + H_2O_2 \xrightarrow{Fe} O_2 + \bullet OH + OH^- \qquad \textbf{(4)}$$

After oxidation to Fe(III), iron is believed to be unreactive in the presence of oxygen in phosphate buffer and incapable of producing hydroxyl radicals *(4)*. Therefore, generation of hydroxyl radicals is limited by the availability of Fe(II) *(1)*. The oxidation of Fe(II)/EDTA in phosphate buffer at neutral pH has been found to be very rapid, with a half-life of less than 15 s and a similar rate of appearance of hydroxyl radicals *(4)*. Hydroxyl radicals have a half-life of about 1 ns in cells and tissues *(6)* and can react *via* abstraction of hydrogen atoms from each of the five carbons of deoxyribose (including the 3'-position of interest here) with rate constants of ~2 x 10^9 M^{-1} s^{-1} *(7)*. The carbon-centered radicals arising from the reaction of hydroxyl radicals with DNA rapidly react

with molecular oxygen at diffusion controlled rates to form organic hydroperoxyl radicals *(7)*. These radicals, in turn, are oxidizers and can partition to form various deoxyribose fragments and abasic sites *(8)*. Therefore, oxygen plays a dual role in this process: it makes the formation of the oxidizing species possible in the first place and, second, it amplifies the damage through subsequent partitioning *(9)*.

An important feature of Fe-mediated DNA damage is the propensity of Fe to form complexes with biological molecules. There are marked differences in the ability of complexed and uncomplexed iron to induce DNA damage. Fe(II)/H_2O_2 shows some sequence specificity in DNA damage that has been explained by preferential localization of Fe(II) ions at specific sites in DNA *(10)*. In addition to binding to the phosphate oxygens in DNA *(5)*, Fe(II) binds with high affinity to nitrogen atoms in DNA bases *via* its inner coordination sphere, particularly to the N7 position in guanine *(10, 11)*. The EDTA complex of Fe(II) presents an opportunity to obviate DNA binding complications since the negative charge of the Fe(II)/EDTA complex prevents binding to DNA by charge repulsion with the sugar-phosphate backbone *(12)*. This may explain the lack of sequence selectivity of strand breaks generated by the complex *(2, 12, 13)*. In general, Fe(II) chelates may serve as a model for more biologically relevant reactions since iron within cells is not "free" but chelated with ubiquitous cellular components or specific proteins *(4)*. On the other hand, use of free Fe(II) provides insight into the DNA damage profile expected when Fe transfers from weak complexes to higher affinity binding sites in DNA.

In an effort to understand the relationship between the reactivity of Fe(II) in its complexed and uncomplexed form towards DNA, we have quantified total deoxyribose oxidation and PGA formation for Fe(II), Fe(II)/EDTA and Fe(II)/EDTA/H_2O_2. We found that the ratio of PGA to strand breaks was not the same for the different ROS generating systems and also varied as a function of concentration for some oxidizing agents. These results are discussed in light of other investigations devoted to oxidizing agents and their mechanisms of inducing distinct DNA damage spectra.

3. MATERIALS AND METHODS

3.1 Materials. All chemicals and reagents were of the highest purity available and were used without further purification unless noted otherwise. Calf thymus DNA, Nuclease P1, $FeSO_4$, $FeCl_3$, *bis*(trimethylsilyl)trifluoroacetamide (containing 1% trimethylchlorosilane) and pentafluorobenzylhydroxylamine were purchased from Sigma Chemical Co. (St. Louis, MO). DNA was dissolved at a concentration of 1 mg/ml in Chelex-treated 50 mM potassium phosphate buffer, pH 7.4 and dialyzed four times against 4 L of phosphate buffer. The first dialysis step was conducted in the presence of 1 mM DTPA. EDTA (the disodium salt) and ethyl acetate were purchased from Mallinckrodt Baker (Phillipsburg, NJ). H_2O_2 (30% v/v) was purchased from EM Science (Gibbstown, NJ, USA). Distilled and deionized water was further purified with a Milli-Q system (Millipore Corporation, Bedford, MA) and was used in all experiments.

3.2 Instrumental Analyses. GC/MS analyses of derivatized PGA were performed with a HP6890 gas chromatograph (HP7673 auto-injector) coupled to a Hewlett Packard 5973N mass selective detector. UV spectra were obtained using a Beckman DU 640 UV-visible spectrophotometer.

3.3 DNA oxidation by iron. Calf thymus DNA (170 μg at 1 mM DNA concentration in nt) in 50 mM Chelex treated phosphate buffer, pH 7.4, was mixed with 200 pmol of [$^{13}C_2$]–PGA (internal standard; synthesis see Chapter 2). To this solution was added an iron-containing solution prepared as follows. A stock solution of 4 mM $FeSO_4$ in the presence or absence of EDTA (as the disodium salt; a 1.1 molar excess of EDTA was used) was freshly prepared by first dissolving EDTA if applicable and then dissolving $FeSO_4$ in ddH_2O and lowering the pH to 2.5 using 6 N HCl. For Fe(III) experiments, a 4 mM $FeCl_3$ stock solution was prepared in ddH_2O. Immediately after preparation of the Fe solutions, DNA samples were treated with 0 to 300 μM final iron concentrations and incubated at 37 °C for 2 h. For studies with Fe(II)/EDTA/H_2O_2, a freshly prepared 5 mM H_2O_2 stock solution was added to DNA samples prior to addition of Fe(II)/EDTA. A DNA sample receiving H_2O_2, but no Fe(II)/EDTA, was used as a control to test for trace metals in stock solutions and for damage induced by H_2O_2. For the preparation of H_2O_2 stock solutions the concentration of the H_2O_2 stock solution was measured using UV/VIS absorbance at 240 nm using the absorption coefficient of ε_{240} = 39.4 M^{-1} cm^{-1} *(14)*.

3.4 Quantification of PGA in oxidized DNA. This analytical method was described in detail in Chapter III, section 3.5.

3.5 Quantification of total deoxyribose oxidation (performed by Mr. Xinfeng Zhou). As an index of total deoxyribose oxidation, plasmid topoisomer analysis was employed to quantify DNA strand breaks and abasic sites produced by iron under identical conditions as for PGA quantification. The experimental procedure was described in detail in Chapter III, section 3.6.

4. RESULTS

4.1 Quantification of PGA in DNA oxidized by Fe(II), Fe(II)/EDTA and Fe(III). Samples containing 170 μg calf thymus DNA and [^{13}C]-labeled internal standard in potassium phosphate buffer (50 mM, pH 7.4) were subjected to oxidation by Fe(II) with and without EDTA and Fe(III) at a range of 0 to 300 μM at 37 °C for 2 h. The samples were processed for GC/MS analysis of PGA and the results are shown in Figure IV-1A. Over the Fe(II)/EDTA dose range studied, the formation of PGA was linear (r^2=0.99) with a slope of 0.5 PGA per 10^6 nt per μM Fe(II)/EDTA. However, PGA formation with Fe(II) was clearly non-linear, as shown in Figure IV-1A. As expected, Fe(III) did not produce any measurable PGA (PGA < 2 per 10^6 nt; data not shown).

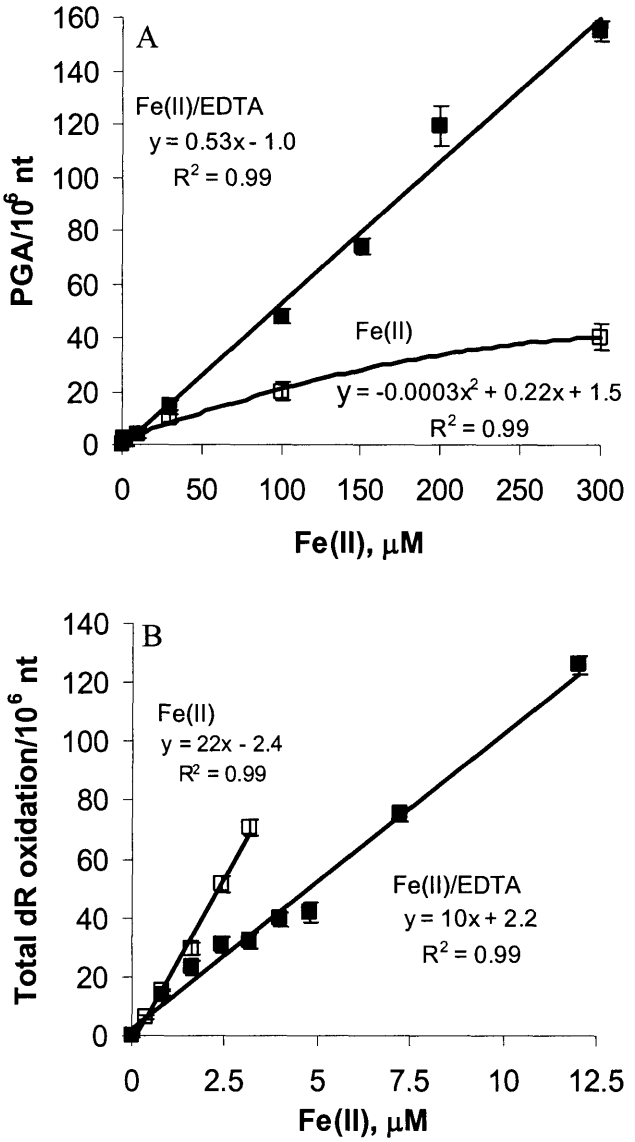

Figure IV-1: (A): PGA levels in calf thymus DNA treated with Fe(II) and Fe(II)/EDTA. DNA was treated with 0 – 300 μM of Fe(II) or Fe(II)/EDTA at 37 °C for 2 h and processed for GC/MS analysis as described in the Experimental Procedures. The data represent the mean ± SD of five independent experiments for Fe(II) and four independent experiments for Fe(II)/EDTA. **(B):** Deoxyribose oxidation events in plasmid DNA as a function of Fe(II) concentration (experiments performed by Mr. Xinfeng Zhou). Supercoiled pUC19 DNA was exposed to 0 – 12.5 μM Fe(II) and then treated with

putrescine to convert abasic sites to strand breaks. The data represents the mean ± SD for three independent experiments

The fraction of deoxyribose oxidation events that produced a PGA residue was estimated by topoisomer analysis (performed by Mr. Xinfeng Zhou) under conditions identical to those used for PGA analysis. The dose response for total deoxyribose oxidation events as a function of Fe concentration yielded a slope of 10 strand breaks per 10^6 nt per μM for Fe(II)/EDTA and 22 strand breaks per 10^6 nt per μM for Fe(II), as shown in Figure IV-1B. A plot of the number of deoxyribose oxidation events *versus* the quantity of PGA residues yields a slope of 0.05 ± 0.002 PGA residues per strand break for Fe(II)/EDTA (data not shown). Due to the nonlinear nature of PGA induction by Fe(II), the number of PGA molecules per deoxyribose oxidation event is not constant and is dependent on the iron concentration.

4.2 Quantification of PGA in DNA oxidized by Fe(II)/EDTA/H_2O_2. It is important to consider the order of addition of reactants in the reaction of Fe(II)/EDTA and H_2O_2 with DNA due to the rapid reaction of Fe(II)/EDTA to generate oxidants in the absence of H_2O_2. That this is the case is shown in Figure IV-1. Colwell *et al.* systematically studied the effects on adding Fe(II), EDTA and H_2O_2 on the formation of 8-hydroxy-2'-deoxyguanine from deoxyguanosine *(11)*. They found that the yield was highly dependent on the order of addition of reactants to deoxyguanosine. The highest yield of hydroxy-2'-deoxyguanine was seen when Fe(II) was allowed to bind to the nucleoside prior to addition of H_2O_2 and EDTA and the lowest yield was observed for the addition of premixed Fe(II)/EDTA before adding H_2O_2 *(11)*. These results, however,

were obtained in unbuffered aqueous solution at pH 6.5, which may not be transferable to a buffered system at physiological pH.

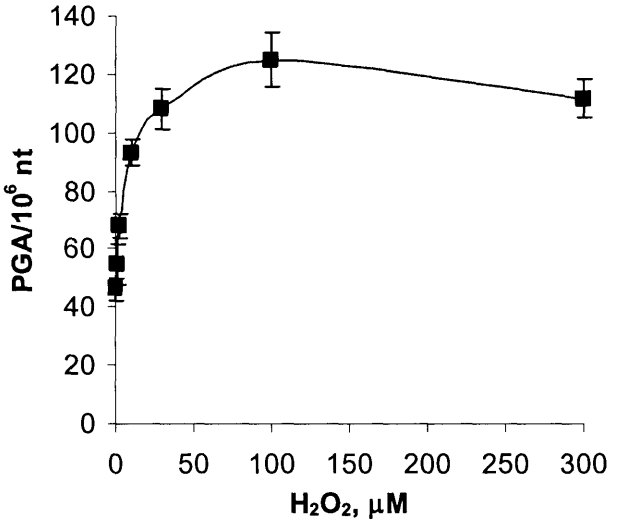

Figure IV-2: PGA levels in calf thymus DNA treated with 30 μM Fe(II)/ETDA and H_2O_2 concentrations between 0 and 300 μM at 37 °C and processed for GC/MS analysis as described in the Experimental Procedures. The data represents the mean ± SD of three independent experiments.

Samples containing 170 μg calf thymus DNA and [^{13}C]-labeled internal standard in potassium phosphate buffer were subjected to oxidation by 30 μM Fe(II)/EDTA and H_2O_2 at a range of 0 to 300 μM at 37°C for 2 h. H_2O_2 was added to samples prior to the addition of Fe(II)/EDTA. The samples were then processed for GC/MS analysis of PGA and the results are shown in Figure IV-2. Over the dose range studied, the data show a bimodal dependence on H_2O_2 concentration. DNA samples treated with only 300 μM H_2O_2 showed no measurable formation of PGA, which indicates the absence of significant quantities of redox active metals in the Chelex treated DNA.

5. DISCUSSION

Given the ubiquitous presence of iron in cells and its genotoxic potential, we undertook a study of iron-induced DNA damage, focusing on the deoxyribose oxidation product PGA. Breiner *et al.* used a gel shift assay to tentatively identify PGA in DNA treated with Fe(II)/EDTA *(15)*. The results presented here provide definitive chemical evidence for the formation of PGA in DNA subjected to Fenton chemistry.

We have shown that the relative level of PGA can vary widely depending on the oxidizing agent, its concentration and complexation state. These results indicate the importance of understanding how the underlying chemistry contributes to different levels and types of oxidative DNA damage. Different chemical mechanisms may lie at the heart of the different levels of PGA produced by Fe(II) and Fe(II)/EDTA. For Fe(II), the response was nonlinear, with a given concentration inducing significantly less PGA than the corresponding concentration of Fe(II)/EDTA. This was not unexpected because it has been shown that EDTA can drastically alter the ability of iron to catalyze oxidation reactions, such as the Haber-Weiss reaction, and can enhance both the rate of iron autoxidation and the radical yield in the Fenton reaction *(14)*. Quian *et al.* attributed this behavior to the formation of Fe(II)–O_2 species, facilitated by the presence of the chelator, which represents an alternative mechanism to the Fenton reaction and involves oxidations initiated by Fe-O or FeO^{2+} complexes (*i.e.*, see references *9, 16, 17*). Due to their high electron affinities, these Fe-O species could be important oxidants with reactivities approaching that of the hydroxyl radical *(14)*. In a marked difference from the Fenton reaction, the Fe-O hypothesis works without the formation of $O_2^{\bullet-}$. Our results could

imply a greater susceptibility of the 3'-position in deoxyribose to oxidation by these Fe-O species formed by Fe(II)/EDTA. It is important to consider the role of phosphate in the DNA oxidation reactions associated with free and chelated Fe(II). Several groups have observed substantial increases in deoxyribose oxidation in DNA cause by both Fe(II) *(5)* and Fe(II)/EDTA *(18, 19)* in the presence of phosphate buffers. The yield of deoxyribose oxidation products was found to be linearly dependent on the phosphate buffer concentration for both oxidants *(5, 19)*. Due to the importance of phosphate *in vivo*, our experiments were conducted in the presence of 50 mM phosphate buffer at the physiological pH 7.4. At 50 mM phosphate concentration, 99% of all iron in solution is complexed to HPO_4^{2-} *(19)* unless it is complexed with EDTA.

The relatively lower level of PGA associate with Fe(II) compared to Fe(II)/EDTA, in spite of the overall deoxyribose oxidation higher level of deoxyribose oxidation, suggests that Fe(II) is bound to sites in DNA that either disfavor 3'-specific oxidation or that favor an alternative partitioning at the 3'-position. There is also the possibility that PGA is oxidized to phosphoglycolate, in a manner analogous to the observed oxidation of glyceraldehydes by Fe(II) *(14)*. Such a model has been proposed by Chevion *et al.* with iron inducing further damage to the same site under conditions of redox cycling *(20)*.

The present studies do not address the chemical identity of the oxidant as either hydroxyl radicals or ferryl complexes. However, Hertzberg *et al.* observed no single-strand break formation with up to 100 μM Fe(II)/EDTA or free Fe(II) treatment in the

presence of 10 mM Tris-HCl buffer *(21)*, which acts as a radical scavenger. This observation suggests that hydroxyl radicals play a dominant role in PGA formation specifically and deoxyribose oxidation generally. In comparison to γ-radiation, the yield of PGA residues induced by Fe(II)/EDTA is 5-fold higher. Even though Fe(II)/EDTA has been described as a radiomimetic agent that induces damage via the production of hydroxyl radicals, the observed differences in PGA production are consistent with marked differences in the yield of DNA base modifications induced by Fe(II)/EDTA and γ-radiation observed by Murata-Kamiya *et al. (22)*.

The observations with H_2O_2 in the Fe(II)/EDTA system serve to further complicate the picture. The introduction of H_2O_2 to the Fe(II)/EDTA system at a fixed Fe(II)/EDTA concentration led to a marked but nonlinear increase in PGA formation, a result consistent with H_2O_2 effects on 8-hydroxy-2'deoxyguanosine formation *(11)*. In contrast, Frelon *et al.*, found a decrease in the level of 2-hydroxy-2'-deoxyadenosine induced by Fe(II)/EDTA in the presence of H_2O_2 *(23)*. H_2O_2 also decreased the production of thiobarbituric acid (TBA) reactive products from deoxyribose *(19)*. The increased formation of PGA observed with Fe(II)/EDTA/H_2O_2 may indicate an increased accessibility of reaction of the C3' position in deoxyribose or a shift in the portioning of C3' oxidation of deoxyribose.

The non-linear dose-response evident for Fe(II) and Fe(II)/EDTA/H_2O_2 has been observed for other DNA oxidation products. For example, base damage induced by Fe(II)/EDTA/H_2O_2 is characterized by nonlinear behavior (*i.e.*, see references *11, 24*) as

is the formation of single strand breaks both *in vitro (25)* and *in vivo (26)* and the formation of phosphoglycolate residues in cells treated with H_2O_2 *(27)*. Aldehydic DNA lesions in HeLa cells investigated using an aldehyde reactive probe (ARP) also exhibit a non-linear response *(28)*. On the other hand, Frelon *et al.* report a linear dose response for seven different base lesions *(29)*. The problem with their studies is that they added Fe(II)/EDTA before adding H_2O_2 which could have affected the DNA oxidation reaction given the rapid reaction of Fe(II)/EDTA with DNA. The authors also claimed that Fe(II)/EDTA and Fe(II) give rise to the same base damage distribution, but failed to show any quantitative comparisons *(29)*.

Our results with Fe/EDTA/H_2O_2 are reminiscent of the studies done by Linn and coworkers. They showed two kinetically different modes of killing *in vivo* with a maximum at lower H_2O_2 concentrations, a progressive decrease as the H_2O_2 concentration is raised and a concentration independent minimum in lethality at higher concentrations *(30)*. Luo *et al.* showed the same complex kinetics using a plasmid nicking assay *(30)*. The authors concluded that there are three types of oxidant based on reactivities with H_2O_2, with alcohols, and with iron chelators. The type I oxidant is sensitive to H_2O_2 concentrations but moderately resistant to the presence of ethanol. In this scenario, iron is loosely associated with DNA. Luo *et al.* suggested that this could be a ferryl oxidant that is formed in Fe(II)/EDTA/H_2O_2 *(30)*. The type II oxidant proved to be very resistant to both H_2O_2 and ethanol, which suggested that iron is intimately associated with DNA through coordination with a base nitrogen alone or simultaneously with the phosphate backbone *(30)*. This would not be expected in our experiments using

Fe(II)/EDTA/H_2O_2 *(30)* but type I and type II oxidants could be responsible for the damage observed for Fe(II). The type III oxidant is sensitive to both H_2O_2 and ethanol, suggesting that iron is not associated with DNA *(30)* as is presumably the case for our Fe(II)/EDTA and Fe/EDTA/H_2O_2 experiments.

Comparing our results for PGA formation induced by Fe(II)/EDTA/H_2O_2 and γ-radiation (Figure III-1) reveals a marked difference in PGA formation. Interestingly, Kennedy *et al.* observed that Fe(II)/EDTA/H_2O_2 and γ-radiation generate similar amounts of 8-oxo-dG *(31)*. In contrast, our findings of greater relative PGA formation induced by Fe(II)/EDTA/H_2O_2 argue that the specific oxidizing species either preferentially targets the C3' position in deoxyribose, especially when compared to the random distribution of damage reported for γ-radiation *(32)*, or that the partitioning of C3' oxidation as shown in Scheme I-3 is affected by the oxidizing species or other aspects of the reaction conditions.

6. REFERENCES

(1) Burkitt, M.J. (2003). Chemical, biological and medical controversies surrounding the Fenton reaction. *Progress in reaction kinetics and mechanism* ***28***, 75-103.

(2) Hertzberg, R.P., Dervan, P.B. (1982). Cleavage of double helical DNA by (methidiumpropyl-EDTA)iron(II). *J Am Chem Soc* ***104***, 313-315.

(3) Bull, C., McClune, G.J., Fee, J.A. (1983). The Mechanism of Fe-EDTA catalyzed superoxide dismutation. *J Am Chem Soc* ***105***, 5290-5300.

(4) Cohen, G., Sinet, P.M. (1980). Fenton's reagent - once more revisited. *Developments in Biochemistry* ***11A***, 27-37.

(5) Svoboda, P., Harms-Ringdahl, M. (2002). Kinetics of phosphate-mediated oxidation of ferrous iron and formation of 8-oxo-2'-deoxyguanosine in solutions

of free 2'-deoxyguanosine and calf thymus DNA. *Biochimica et biophysica acta.* ***1571(1)***, 45-54.

(6) von Sonntag, C. (1987). The Chemical Basis of Radiation Biology (New York: Taylor & Francis).

(7) Dizdaroglu, M., Jaruga, P., Birincioglu, M., Rodriguez, H. (2002). Free radical-induced damage to DNA: mechanisms and measurement. *Free radical biology & medicine.* ***32(11)***, 1102-1115.

(8) Pogozelski, W.K., Tullius, T.D. (1998). Oxidative strand scission of nucleic acids: routes initiated by hydrogen abstraction from the sugar moiety. *Chem. Rev.* ***98***, 1089-1107.

(9) Rush, J.D., Maskos, Z., Koppenol, W.H. (1990). Distinction between hydroxyl radical and ferryl species. *Methods in enzymology.* ***186***, 148-156.

(10) Rai, P., Cole, T.D., Wemmer, D.E., Linn, S. (2001). Localization of Fe(2+) at an RTGR sequence within a DNA duplex explains preferential cleavage by Fe(2+) and H2O2. *Journal of molecular biology.* ***312(5)***, 1089-1101.

(11) Colwell, B.A., Morris, D.L., Jr. (2003). Formation of the oxidative damage marker 8-hydroxy-2'-deoxyguanosine from the nucleoside 2'-deoxyguanosine: parameter studies and evidence of Fe(II) binding. *Journal of inorganic biochemistry.* ***94(1-2)***, 100-105.

(12) Celender, D.W., Cech, T.R. (1990). Iron(II)-ethylenediaminetetraacetic acid catalyzed cleavage of RNA and DNA oligonucleotides: similar reactivity toward single-and double-stranded forms. *Biochemistry* ***29***, 1355-1361.

(13) Tullius, T.D., Dombroski, B.A. (1985). Iron(II) EDTA used to measure the helical twist along any DNA molecule. *Science* ***230***, 679-681.

(14) Qian, S.Y., Buettner, G.R. (1999). Iron and dioxygen chemistry is an important route to initiation of biological free radical oxidations: an electron paramagnetic resonance spin trapping study. *Free radical biology & medicine.* ***26(11-12)***, 1447-1456.

(15) Breiner, K.M., Daugherty, M.A., Oas, T.G., Thorp, H.H. (1995). An anionic diplatinum DNA photocleavage agent: chemical mechanism and footprinting of the lambda repressor. *J Am Chem Soc* ***117***, 11673-11679.

(16) Rush, J.D., Koppenol, W.H. (1986). Oxidizing intermediates in the reaction of ferrous EDTA with hydrogen peroxide. Reactions with organic molecules and ferrocytochrome c. *The Journal of biological chemistry.* ***261(15)***, 6730-6733.

(17) Wink, D.A., Nims, R.W., Saavedra, J.E., Utermahlen, W.E., Jr.;, Ford, P.C. (1994). The Fenton oxidation mechanism: reactivities of biologically relevant substrates with two oxidizing intermediates differ from those predicted for the hydroxyl radical. *Proceedings of the National Academy of Sciences of the United States of America.* ***91(14)***, 6604-6608.

(18) Gutteridge, J.M. (1984). Reactivity of hydroxyl and hydroxyl-like radicals discriminated by release of thiobarbituric acid-reactive material from deoxy sugars, nucleosides and benzoate. *The Biochemical journal.* ***224(3)***, 761-767.

(19) Winterbourn, C.C. (1991). Factors that influence the deoxyribose oxidation assay for Fenton reaction products. *Free radical biology & medicine.* ***11(4)***.

(20) Chevion, M. (1988). A site-specific mechanism for free radical induced biological damage: the essential role of redox-active transition metals. *Free radical biology & medicine.* ***5(1)***.

(21) Hertzberg, R.P., Dervan, P.B. (1984). Cleavage of DNA with methidiumpropyl-EDTA-iron(II): Reaction conditions and product analyses. *Biochemistry* ***23***, 3934-3945.

(22) Murata-Kamiya, N., Kamiya, H., Muraoka, M., Kaji, H., Kasai, H. (1997). Comparison of oxidation products from DNA components by gamma- irradiation and Fenton-type reactions. *J. Radiat. Res. (Tokyo)* ***38***, 121-131.

(23) Frelon, S., Douki, T., Cadet, J. (2002). Radical oxidation of the adenine moiety of nucleoside and DNA: 2-hydroxy-2'-deoxyadenosine is a minor decomposition product. *Free radical research.* ***36(5)***, 499-508.

(24) Lloyd, D.R., Phillips, D.H. (1999). Oxidative DNA damage mediated by copper(II), iron(II) and nickel(II) Fenton reactions: evidence for site-specific mechanisms in the formation of double-strand breaks, 8-hydroxydeoxyguanosine and putative intrastrand cross-links. *Mutation research.* ***424(1-2)***, 23-36.

(25) Ambroz, H.B., Bradshaw, T.K., Kemp, T.J., Kornacka, E.M., Przybytnia, G.K. (2001). Role of ions in damage to DNA: influence of ionizing radiation, UV light and H2O2. *Journal of Photochemistry and Photobiology A: Chemistry* ***142***, 9-18.

(26) Hoffmann, M.E., Mello-Filho, A.C., Meneghini, R. (1984). Correlation between cytotoxic effect of hydrogen peroxide and the yield of DNA strand breaks in cells of different species. *Biochimica et biophysica acta.* ***781(3)***, 234-238.

(27) Bertoncini, C.R., Meneghini, R. (1995). DNA strand breaks produced by oxidative stress in mammalian cells exhibit 3'-phosphoglycolate termini. *Nucleic Acids Res* ***23***, 2995-3002.

(28) Nakamura, J., Purvis, E.R., Swenberg, J.A. (2003). Micromolar concentrations of hydrogen peroxide induce oxidative DNA lesions more efficiently than millimolar concentrations in mammalian cells. *Nucleic acids research.* ***31(6)***, 1790-1795.

(29) Frelon, S., Douki, T., Favier, A., Cadet, J. (2002). Comparative study of base damage induced by gamma radiation and Fenton reaction in isolated DNA. *J Chem Soc Perkin Trans 1*, 2866-2870.

(30) Luo, Y., Han, Z., Chin, S.M., Linn, S. (1994). Three chemically distinct types of oxidants formed by iron-mediated Fenton reactions in the presence of DNA. *Pro. Natl. Acad. Sci. USA* ***91***, 12438-12442.

(31) Kennedy, L.J., Moore Jr., K., Caulfield, J.L., Tannenbaum, S.R., Dedon, P.C. (1997). Quantitation of 8-oxoguanine and strand breaks produced by four oxidizing agents. *Chem. Res. Toxicol.* ***10***, 386-392.

(32) Goodhead, D.T. (1989). The initial physical damage produced by ionizing radiations. *International journal of radiation biology.* ***56(5)***, 623-634.

Chapter V

The Chemistry of Peroxynitrite-induced 3'-Phosphoglycolaldehyde

1. ABSTRACT

Peroxynitrite ($ONOO^-$) is a chemical mediator of macrophage-induced inflammation and it may represent an important source of endogenous damage to biomolecules such as proteins, lipids and DNA. The observation of the modulation of $ONOO^-$ chemistry in the presence of carbon dioxide due to the formation of nitrosoperoxycarbonate ($ONOOCO_2^-$) has led to an increased interest in understanding $ONOO^-$ and $ONOOCO_2^-$ damage chemistries. To extend our efforts to relate $ONOO^-$ and $ONOOCO_2^-$ chemistries to DNA deoxyribose oxidation, we measured the total deoxyribose oxidation and 3'-phosphoglycolaldehyde (PGA) formation in DNA after exposure to $ONOO^-$ (0 – 1000 μM for PGA formation and 0 – 32 μM for total deoxyribose oxidation) in the presence of bicarbonate concentrations between 0 and 100 mM. The calculated concentration of carbon dioxide associated with these bicarbonate concentrations range from 11 μM to 10 mM. As expected, we found that PGA formation and deoxyribose oxidation in general were suppressed by increasing bicarbonate concentrations. The suppression is nonlinear and becomes independent of $ONOO^-$

concentration at high $ONOO^-$ concentrations. To further understand this nonlinear behavior, we studied the $ONOO^-$ induced oxidation of PGA, both free and bound to an oligodeoxynucleotide, in the presence and absence of 25 mM bicarbonate. Carbon dioxide was also found to affect the selectivity of the reaction of $ONOO^-$ with free and oligodeoxynucleotide-bound PGA. In the absence of bicarbonate, free PGA was more readily oxidized than PGA incorporated into an oligodeoxynucleotide, with the situation reversed in the presence of 25 mM bicarbonate. By itself, the level of PGA oxidation by $ONOO^-$ and $ONOOCO_2^-$ cannot account for the non-linearity of PGA formation and total deoxyribose oxidation.

2. INTRODUCTION

It has been demonstrated that there is an association between chronic inflammation and increased cancer risk. Examples are inflammatory bowel disease and colon cancer *(1)*, *Heliobacter pylori* infection and gastric cancer *(2)*, and *Schistosoma heamatobium* infection and bladder cancer *(3)*. During the process of inflammation, activated macrophages generate large amounts of nitric oxide ($NO^\bullet$) by up-regulation of inducible $NO^\bullet$ synthase. At the same time, there is concomitant production of superoxide ($O_2^{\bullet-}$) *(4)*. These two species react to produce peroxynitrite ($ONOO^-$) with a rate constant between 6.6 and 19 x 10^9 M^{-1} s^{-1}, which is at least 3- to 8-times greater than the rate of $O_2^{\bullet-}$ decomposition by superoxide dismutase *(4)* and therefore of potential importance *in vivo*. $ONOO^-$ is formed either within generator cells or extra-cellularly, or $NO^\bullet$ can diffuse into adjacent cells and react with intra cellular $O_2^{\bullet-}$. Both mechanisms allow cells

to be exposed to $ONOO^-$, which has been shown to be both cytotoxic and mutagenic in cultured mammalian cells *(5, 6)*.

Prerequisite to an understanding of $ONOO^-$ oxidation reactions is an understanding of the complex underlying chemistries and the impact of CO_2 on $ONOO^-$ chemistry. Even though there is much controversy surrounding the mechanism of $ONOO^-$ decomposition, NO_3^- is a major product in the absence of CO_2. In solution, the radical intermediates of the decomposition of $ONOO^-$ are surrounded by a solvent cage that hinders the radicals from separation by diffusion. Therefore the majority of formed radicals will react with each other, but not necessarily to form the precursor $ONOO^-$. Approximately two-third of the radicals degrading into NO_3^- never escape the solvent cage, whereas one-thirds diffuse from the solvent cage and become free radicals (see Scheme V-1) *(7)*. There is, however, some evidence for peroxynitrous acid as the mediator of oxidation *(8)*. Approximately 5% of $ONOO^-$ decomposes to NO_2^- and O_2 *(9)*, which is not the case in the presence of bicarbonate.

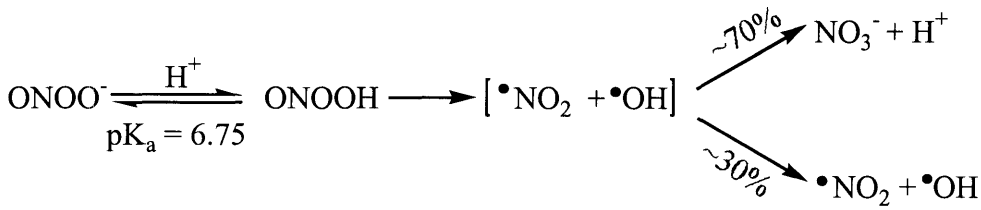

Scheme V-1: Decomposition of $ONOO^-$ *(10)*.

The known reactions of $ONOO^-$ can be divided into at least five mechanistic classes: (a) isomerization to nitrate, (b) one-electron or (c) two-electron oxidations, (d)

oxygen atom transfers, and (e) electrophilic nitrations *(11)*. $ONOO^-$ has also been shown to diffuse across biological membranes *(12)*, to react with proteins, lipids and other biologically relevant molecules. The reaction of $ONOO^-$ with DNA produces three major types of damage: direct strand breaks due to oxidation of deoxyribose, nitration of guanine, and oxidation of guanine *(13)*.

In contrast to the proton catalyzed decomposition as shown in Scheme V-1, the presence of carbon dioxide leads to an alternative route of decomposition (*i.e.* reference *10*) at a rate of $3 - 6 \times 10^4\ M^{-1}\ s^{-1}$ *(14)*, with the generation of nitrosoperoxycarbonate ($ONOOCO_2^-$) (see Scheme V-2). This species has a significantly shorter half-life (~ 50 ms) than $ONOO^-$ (~ 1 s) *(15)*. Homolysis of the O-O bond produces the carbonate radical anion ($CO_3^{\bullet-}$) and the $NO_2^\bullet$ radical (*i.e.* references *9, 11, 16*). About two-thirds of the $ONOOCO_2^-$ decomposes to NO_3^-, while about one-third of the caged $CO_3^{\bullet-}$ and $NO_2^\bullet$ escape as free radicals *(9, 17)* capable of reacting with biomolecules or recombining to give NO_3^- and CO_2 (see Scheme V-2). $CO_3^{\bullet-}$, with a reducing potential of E = 1.78 V *(18)*, is a much stronger oxidizing agent than $NO_2^\bullet$ (E = 0.99 V *(19)*) and is responsible for many of the observed one-electron oxidations, whereas $NO_2^\bullet$ plays a role in nitrations. Normal plasma bicarbonate and CO_2 concentrations are 25 and 1.3 mM, respectively, but higher levels could be achieved during pathologic events in tissues, such as respiratory distress or ischemia reperfusion *(20)*. Excess production of $ONOO^-$ has been documented to occur during these and other instances of accelerated tissue $O_2^{\bullet-}$ and $NO^\bullet$ production, which enhances the potential for coordinated reaction mechanisms to occur between CO_2/HCO_3^-, $ONOO^-$ and tissue target molecules *(20)*.

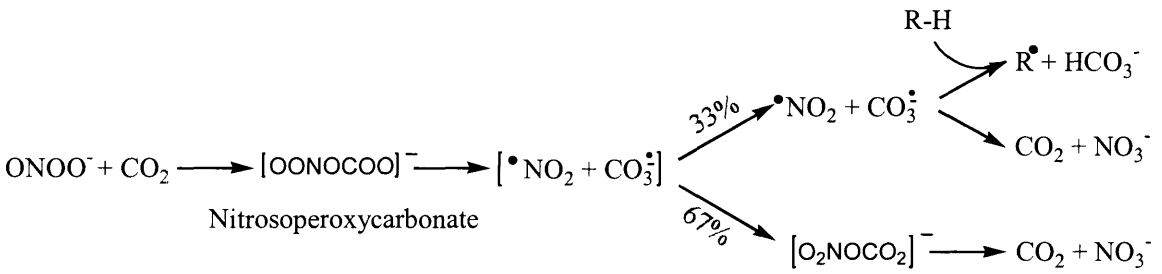

Scheme V-2: Reaction of $ONOO^-$ with CO_2 *(10)*.

$ONOO^-$ has been found to be a very potent bactericidal agent *(21, 22)*. However, introducing bicarbonate (24 mM) at pH 7.4 to *E. coli* suspensions was sufficient to protect the bacteria from otherwise lethal $ONOO^-$ concentrations *(22)*. The authors concluded that $ONOOCO_2^-$ is physically excluded from reaching the vulnerable bacterial sites such as DNA or alternatively that the life-time of the resulting $ONOOCO_2^-$ is too short to allow appreciable reaction with the bacterium *(22)*. It has been recognized recently that the proportions of the various DNA products strongly depend on the presence of CO_2 and thus the formation of $ONOOCO_2^-$ *(13, 23)*. $ONOO^-$ causes predominantly deoxyribose oxidation *(13)*, while in the presence of 25 mM bicarbonate at pH 7.4, base damage involving mainly guanine becomes the predominant oxidation target with a large increase in the production of 8-nitro-dG *(13)*. While there is a shift from sugar to base damage chemistry in the presence of CO_2, the total quantity of DNA damage remains unchanged *(13)*.

The effect of bicarbonate, and thus CO_2, on DNA strand breaks and nitro-8-G formation has been studied by Yermilov *et al. (23)* at a $ONOO^-$ concentration of 0.1 mM and bicarbonate concentrations between 0 – 50 mM. While their results revealed a

suppression of strand break formation as a function of bicarbonate concentration, their studies were plagued by a flawed strand break assay that caused an underestimation of actual induced damage. Therefore, we decided to repeat the experiment performed by Yermilov *et al.* under so-called single-hit conditions where damage does not exceed 30% nicking.

Since there is ample evidence for the formation of increased base damage at increased bicarbonate concentrations *(4, 13, 24)*, we decided to study the effects of CO_2 on a specific deoxyribose $ONOO^-$ oxidation product, 3'-phosphoglycolaldehyde (PGA), and relate this to total deoxyribose oxidation. PGA has been shown earlier to be a general deoxyribose oxidation product induced by Fenton chemistry (see Chapter IV) and radiation (see Chapter III), both oxidative agents that have historically been associated with hydroxyl radical-induced damage. However, it is not known whether $CO_3^{\bullet-}$ is capable of inducing deoxyribose oxidation.

3. MATERIALS AND METHODS

3.1 Materials. All chemicals and reagents were the highest purity available and were used without further purification unless noted otherwise. Calf thymus DNA, Nuclease P1, *bis*(trimethylsilyl)trifluoroacetamide (containing 1% trimethylchlorosilane), diethylenetriaminepentaacetic acid, 1 N NaOH and pentafluorobenzylhydroxylamine were purchased from Sigma Chemical Co. (St. Louis, MO). K_2HPO_4, KH_2PO_4, $NaHCO_3$ and ethyl acetate were purchased from Mallinckrodt Baker (Phillipsburg, NJ). Chelex

resin was purchased from BioRad. Distilled and deionized water was further purified with a Milli-Q system (Millipore Corporation, Bedford, MA) and was used in all experiments.

3.2 Instrumental Analyses. GC/MS analyses of derivatized PGA were performed with a HP6890 gas chromatograph (HP7673 auto-injector) coupled to a Hewlett Packard 5973N mass selective detector. UV spectra were obtained using a Beckman DU 640 UV-visible spectrophotometer.

3.3 Preparations of buffers. Buffers containing 50 mM phosphate buffer, pH 7.4 were prepared containing between 0 and 100 mM $NaHCO_3$. The buffers were treated with Chelex resin at 4 °C overnight (5 g Chelex resin for 4 L of buffer) and then buffers were filtered using a 0.2 μm filter. Buffers were stored at 4 °C.

3.4 Preparations of DNA. Calf thymus DNA and plasmid pUC19 were dissolved at a concentration of 1 mg/ml in Chelex-treated 50 mM potassium phosphate buffer, pH 7.4 containing various concentrations of $NaHCO_3$, and dialyzed four times against 4 L of the respective buffer. The first dialysis step was conducted in the presence of 1 mM diethylenetriaminepentaacetic acid.

3.5 Calf thymus DNA oxidation by $ONOO^-$. $ONOO^-$ was prepared as described by Pryor *et al. (25)*. Briefly, ozone generated in a Welsbach ozonator was bubbled into 100 ml of 0.1 M sodium azide in water chilled in an ice bath. After 45 min of ozonation,

the $ONOO^-$ concentration was measured in 0.1 N NaOH using an absorption coefficient of ε_{302} = 1670 M^{-1} cm^{-1} *(25)*. The 30 mM $ONOO^-$ stock solution in 0.1 N NaOH was stored at -80 °C. The thawed $ONOO^-$ stock was kept on ice at all times during use. The $ONOO^-$ concentration was determined as described above immediately before use. A 25 mM stock solution of $ONOO^-$ was prepared by dilution of the stock with ice cold 0.1 N NaOH. Calf thymus DNA (170 μg; 1 mM nt) in Chelex-treated buffer, pH 7.4, was treated with $ONOO^-$ by addition of up to 10 μl increments *via* bolus addition to give a final concentration between 0 and 1 mM. [$^{13}C_2$]–PGA (200 pmol; internal standard; synthesis described in Chapter II, section 3.4) was added immediately after damage induction, due to the observation that $ONOO^-$ oxidizes the internal standard. Samples treated with less than 1000 μM $ONOO^-$ received additional 0.1 N NaOH to achieve a final NaOH concentration of 4 mM. Calibration samples also received 4 mM of 0.1 N NaOH. Quantification of PGA was performed as described in Chapter III, section 3.5.

3.6 Quantification of PGA oxidation by $ONOO^-$. Samples containing 170 μg of calf thymus DNA (1 mM nt) in Chelex-treated 50 mM potassium phosphate buffer with and without 25 mM sodium bicarbonate, pH 7.4, were treated with $ONOO^-$ by addition of up to 10 μl increments via bolus addition to final concentrations of 10, 100 and 1000 μM $ONOO^-$ either in the presence or absence of 1, 10 and 100 pmol PGA or a PGA-containing oligodeoxynucleotide (oligo-PGA; for syntheses, see Chapter II, sections 3.3 and 3.5). To samples that contained no PGA and oligo-PGA during $ONOO^-$ treatment, 1, 10 and 100 pmol PGA or PGA-containing oligonucleotide were added immediately after $ONOO^-$ addition. All samples received 200 pmol of [$^{13}C_2$]–PGA as an

internal standard immediately after damage induction. Samples treated with less than 1000 μM $ONOO^-$ received additional 0.1 N NaOH to achieve a final NaOH concentration of 4 mM. . Calibration samples also received 4 mM of 0.1 N NaOH. Samples were then subjected to PGA quantification as described in Chapter III, section 3.5. PGA signals obtained from samples treated with $ONOO^-$ in the absence of added PGA and oligo-PGA were subtracted from signals obtained from samples where PGA and oligo-PGA was added before $ONOO^-$ treatment. This constitutes the amount of PGA oxidized by $ONOO^-$, leading to a loss in PGA signal.

3.7 Quantification of total deoxyribose oxidation (performed by Mr. Xinfeng Zhou). As an index of total deoxyribose oxidation, plasmid topoisomer analysis was employed to quantify DNA strand breaks and abasic sites produced by $ONOO^-$ under identical conditions as for the oxidation of calf thymus DNA. Plasmid pUC19 (20 μg in a total reaction volume of 60 μl) was treated with $ONOO^-$ as described above for calf thymus DNA. For the experimental procedure to quantify total deoxyribose oxidation see Chapter III, section 3.6.

4. RESULTS

4.1 Modulation of PGA in DNA oxidized by $ONOO^-$. Samples containing calf thymus DNA and 0 to 100 mM sodium bicarbonate (or 0.3 mM sodium bicarbonate and 99.7 mM NaCl to assess the effect of ionic strength) were subjected to oxidation by $ONOO^-$ over the range of 0 to 1 mM *via* bolus addition. $ONOO^-$ has a half-life of ~ 1 s at pH 7.4 and the nitrate breakdown products are inert *(26)*. Immediately after damage induction, the internal standard [^{13}C]-PGA was added. The samples were then processed for GC/MS analysis of PGA. The results for PGA formation are shown in Figure V-1A. Over the $ONOO^-$ dose range studied, PGA formation in the absence of bicarbonate was found to be reasonably linear (r^2=1) with a slope of 0.2 PGA molecules per 10^6 nt per μM $ONOO^-$. PGA formation in the presence of 25 and 100 mM sodium bicarbonate were below the detection limit of 2 PGA per 10^6 nt (data not shown). With increasing bicarbonate concentration, PGA formation deviated from linearity and could better be described by a second-order polynomial function.

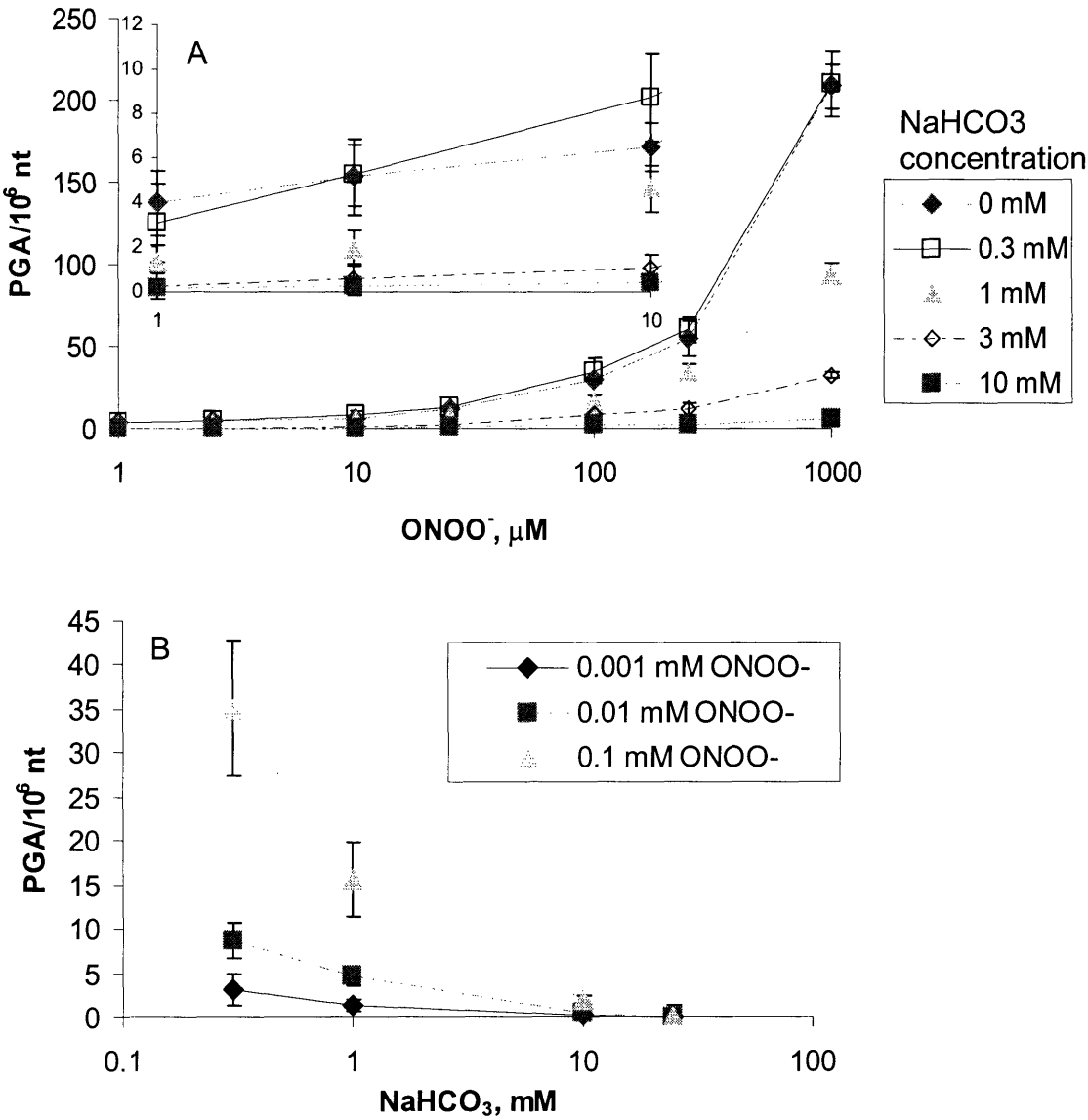

Figure V-1: PGA levels in calf thymus DNA treated with 0 – 1 mM $ONOO^-$ in 50 mM phosphate buffer containing 0 – 10 mM sodium bicarbonate. DNA samples were processed for GC/MS analysis as described in the Chapter III, section 3.5. The data represent the mean ± SD of three independent experiments. **A:** Plots $ONOO^-$-induced PGA formation at constant bicarbonate concentrations; **B:** Effects of sodium bicarbonate concentration on $ONOO^-$-induced PGA formation.

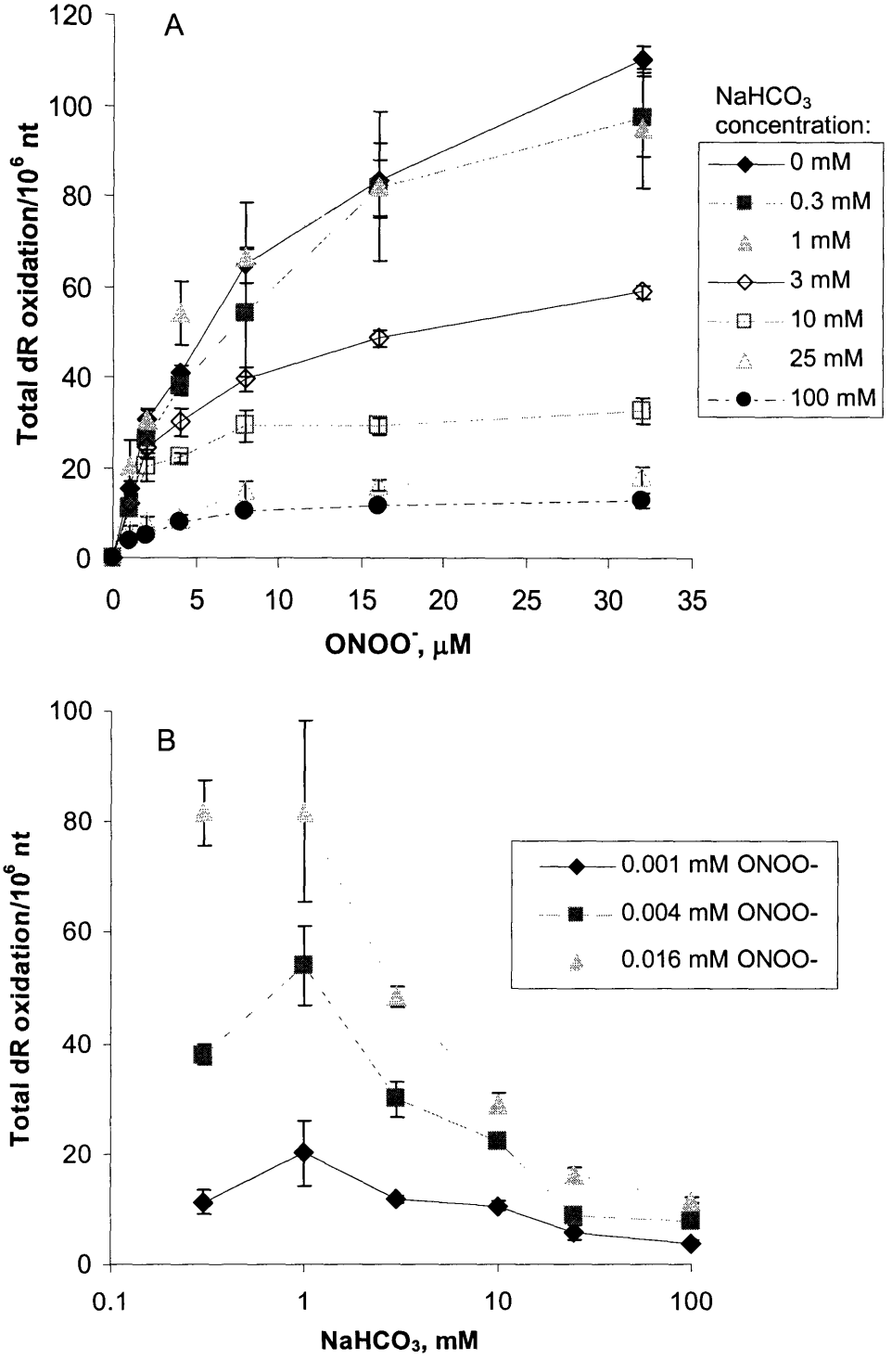

Figure V-2: Effect of bicarbonate concentration on the total quantity of deoxyribose oxidation events produced by $ONOO^-$. Experiments were performed by Mr. Xinfeng

Zhou. Supercoiled pUC19 DNA was exposed to 0 – 32 μM $ONOO^-$ and then treated with putrescine to convert abasic sites to strand breaks. The proportion of nicked, circular plasmid (*i.e.*, strand breaks + abasic sites) closely approximates the total number of deoxyribose oxidation events. The data represents the mean ± SD for three independent experiments.

The fraction of deoxyribose oxidation events that produced a PGA residue was estimated by topoisomer analysis (experiments performed by Mr. Xinfeng Zhou). Variation in the quantity of total deoxyribose oxidation events per μM of $ONOO^-$ was nonlinear, as shown in Figure V-2. The dose response in this case can best be described by a logarithmic function. Due to the nonlinear nature of PGA induction by $ONOO^-$ the number of PGA molecules per total deoxyribose oxidation event is not constant but $ONOO^-$ concentration dependent.

4.2 Fate of PGA in DNA oxidized by $ONOO^-$. To investigate the basis for our observation that samples containing the internal standard before $ONOO^-$ treatment exhibited a marked decrease in signal intensity in comparison to calibration samples, we quantified the disappearance of PGA induced by $ONOO^-$ treatment. For this purpose, samples containing 170 μg calf thymus DNA in potassium phosphate buffer (50 mM, pH 7.4) with or without 25 mM sodium bicarbonate were subjected to oxidation by $ONOO^-$ before or after the addition of PGA or a 3'-PGA-containing oligodeoxynucleotide. In all cases, the internal standard [^{13}C]-PGA was added after $ONOO^-$ treatment. The samples were then processed for GC/MS analysis of PGA. The loss of PGA as a function of PGA or $ONOO^-$ and bicarbonate concentration is shown in Figure V-3.

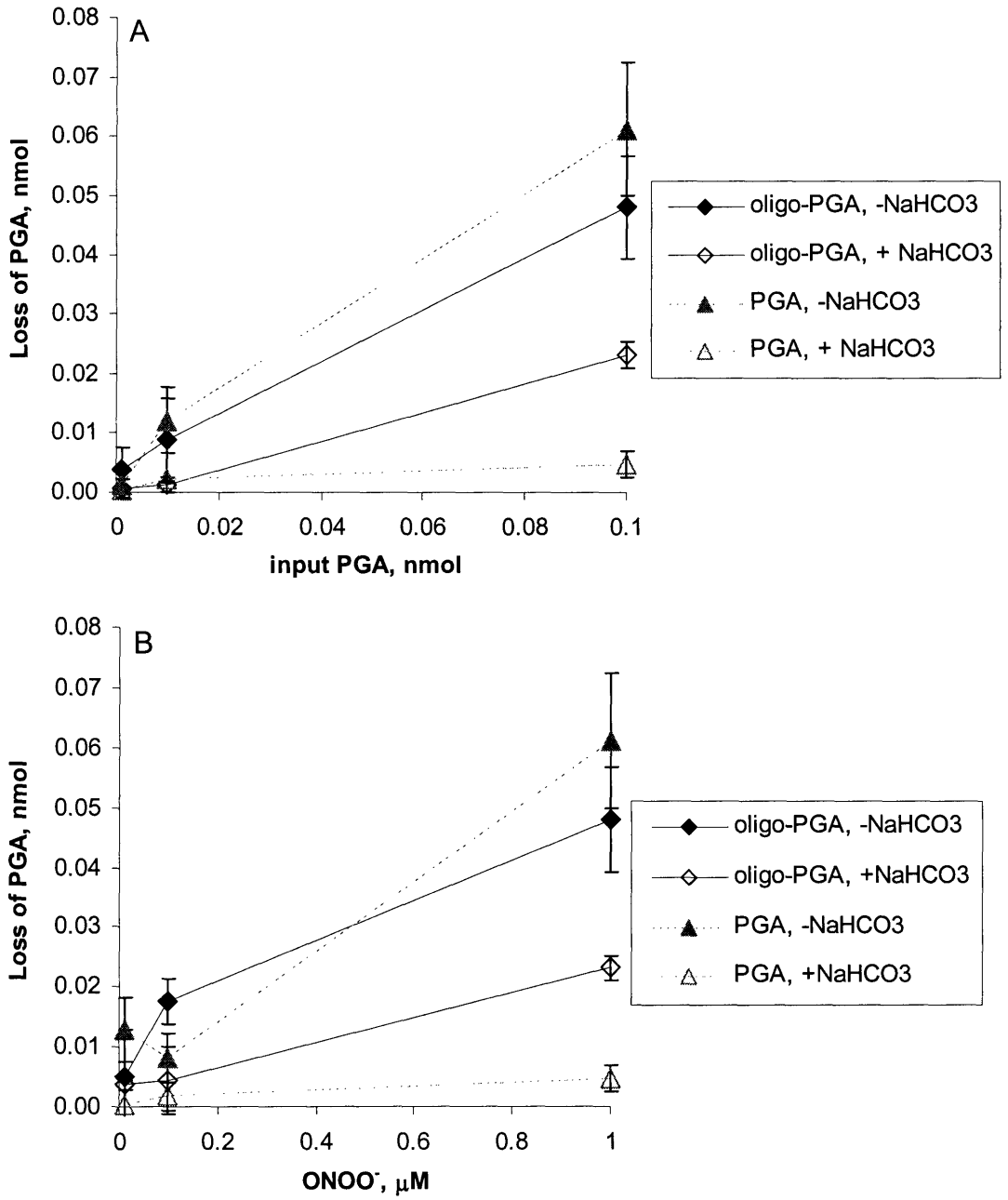

Figure V-3: The loss of PGA in calf thymus DNA treated with $ONOO^-$ in 50 mM phosphate buffer (pH 7.4) with or without 25 mM sodium bicarbonate. **A:** 1, 10 or 100 pmol of PGA or a 3-PGA-containing oligonucleotide were added either before or after $ONOO^-$ treatment. **B:** Samples were treated with 0.01, 0.1 and 1 mM $ONOO^-$ in the presence or absence of 100 pmol PGA or oligo-PGA. After oxidation, samples were

processed for GC/MS analysis as described in Chapter III, section 3.5. The data represents the mean ± SD of three independent experiments.

In the presence of 25 mM bicarbonate, $ONOO^-$ is less efficient in oxidizing PGA free in solution and bound to DNA. However, free PGA is less readily oxidized than PGA in the oligo. In contrast, in the absence of bicarbonate, the opposite effect is observed: free PGA shows a greater loss than PGA bound to DNA.

5. DISCUSSION

Mounting evidence suggests that $ONOO^-$ causes mainly deoxyribose oxidation in DNA, while the presence of carbon dioxide causes damage to shift to guanine *(13)*. As has been shown by Yermilov *et al.*, the presence of bicarbonate inhibits the production of $ONOO^-$-induced strand breaks in plasmid DNA *(23)*. However, Yermilov *et al.* studied only one $ONOO^-$ concentration, so little insight was gained into the effect of carbon dioxide chemistry on $ONOO^-$ reactivity with DNA. We expected to see biphasic behavior at low bicarbonate concentrations, in which carbon dioxide would suppress $ONOO^-$ induced deoxyribose oxidation until the $ONOO^-$ concentration exceeded the carbon dioxide concentration, at which point there would be an increase in $ONOO^-$ induced deoxyribose oxidation. However, while our results reveal carbon dioxide-induced suppression of deoxyribose oxidation and PGA formation (see Figure V-1 and Figure V-2) the suppression of deoxyribose oxidation was never complete, even at 100 mM bicarbonate. These results lead to three main points of discussion: (1), that bicarbonate

suppresses the formation of PGA and deoxyribose oxidation; (2), that deoxyribose oxidation occurs even at high bicarbonate concentrations; and (3), that deoxyribose oxidation and PGA formation eventually become independent of $ONOO^-$ concentration.

First, we will discuss the overall suppression of PGA formation and deoxyribose oxidation by bicarbonate. Tretyakova *et al.* have shown that, in the presence of bicarbonate, the damage spectrum induced by $ONOO^-$ shifts towards base oxidation *(13)*, which explains the decrease in PGA formation and deoxyribose oxidation with increasing bicarbonate concentration. They hypothesized that $ONOOCO_2^-$ favors nitration over oxidation reactions at the expense of deoxyribose oxidation in DNA *(13)*. Alternatively, it is possible that the $CO_3^{\bullet-}$ radical is not energetic enough or too selective to abstract the 3'-hydrogen from deoxyribose. This is supported by observations that, in contrast to the hydroxyl radical, the $CO_3^{\bullet-}$ radical is relatively selective and discriminating for phenolic residues (*e.g.*, tyrosine), indolic moieties (*e.g.*, tryptophan, melatonin), sulfides *(e.g.*, methionine) and selenides (*e.g.*, selenomethionine, selenocysteine) *(10)*, as well as guanine in DNA *(27)*. All $CO_3^{\bullet-}$ radical hydrogen abstraction reactions studied so far involve hydrogens from OH and SH groups and αC-hydrogen atoms in primary amines *(28)*. In general, hydrogen atom abstraction reactions mediated by $CO_3^{\bullet-}$ were found to be slower than electron transfer reactions *(28)*. This may explain the decrease in total deoxyribose oxidation, and thus in PGA formation, presented here, since deoxyribose oxidation as discussed in Chapter I involves carbon-hydrogen bond breaking. The negative charge of $CO_3^{\bullet-}$ could lead to charge repulsion with the sugar-phosphate backbone in DNA and thus to lower deoxyribose reactivity. This is supported by the

hypothesis that solvent exposure of the sites of hydrogen atom abstraction plays a role in reaction with $CO3^{\bullet-}$ radicals *(28)*. However, this does not support the increase in guanine oxidation in the presence of carbon dioxide.

Second, we will discuss why deoxyribose oxidation occurs even at high bicarbonate concentrations. The presence of sodium bicarbonate has been shown to inhibit the oxidation of thiols, dimethylsulfoxide, cytochrome C *(20)* and glutathione *(29)*. Sodium bicarbonate has also been shown to inhibit $ONOO^-$-mediated formation of base propenals from DNA, a products of C4'-oxidation of deoxyribose. However, these workers used a non-physiological pH of 4.3 for these experiments *(23)*. From their results, Yermilov *et al.* concluded that the reactive species involved in strand breakage and base propenal formation were different from those involved in the nitration of guanine. They argue that deoxyribose oxidation is caused by residual $ONOO^-$ in solutions containing carbon dioxide, and that the presence of $ONOO^-$ is decreased by increasing amounts of bicarbonate. Further they argue that nitrosoperoxycarbonate is responsible for nitration but incapable of oxidation of deoxyribose due to the low hydroxyl-like activity of $ONOOCO_2^-$. This hypothesis is supported by the observation of Romero *et al.* who studied the oxidation of intracellular oxyhemoglobin by $ONOO^-$ in the presence of bicarbonate *(12)*. They observed that the oxidation of oxyhemoglobin was due solely to $ONOO^-$ because $ONOOCO_2^-$ is incapable of entering the cell and oxidizing the target. The physiological level of 25 mM bicarbonate in plasma corresponds to a concentration of 1.3 mM carbon dioxide *(20)*. In the presence of 25 mM bicarbonate, more than 20% of oxyhemoglobin was oxidized *(12)*, which suggests that at least 20% of $ONOO^-$ was not

converted to $ONOOCO_2^-$ in the presence of carbon dioxide regardless of the very fast reaction kinetics of $ONOOCO_2^-$ formation. The 1.3 mM carbon dioxide concentration at 25 mM bicarbonate exceeds our maximal $ONOO^-$ concentration and should lead to a total conversion of $ONOO^-$ to $ONOOCO_2^-$. However, we still observe residual deoxyribose oxidation at 25 mM bicarbonate, which may indicate that indeed residual $ONOO^-$ is responsible for the observed deoxyribose oxidation.

In the following, we discuss the observation that PGA formation and deoxyribose oxidation are suppressed even at bicarbonate concentrations well below $ONOO^-$ concentrations. In general, carbon dioxide represents about 10% of the total concentration of carbonate species at pH 7 *(30)*. Buffers containing no sodium bicarbonate that are equilibrated with dry, clean air contain 11 μM carbon dioxide (pH 7.4, 50 mM phosphate buffer, ambient temperature) *(30, 31)*. Therefore, carbon dioxide was present in all our experiments, since no effort was made to exclude carbon dioxide absorption from air into the buffers or stock solutions. The disappearance of $ONOO^-$ in the presence of excess bicarbonate, as is the case for the present experiments, follows pseudo-first-order kinetics *(20)*. The pseudo-first-order rate constants measured by Denicola *et al.* showed a linear dependence on bicarbonate concentrations at pH 7.4 and 25°C and represented an apparent second-order rate constant of 2.3×10^3 M^{-1} s^{-1} *(20)*. The half-life of the hydration-dehydration equilibrium of carbon dioxide is ~25 s in neutral solutions at ambient temperature *(14)*, and therefore is too slow to be a major source to replenish the carbon dioxide removed by reaction with $ONOO^-$. However, carbon dioxide has been shown to be a true catalyst for the decomposition of $ONOO^-$. The regeneration of carbon

dioxide from $ONOOCO_2^-$ adducts amounts to 92% at 1 mM bicarbonate under physiological conditions, and thus the carbon dioxide concentration even at excess ONOO- is never appreciably changed *(31)*. This explains our finding of the overall suppression of deoxyribose oxidation and PGA formation even at carbon dioxide concentrations that are well below $ONOO^-$ concentrations.

Finally, we discuss that deoxyribose oxidation and PGA formation eventually become independent of $ONOO^-$ concentration. The suppression of strand breaks as shown in Figure V-2B is reminiscent of the suppression of glutathione, bovine serum albumin and dimethylsulfoxide oxidation in reaching saturation after a certain $ONOO^-$ threshold concentration *(20)*. The authors explain this effect by the formation of a secondary oxidizing intermediate with a different reactivity toward the target molecule *(20)*. Lymar *et al.* made a similar observation in their studies of the carbon dioxide-catalyzed tyrosine nitration reaction *(15)* where only ~ 20% of the added $ONOO^-$ could be converted to products. The authors concluded that this observation indicated the existence of at least two forms of the reactive intermediate generated from $ONOOCO_2^-$, one that is reactive and the other that is unreactive towards tyrosine *(15)*. A similar observation was made by Lermercier *et al.* who studied the nitration of phenol and found direct correlation of bicarbonate concentration and nitration yield increase that, however, is limited to a maximum of 20% based on $ONOO^-$ converted to nitration products *(32)*. They added to the model of Lymar *et al.* that the solvent cage limits the escape of $CO_3^{\bullet-}$ and $NO_2^\bullet$ and therefore could be responsible for this observation *(32)*. Koppenol *et al.* offer a different explanation for the coexistence of reactive and unreactive forms of $ONOO^-$ *(19)*. In this

case, reactivity was proposed to be dictated by partitioning between *cis* and *trans* rotameric states, of which only the *trans* rotamer (or a reactive intermediate derived from it) is reactive *(22)*. Lymar *et al.* counter this model by arguing that changes in molecular conformation could not lead to differences in oxidizing potential between reactive and unreactive intermediates as large as have been observed *(9)*. They proposed that the unreactive intermediate is too short lived to engage in bi-molecular reactions *(9)*.

All of these models mentioned above could account for the overall decrease in PGA formation and deoxyribose oxidation in the presence of bicarbonate. However, none of the hypotheses plausibly explain the nonlinearity of the data presented here and in the literature (*i.e.*, references *(19, 20, 29, 32)*). Overall, there seems to be a factor that limits deoxyribose oxidation by $ONOO^-$ as a function of $ONOO^-$ concentration.

One explanation for the observed non-linear DNA damage dose response involves the further oxidation of the products with excess $ONOO^-$. Uppu *et al.* showed that aldehydes react with $ONOO^-$ to form addition products in a manner analogous to the carbon dioxide reaction *(33)*. This explains our observation that the internal PGA standard was lost during reaction with $ONOO^-$ and had to be added after damage induction, contrary to all other oxidizing agents we have studied. Nakao *et al.* demonstrated that $ONOO^-$ oxidizes acetaldehyde to formate and acetate at a total yield of 30 % of the initial $ONOO^-$ concentration and produces 10% methyl radicals (see Scheme V-3) *(34)*. Bicarbonate concentrations of 1 and 10 mM decreased the yield of methyl radicals produced by the oxidation of acetaldehyde by 20 and 80%, respectively *(34)*.

Interestingly, ketones have been shown to catalyze the decomposition of $ONOO^-$ at rate constants up to half of the reaction of $ONOO^-$ with CO_2 *(35, 36)*.

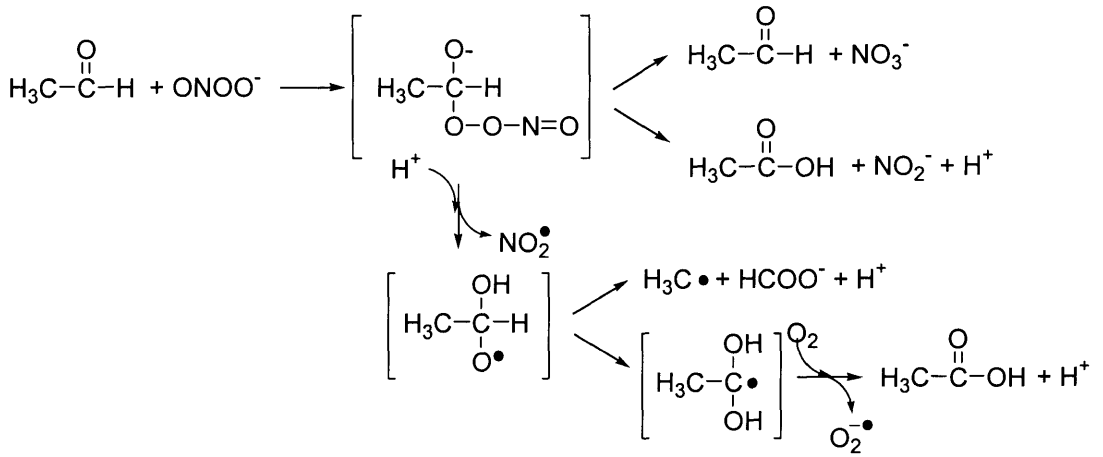

Scheme V-3: Oxidation of acetaldehyde by $ONOO^-$ *(34, 36)*.

A similar situation could occur in a reaction of PGA with $ONOO^-$. Since spontaneous decomposition of $ONOO^-$ to hydroxyl radicals and NO_3^- is slower than the direct reaction of $ONOO^-$ with aldehydes *(34)*, we would expect nucleophilic attacks as illustrated in Scheme V-3. However, the negative charge of PGA and $ONOO^-$ there could lead to charge repulsion that could influence the reaction rate. In our system, PGA is also competing with DNA for reaction with $ONOO^-$ and related $ONOO^-$ decomposition products, which complicates the interpretation of results. The rate of reaction of acetaldehyde with $ONOO^-$ (680 M^{-1} s^{-1}) is much slower than the rate of $ONOO^-$ reaction with CO_2 (3 x 10^4 M^{-1} s^{-1}) *(34)*, so we expected the yield of PGA oxidation to decrease in the presence of bicarbonate. This is indeed the case. However, the oxidation of PGA is not totally suppressed in the presence of 25 mM bicarbonate (1.3 mM carbon dioxide), even though the formation of PGA is below our detection limit. This may indicate that

$CO_3^{\bullet-}$ or $NO_2^{\bullet}$ are able to react with PGA but not form it. Similar observations were made by Uppu *et al.* for the nitration of ethyl-acetoacetate in the presence of bicarbonate *(37)*.

In conclusion, we have determined that the suppression of PGA formation and total deoxyribose oxidation by carbon dioxide varies as a function of the chemistry and concentration of $ONOO^-$. The results are consistent with several previous studies and extend the quantification of a little-explored deoxyribose oxidation product. However, the non-linearity of deoxyribose oxidation by ONOO- remains unexplained, although this effect has been observed for other reactants by other researchers (*i.e.*, references *19, 20, 29, 32*). Taken together, our findings suggest that $ONOOCO_2^-$ damage chemistry is far more complex than previously assumed and further studies are needed to investigate the precise kinetics of $ONOOCO_2^-$ reactions.

6. REFFERENCES

(1) Farrell, R.J., Peppercorn, M.A. (2002). Ulcerative colitis. *Lancet.* ***359(9303)***, 331-340.

(2) Asaka, M., Takeda, H., Sugiyama, T., Kato, M. (1997). What role does Helicobacter pylori play in gastric cancer? *Gastroenterology.* ***113(6) Suppl***, S56-60.

(3) Mostafa, M.H., Sheweita, S.A., O'Connor, P.J. (1999). Relationship between schistosomiasis and bladder cancer. *Clinical microbiology reviews.* ***12(1)***, 97-111.

(4) Dedon, P.C., Tannenbaum, S.R. (2004). Reactive nitrogen species in the chemical biology of inflammation. *Archives of biochemistry and biophysics.* ***423***, 12-22.

(5) Zhuang, J.C., Wright, T.L., deRojas-Walker, T., Tannenbaum, S.R., Wogan, G.N. (2000). Nitric oxide-induced mutations in the HPRT gene of human lymphoblastoid TK6 cells and in Salmonella typhimurium. *Environmental and molecular mutagenesis.* ***35(1)***.

(6) Zhuang, J.C., Lin, C., Lin, D., Wogan, G.N. (1998). Mutagenesis associated with nitric oxide production in macrophages. *Proceedings of the National Academy of Sciences of the United States of America.* ***95(14)***, 8286-8291.

(7) Gerasimov, O., Lymar, S.V. (1999). The yield of hydroxyl radical from the decomposition of peroxynitrous acid. *Inorg. Chem.* ***38***, 4317-4321.

(8) Maurer, P., Thomas, C.F., Kissner, R., Ruegger, H., Greter, O., Roethlisberger, U., Koppenol, W.H. (2003). Oxidation of nitrite by peroxynitrous acid. *J Phys Chem A* ***107***, 1763-1769.

(9) Lymar, S.V., Hurst, J.K. (1998). CO2-catalyzed one-electron oxidations by peroxynitrite: properties of the reactive intermediate. *Inorg. Chem.* ***37***, 294-301.

(10) Squadrito, G.L., Pryor, W.A. (2002). Mapping the reaction of peroxynitrite with CO2: energetics, reactive species, and biological implications. *Chemical research in toxicology.* ***15(7)***, 885-895.

(11) Uppu, R.M., Squadrito, G.L., Pryor, W.A. (1996). Acceleration of peroxynitrite oxidations by carbon dioxide. *Archives of biochemistry and biophysics.* ***327(2)***, 335-343.

(12) Romero, N., Denicola, A., Souza, J.M., Radi, R. (1999). Diffusion of peroxynitrite in the presence of carbon dioxide. *Archives of biochemistry and biophysics.* ***368(1)***, 23-30.

(13) Tretyakova, N.Y., Burney, S., Pamir, B., Wishnok, J.S., Dedon, P.C., Wogan, G.N., Tannenbaum, S.R. (2000). Peroxynitrite-induced DNA damage in the supF gene: correlation with the mutational spectrum. *Mutation research.* ***447(2)***, 287-303.

(14) Lymar, S.V., Hurst, J.K. (1995). Rapid reaction between peroxynitrite ion and carbon dioxide: implications for biological activity. *J Am Chem Soc* ***117***, 8867-8868.

(15) Lymar, S.V., Jiang, Q., Hurst, J.K. (1996). Mechanism of carbon dioxide-catalyzed oxidation of tyrosine by peroxynitrite. *Biochemistry.* ***35(24)***, 7855-7861.

(16) Bonini, M.G., Radi, R., Ferrer-Sueta, G., Ferreira, A.M., Augusto, O. (1999). Direct EPR detection of the carbonate radical anion produced from peroxynitrite and carbon dioxide. *The Journal of biological chemistry.* ***274(16)***, 10802-10806.

(17) Goldstein, S., Czapski, G. (1998). Formation of Peroxynitrate from the Reaction of Peroxynitrite with CO2: Evidence for Carbonate Radical Production. *J Am Chem Soc* ***120***, 3458-3463.

(18) Bonini, M.G., Augusto, O. (2001). Carbon dioxide stimulates the production of thiyl, sulfinyl, and disulfide radical anion from thiol oxidation by peroxynitrite. *The Journal of biological chemistry.* ***276(13)***, 9749-9754.

(19) Koppenol, W.H., Moreno, J.J., Pryor, W.A., Ischiropoulos, H., Beckman, J.S. (1992). Peroxynitrite, a cloaked oxidant formed by nitric oxide and superoxide. *Chemical research in toxicology.* ***5(6)***, 834-842.

(20) Denicola, A., Freeman, B.A., Trujillo, M., Radi, R. (1996). Peroxynitrite reaction with carbon dioxide/bicarbonate: kinetics and influence on peroxynitrite-mediated oxidations. *Archives of biochemistry and biophysics.* ***333(1)***, 49-58.

(21) Zhu, L., Gunn, C., Beckman, J.S. (1992). Bactericidal activity of peroxynitrite. *Archives of biochemistry and biophysics.* ***298(2)***, 452-457.

(22) Lymar, S.V., Hurst, J.K. (1996). Carbon dioxide: physiological catalyst for peroxynitrite-mediated cellular damage or cellular protectant? *Chemical research in toxicology.* ***9(5)***, 845-850.

(23) Yermilov, V., Yoshie, Y., Rubio, J., Ohshima, H. (1996). Effects of carbon dioxide/bicarbonate on induction of DNA single-strand breaks and formation of 8-nitroguanine, 8-oxoguanine and base-propenal mediated by peroxynitrite. *FEBS letters.* ***399(1-2)***, 67-70.

(24) Burney, S., Caulfield, J.L., Niles, J.C., Wishnok, J.S., Tannenbaum, S.R. (1999). The chemistry of DNA damage from nitric oxide and peroxynitrite. *Mutation research.* ***424(1-2)***, 37-49.

(25) Pryor, W.A., Cueto, R., Jin, X., Koppenol, W.H., Ngu-Schwemlein, M., Squadrito, G.L., Uppu, P.L., Uppu, R.M. (1995). A practical method for preparing peroxynitrite solutions of low ionic strength and free of hydrogen peroxide. *Free radical biology & medicine.* ***18(1)***, 75-83.

(26) Kennedy, L.J., Moore Jr., K., Caulfield, J.L., Tannenbaum, S.R., Dedon, P.C. (1997). Quantitation of 8-oxoguanine and strand breaks produced by four oxidizing agents. *Chem. Res. Toxicol.* ***10***, 386-392.

(27) Shafirovich, V., Dourandin, A., Huang, W., Geacintov, N.E. (2001). The carbonate radical is a site-selective oxidizing agent of guanine in double-stranded oligonucleotides. *The Journal of biological chemistry.* ***276(27)***, 24621-24626.

(28) Augusto, O., Bonini, M.G., Amanso, A.M., Linares, E., Santos, C.C., De Menezes, S.L. (2002). Nitrogen dioxide and carbonate radical anion: two emerging radicals in biology. *Free radical biology & medicine.* ***32(9)***, 841-859.

(29) Zhang, H., Squadrito, G.L., Uppu, R.M., Lemercier, J.N., Cueto, R., Pryor, W.A. (1997). Inhibition of peroxynitrite-mediated oxidation of glutathione by carbon dioxide. *Archives of biochemistry and biophysics.* ***339(1)***, 183-189.

(30) Alberty, R.A. (1995). Standard Transformed Formation Properties of Carbon Dioxide in Aqueous Solutions t specified pH. *J. Phys. Chem.* ***99***, 11028-11034.

(31) Pryor, W.A., Lemercier, J.N., Zhang, H., Uppu, R.M., Squadrito, G.L. (1997). The catalytic role of carbon dioxide in the decomposition of peroxynitrite. *Free radical biology & medicine.* ***23(2)***, 331-338.

(32) Lemercier, J.N., Padmaja, S., Cueto, R., Squadrito, G.L., Uppu, R.M., Pryor, W.A. (1997). Carbon dioxide modulation of hydroxylation and nitration of phenol by peroxynitrite. *Archives of biochemistry and biophysics.* ***345(1)***, 160-170.

(33) Uppu, R.M., Winston, G.W., Pryor, W.A. (1997). Reactions of peroxynitrite with aldehydes as probes for the reactive intermediates responsible for biological nitration. *Chemical research in toxicology.* ***10(12)***, 1331-1337.

(34) Nakao, L.S., Ouchi, D., Augusto, O. (1999). Oxidation of acetaldehyde by peroxynitrite and hydrogen Peroxide/Iron(II). Production Of acetate, formate, and methyl radicals. *Chemical research in toxicology.* ***12(10)***, 1010-1018.

(35) Yang, D., Tang, Y.-C., Wang, X.-C., Bartberger, M.D., Houk, K.N., Olson, L. (1999). Ketone-catalyzed decomposition of peroxynitrite via dioxirane intermediates. *J Am Chem Soc* ***121***, 11976-11983.

(36) Merenyi, G., Lind, J., Goldstein, S. (2001). The rate of homolysis of adducts of peroxynitrite to the C=O double bond. *J Am Chem Soc* ***124***, 40-48.

(37) Uppu, R.M., Pryor, W.A. (1996). Carbon dioxide catalysis of the reaction of peroxynitrite with ethyl acetoacetate: an example of aliphatic nitration by peroxynitrite. *Biochemical and biophysical research communications.* ***229(3)***, 764-769.

CHAPTER VI

Formation of 3'-Phosphoglycolaldehyde in Human Cells

1. ABSTRACT

DNA strand breaks are among the most common types of radiation-induced DNA damage, and arise mainly as a product of oxidation of the deoxyribose moiety. Therefore, definition of deoxyribose oxidation chemistry within DNA is required for a better understanding of the biological effects of ionizing radiation. Toward the goal of quantifying deoxyribose oxidation chemistry in cells, we report here the quantification of 3'-phosphoglycolaldehyde (PGA) residues, which arise from C3'-oxidation of deoxyribose in DNA, induced by γ-radiation in human TK6 cells. Samples were exposed to 0-1000 Gy of ^{60}Co γ-radiation, which resulted in a linear dose-response of 0.0024 PGA residues per 10^6 nucleotides per Gy. When compared to the results obtained for *in vitro* irradiation of calf thymus DNA (1.5 PGA residues per 10^6 nucleotides per Gy), the yield of PGA experiences an almost 1000-fold quenching effect *in vivo*.

2. INTRODUCTION

The analytical method developed and applied in previous chapters will now be applied to cells. The most frequent types of DNA damage produced by ionizing radiation are single- and double-strand breaks, base and sugar modifications and DNA-protein crosslinks *(1, 2)*. Therefore, the determination of the level of sugar oxidation within DNA is a requisite for a better understanding of the biological effects of ionizing radiation. Most DNA damage induced by γ-radiation arise as a result of hydroxyl radicals. Other radical species such as e^-_{aq} and H atom also can cause DNA damage partially due to their reaction with oxygen at diffusion controlled rates to yield superoxide *(3)*.

Several other groups have undertaken studies of radiation-induced DNA damage in cells. Le *et al.* measured the induction and repair of thymine glycol in human A549 lung carcinoma cells using an immunochemical recognition technique coupled with capillary electrophoresis *(4)*. They found that thymine glycol is induced at a level of 0.9 lesions per 10^7 nt per Gy in cells and 6.5 molecules per 10^6 nt per Gy for calf thymus DNA *(4)*. Douki *et al.* measured UV light-induced *cis-syn* cyclobutane thymine dimers and *trans-syn* I cyclobutane thymine photoproducts in acute leukemia THP1 monocytes using high-performance liquid chromatography/tandem mass spectrometry (HPLC/MS/MS) *(5)*. The yield of lesions depended on the wavelength of UV light and cell density used and ranged from 2.4 lesions per J m^{-2} per 10^6 nt, to 0.01 lesions per J m^{-2}

per 10^6 nt *(5)*. The same methodology was used to quantify a variety of DNA lesions in THP1 cells exposed to 90-450 Gy of γ-radiation, shown in Table VI-1.

Table VI-1: Oxidative DNA lesions measured in cells induced by γ-radiation

Lesion	lesions/10^6 nt/Gy	Reference
thymine glycol	0.09	*(4)*
5,6-dihydroxy-5,6-dihydrothymidine	0.097	*(6)*
5-(hydroxymethyl)-2'-deoxyuridine	0.029	*(6)*
5-formyl-2'-deoxyuridine	0.022	*(6)*
8-oxo-dG	0.020	*(6)*
8-oxo-dG *	0.044	*(7)*
8-oxo-7,8-dihydro-2'-adenosine	0.003	*(6)*
4,6-diamino-5-formamidopyrimidine	0.005	*(6)*
2,6-diamino-4-hydroxy-5-formamidopyrimidine	0.039	*(6)*
5-hydroxy-2'deoxyuridine	< 0.0002	*(6)*
PGA **	0.0024	

All lesions measured using HPLC/MS/MS unless otherwise indicated; * measured using HPLC/ECD; ** measured using GC/MS as described in Chapter III.

Several analytical techniques are available to study oxidative DNA modification in cells. Strand breaks can be measured using the comet assay *(7)* or alkaline elution *(8)*. Methods that can measure specific DNA oxidation products in cells include ^{32}P-postlabeling, HPLC/MS/MS, and immunological detection *(4)*. However, the use of antibodies targeted against specific DNA lesions is limited due to cross reactivity with unmodified DNA bases *(9)*. ^{32}P-postlabeling consists of enzymatic hydrolysis of DNA, followed by the introduction of a radioactive phosphate on the 5'-OH end of the digested nucleoside 3'-monophosphates. The modified and normal nucleotides are then separated

by either thin-layer chromatography, gel electrophoresis, or reverse phase HPLC prior to quantification *(10, 11)*. This method often exhibits a high background because of artefactual oxidation induced by radioactivity *(9)*. HPLC coupled to electrochemical detection has been employed for the measurement of several DNA base lesions such as 8-oxo-7,8-dihydro-2'-deoguanosine (8-oxo-G) *(12-14)*. A highly sensitive and specific method that combines HPLC separation with electrospray ionization tandem mass spectrometry has been used to assess DNA adducts of bulky chemicals such as benzo[a]pyrene *(15)* and UV-induced pyrimidine dimer photoproducts *(5)* and other modified DNA bases such as 8-oxo-G *(9)*.

We report here the expansion of our previously developed GC/MS method to the detection of 3-phosphoglycolaldehyde (PGA) *in vivo*. The measurement of specific deoxyribose oxidation products requires both sensitive and specific techniques since the modification level of cellular DNA for most base lesions as discussed above is in the range of 1 lesion per 10^7 nt per Gy (*i.e.* reference *16*). The expanded method, now including a DNA isolation step, was used to detect PGA in γ-irradiated human TK6 lymphoblastoma cells. Our method is both specific and comparable in sensitivity in detection of oxidative DNA lesions in comparison to published HPLC/MS/MS results for γ-radiation-induced nucleobase lesions (i.e. reference *6*).

3. MATERIALS AND METHODS

3.1 Materials. All chemicals and reagents were of the highest purity available and were used without further purification unless noted otherwise. Pentafluorobenzylhydroxylamine and *bis*(trimethylsilyl)trifluoroacetamide (containing 1% trimethylchlorosilane) were purchased from Sigma Chemical Co. (St. Louis, MO). Nuclease P1, RNase A (DNase free), and proteinase K were from Roche Diagnostic Co. (Indianapolis, IN). Ethyl acetate was purchased from Mallinckrodt Baker (Phillipsburg, NJ). Distilled and deionized water was further purified with a Milli-Q system (Millipore Corporation, Bedford, MA) and was used in all experiments.

3.2 Instrumental Analyses. GC/MS analyses of derivatized PGA were performed with a HP6890 gas chromatograph (HP7673 auto-injector) coupled to a Hewlett Packard 5973N mass selective detector. UV spectra were obtained using a Beckman DU 640 UV-visible spectrophotometer.

3.3 Cell culture (performed by Dr. Tao Jiang). TK6 human lymphoblastoid cells were maintained in exponentially growing suspension culture at 37 °C in a humidified 5% CO_2 atmosphere in RPMI-1640 medium supplemented with 10% heat-inactivated calf bovine serum in the presence of 100 units/ml of penicillin, 100 μg/ml of streptomycin, and 4 mM of L-glutamine.

3.4 γ-Irradiation of TK6 cells. Samples were irradiated at room temperature in a Gammacell-220E (Atomic Energy of Canada, Ltd.) with an annular ^{60}Co source. On the date of calibration (10/15/2003), the sealed source contained 23,654 Ci of ^{60}Co and delivered γ-radiation at a rate of 5.215 Gy/s. Cells (2×10^7) were sedimented at 200 g for 5 min, the cell pellet was rinsed three times with 10 ml of PBS (0.9% NaCl, 10 mM sodium phosphate, pH 7.2) and resuspended in 10 ml PBS. After resuspension the cells were irradiated, pelleted and stored at -80 °C overnight.

3.5 Isolation of genomic DNA (performed by Ms. Marita C. Barth; method development by Ms. Min Dong). The pelleted cells were resuspended in 800μL of buffer A (300 mM sucrose, 60 mM KCl, 15 mM NaCl, 60 mM Tris-HCl, pH 8.0, 0.5 mM spermidine, 0.15 mM spermine, and 2 mM EDTA) containing 1% (octylphenoxy)polyethoxyethanol (IGEPA CA-630). Each sample was split into two tubes, each containing 400 μL. The cell suspension was vortexed at moderate speed for 1 min and incubated on ice for 5 min. The nuclei were sedimented by centrifugation at 4500 g for 10 min at 4 °C. The pelleted nuclei were resuspended in 300 μL buffer A. The cell suspension was vortexed again at moderate speed for 1 min and nuclei were re-sedimented at 4500 g for 10 min at 4 °C. The pelleted nuclei were resuspended in 200 μL buffer B (150 mM NaCl and 5 mM EDTA, pH 7.8) and consecutively, 200 μL buffer C (20 mM Tri-HCl, pH 8.0, 20 mM NaCl, 20 mM EDTA, and 1% sodium dodecyl sulfate) was added to the nuclei suspension before adding proteinase K to a final concentration of 450 μg/ml. The nuclei suspension was incubated at 37 °C for 3 h with occasional mixing by inversion of the sample tubes. RNase A was added to a final

concentration of 150 μg/ml followed by incubation at 37 °C for 1 h. DNA was purified by successive extraction with 1 volume of phenol (equilibrated with 0.1 M Tris-HCl, pH 8.0, also containing 0.1 % 8-hydroxyquinoline (w/w)), 1 volume of phenol: chloroform (1:1, v/v), and 1 volume of chloroform. DNA was recovered by precipitation in 200 mM NaCl and 2 volumes of ice cold absolute ethanol. The floating DNA filament was recovered with a micropipette tip or DNA was pelleted by centrifugation at 5000 g for 30 min. The recovered DNA pellet was washed with 70% ethanol, air-dried at room temperature and dissolved in 50 mM Chelex-treated phosphate buffer, pH 7.4. DNA concentration was measured for combined samples by absorption at 260 nm and stored at –80 °C overnight.

3.6 Quantification of PGA. PGA was measured using our GC/MS method as described in Chapter III, section 3.5.

4. RESULTS AND DISCUSSION

Samples containing 2 x 10^8 TK6 cells in PBS buffer were subjected to γ-radiation over the range of 0 to 1000 Gy. The samples were processed for DNA isolation and GC/MS analysis of PGA. The results are shown in Figure VI-1. Over the dose range of 250 to 1000 Gy, the data show linearity (r^2=1.0), with a slope of 0.0024 PGA residues per 10^6 nt per Gy. Between 0 and 250 Gy the curve shows a different slope, however, no measurements can be taken to investigate this behavior, because PGA levels are below

our detection limit. *In vitro*, we observed a slope of 1.5 PGA residues per 10^6 nt per Gy, which represents a quenching effect of about 1000-fold for PGA induction *in vivo*.

Measurement of PGA levels in un-irradiated cells has been unexpectedly difficult, due to extreme difficulties in re-dissolving DNA after ethanol precipitation. Attempts to alleviate this problem by incubation of the solution at 37 °C with gentle shaking, vortexing or freezing, and subsequent thawing of samples failed. In addition, with the measured PGA levels in irradiated cells being very close to detection limit, optimization of the DNA isolation procedure and further optimization of the PGA method for the measurement of PGA in cells is a prerogative to further investigate PGA levels in cells treated with other oxidative agents.

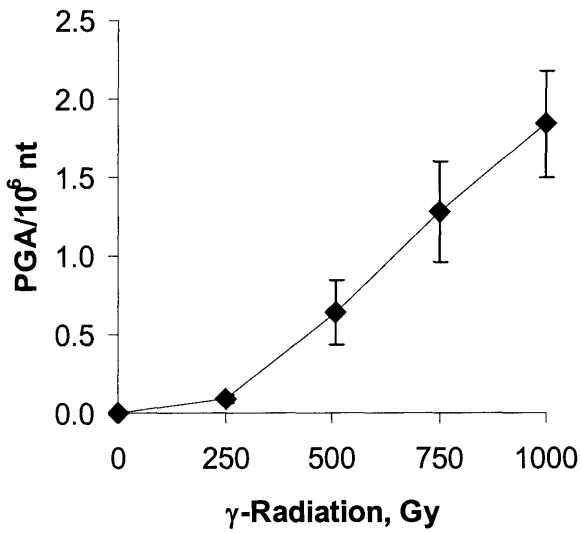

Figure VI-1: PGA levels in γ-irradiated TK6 cells. Cells were subjected to 0-1000 Gy of γ-radiation in a ^{60}Co source and processed for GC/MS analysis as described in Chapter III, section 3.5. The data represent mean ± SD for three independent experiments.

The method of DNA extraction from cells has been shown to be of great importance in the avoidance of DNA oxidation artifacts. Helbock *et al.* showed that phenol extraction contributes a real but minor increase in the level of 8-oxo-dG when compared to the chaotropic sodium iodide method *(17)*. Far more problematic was air exposure of DNA while drying DNA in the presence of free-radical producing impurities *(17)*. The background level of 8-oxo-dG is also influenced by nuclease P1 incubation (which is also used in our method) for DNA hydrolysis in the presence of redox-active iron, which Helbock *et al.* suppressed by addition of 0.1 mM desferal *(17)*. Even though the contribution of redox-active metals after DNA extraction during nuclease P1 digestion is a possibility, it would equally affect all samples and therefore just increase the background level of PGA. However, NP1 incubation in the presence of 0.1 mM desferal might decrease this background and lead to greater sensitivity, if desferal does not extract into ethyl acetate or interferes with the GC/MS assay in any other way *(17)*. Helbock *et al.* suggested that the digestion of DNA samples of more than 100 μg of DNA per sample is preferable to allow for a greater margin of methodological error *(17)*. We have used on average 300 μg of DNA per sample for PGA measurements. However, the use of greater quantities of DNA may require re-optimization of the nuclease P1 digestion step in our assay to insure complete digestion of genomic DNA.

The chaotropic DNA isolation method in combination with HPLC/MS/MS was used by Frelon *et al.* to measure five modified DNA bases in cells exposed to γ-radiation. At the lowest irradiation level of 90 Gy, 8-oxo-G was observed at approximately 2 lesions per 10^6 unmodified nt *(9)*. We are able to detect similarly low levels of PGA in

cells with our GC/MS method using the same amount of cells but higher radiation levels, indicating that PGA is a rarer lesion induced by γ-radiation than 8-oxo-G. Pouget *et al.* used HPLC/MS/MS to determine 8-oxo-G levels in γ-irradiated cells at a dose range between 90 and 450 Gy. The response was linear ($r^2 = 0.97$) and amounted to 0.02 lesions per Gy *(6)*. This is about 10-fold higher than our results with PGA. However, Frelon *et al.* used the same technique for isolated DNA and obtained a formation rate of 35.1 ± 0.9 lesions per 10^6 unmodified nt per Gy *(9)*, which is similar to our results and represents a roughly 1000-fold quenching when comparing *in vivo* to *in vitro* results.

Using the comet assay, a single-cell electrophoresis method, Pouget *et al.* have shown that in human acute monocytic THP1 cells exposed to γ-radiation the yield of single- and double-strand breaks and alkaline-labile sites per Gy is close to 0.13 per 10^6 nt, corresponding to 1600 DNA lesions per cell per Gy *(18)*. In order to obtain quantitative information from the comet assay, calibrations where preformed to correlate the comet tail moment with 8-oxo-G yields obtained by HPLC-EC measurements *(18)*. The authors claim that this corresponds favorably with the finding of Goodhead, who found that a dose of 1 Gy of γ-radiation corresponds to about 1000 radiation tracks through the cell nucleus as established by Monte-Carlo simulations *(19)*. Assuming that the strand breaks and alkaline-labile sites mainly correspond to deoxyribose oxidation, the number obtained by Pouget *et al. (18)* and our yield of PGA per nt per Gy indicates that about 2% of all deoxyribose oxidation induced by γ-radiation contain a PGA residue. This corresponds favorably with the value established in our in vitro studies of a 1% yield of PGA per deoxyribose oxidation event (see Chapter III, section 4.3).

5. REFERENCES

(1) O'Neill, P. (2001). Radiation-induced damage in DNA. In Radiation chemistry: present status and future trends, **87**, 1 Edition, C.D. Jonah, B.S.M. Rao, eds. (Elsevier Science), 585-622.

(2) Douki, T., Martini, R., Ravanat, J.L., Turesky, R.J., Cadet, J. (1997). Measurement of 2,6-diamino-4-hydroxy-5-formamidopyrimidine and 8-oxo-7,8-dihydroguanine in isolated DNA exposed to gamma radiation in aqueous solution. *Carcinogenesis.* ***18(12)***, 2385-2391.

(3) von Sonntag, C. (1987). The Chemical Basis of Radiation Biology (New York: Taylor & Francis).

(4) Le, X.C., Xing, J.Z., Lee, J., Leadon, S.A., Weinfeld, M. (1998). Inducible repair of thymine glycol detected by an ultrasensitive assay for DNA damage. *Science* ***280***, 1066-1069.

(5) Douki, T., Court, M., Sauvaigo, S., Odin, F., Cadet, J. (2000). Formation of the main UV-induced thymine dimeric lesions within isolated and cellular DNA as measured by high performance liquid chromatography-tandem mass spectrometry. *The Journal of biological chemistry.* ***275(16)***, 11678-11685.

(6) Pouget, J.P., Frelon, S., Ravanat, J.L., Testard, I., Odin, F., Cadet, J. (2002). Formation of modified DNA bases in cells exposed either to gamma radiation or to high-LET particles. *Radiation research.* ***157(5)***, 589-595.

(7) Pouget, J.P., Ravanat, J.L., Douki, T., Richard, M.J., Cadet, J. (1999). Measurement of DNA base damage in cells exposed to low doses of gamma-radiation: comparison between the HPLC-EC and comet assays. *Int J Radiat Biol* ***75***, 51-58.

(8) Epe, B., Pflaum, M., Boiteux, S. (1993). DNA damage induced by photosensitizers in cellular and cell-free systems. *Mutation research.* ***299(3-4)***, 135-145.

(9) Frelon, S., Douki, T., Ravanat, J.L., Pouget, J.P., Tornabene, C., Cadet, J. (2000). High-performance liquid chromatography--tandem mass spectrometry measurement of radiation-induced base damage to isolated and cellular DNA. *Chemical research in toxicology.* ***13(10)***, 1002-1010.

(10) Weinfeld, M., Soderlind, K.J. (1991). 32P-postlabeling detection of radiation-induced DNA damage: identification and estimation of thymine glycols and phosphoglycolate termini. *Biochemistry* ***30***, 1091-1097.

(11) Weinfeld, M., Buchko, G.W. (1993). Postlabeling methods for the detection of apurinic sites and radiation- induced DNA damage. *IARC Sci Publ* ***124***, 95-103.

(12) Douki, T., Delatour, T., Paganon, F., Cadet, J. (1996). Measurement of oxidative damage at pyrimidine bases in gamma-irradiated DNA. *Chemical research in toxicology.* ***9(7)***, 1145-1151.

(13) Berger, M., Anselmino, C., Mouret, J.-F., Cadet, J. (1990). High performance liquid chromatography-electrochemical assay for monitoring the formation of 8-oxo-7,8-dihydroadenine and its related 2'-deoxyribonucleoside. *Journal of liquid chromatography* ***13***, 929-940.

(14) Wagner, J.R., Hu, C.C., Ames, B.N. (1992). Endogenous oxidative damage of deoxycytidine in DNA. *Proceedings of the National Academy of Sciences of the United States of America.* ***89(8)***, 3380-3384.

(15) Fang, A.H., Smith, W.A., Vouros, P., Gupta, R.C. (2001). Identification and characterization of a novel benzo[a]pyrene-derived DNA adduct. *Biochem Biophys Res Commun* ***281***, 383-389.

(16) Cadet, J., Douki, T., Frelon, S., Sauvaigo, S., Pouget, J.P., Ravanat, J.L. (2002). Assessment of oxidative base damage to isolated and cellular DNA by HPLC-MS/MS measurement. *Free radical biology & medicine.* ***33(4)***, 441-449.

(17) Helbock, H.J., Beckman, K.B., Shigenaga, M.K., Walter, P.B., Woodall, A.A., Yeo, H.C., Ames, B.N. (1998). DNA oxidation matters: the HPLC-electrochemical detection assay of 8-oxo-deoxyguanosine and 8-oxo-guanine. *Proceedings of the National Academy of Sciences of the United States of America.* ***95(1)***, 288-293.

(18) Pouget, J.P., Douki, T., Richard, M.J., Cadet, J. (2000). DNA damage induced in cells by gamma and UVA radiation as measured by HPLC/GC-MS and HPLC-EC and Comet assay. *Chem Res Toxicol* ***13***, 541-549.

(19) Goodhead, D.T. (1989). The initial physical damage produced by ionizing radiations. *International journal of radiation biology.* ***56(5)***, 623-634.

Chapter 7

Conclusions and Future Studies

We have developed a reproducible, sensitive and specific method to quantify phosphoglycolaldehyde (PGA) *in vitro* and *in vivo*. The method can also be applied to virtually all carbonyl-containing deoxyribose oxidation products. We have used our method to establish that PGA is a general deoxyribose oxidation product for reactive oxygen and nitrogen species (see Table VII-1). Our results confirm the long-standing qualitative and chemically unrigorous claims of PGA formation *in vitro (1, 2)*. In addition for the first time, we provide a rigorous measure of this deoxyribose oxidation product in cells.

There remains one crucial step to identify PGA as a product of deoxyribose C3' hydrogen atom abstraction. At this point we cannot rule out 2'-oxidation given the observation of Saito and coworkers of the C2' oxidation product erythrose abasic site that yielded PGA residues, following an alkali-induced retroaldol rearrangement *(3)*. The use of a ^{13}C labeled deoxyribose in the C2' position would prove the formation of PGA resulting from the 3'-position if the measured PGA does not contain the ^{13}C label. PGA

formed by the C3' position consists of the C4' and C5' carbon of the deoxyribose (see Scheme I-3).

Summary of results:

Oxidizing agent	Total deoxyribose oxidation/10^6 nt	PGA/10^6 nt	% dR oxidation events containing PGA
Fe(II)	22/μM ± 2	Nonlinear	n/a
Fe(II)/EDTA	10/μM ± 1	0.5/μM ± 0.4	5% ± 0.2 %
Fe(II)/EDTA/H_2O_2		Nonlinear	n/a
γ-Radiation (*in vitro*)	144/Gy ± 10	1.5/Gy ± 0.05	1 % ± 0.02 %
α -Particles	1.9/Gy ± 0.1	0.1/Gy ± 0.02	7 % ± 0.5 %
$ONOO^-$	Nonlinear	0.2/μM ± 0.006	12 % *
$ONOOCO_2^-$	Nonlinear	n/d	n/a

Table VII-1: Summary of total deoxyribose oxidation events (experiments performed by Xinfeng Zhou), and PGA yields per 10^6 nt, for the oxidizing agents studied in this thesis. $ONOOCO_2^-$ refers to the exposure of DNA to $ONOO^-$ in the presence of 25 mM bicarbonate. n/d: below the detection limit of 2 PGA per 10^6 nt; n/a: not applicable, because PGA formation is below our detection limit; *: calculated for 25 mM $ONOO^-$, but this value is $ONOO^-$ concentration dependent due to the nonlinear nature of the total deoxyribose oxidation.

The GC/MS method developed for this thesis was proven to be applicable to the measurement of PGA *in vitro* and *in vivo* with great sensitivity, reproducibility and specificity. The method remains robust and sensitive even in the presence of iron and peroxynitrite decomposition products, thus making prepurification before enzyme

hydrolysis unnecessary. Our PGA method has sensitivity similar to the HPLC/MS/MS measurement of 8-oxo-G *(4)*.

We have successfully quantified PGA in human cells, the first time to our knowledge that a specific deoxyribose oxidation product has been quantified *in vivo*. However, as discussed in Chapter VI, *in vivo* measurement of PGA remains to be optimized. After optimization, the method can be used to quantify PGA in tissues, comparing for instance normal tissues to chronically inflamed tissues or tissues that experienced chronic iron overload. Further *in vitro* studies of PGA production using copper, chromium and other transition metals, that have been shown to react in a similar way to the Fenton reaction *(5, 6)*, are also worthwhile pursuing to further characterize deoxyribose oxidation.

Furthermore, our assay can be extended to study other deoxyribose oxidation products, such as the C5' oxidation product 2'-phosphoryl-1,4-dioxobutane, the C4' oxidation product 4'-keto-1'-aldehyde abasic site, or the C2' oxidation product erythrose-abasic site. Pentafluorobenzylhydroxylamine reacts quantitatively with all aldehydes and ketones, therefore all deoxyribose oxidation products featuring such a carbonyl group can be studied with our method. However, the method would have to be re-optimized to ensure quantitative enzymatic hydrolysis from DNA. Also, synthesis of standards and positive controls, including an oligodeoxynucleotide containing the lesion of interest, is non-trivial.

The pathway leading to PGA may not be the only pathway involved in the degradation of the 3'-carbon radical. Stubbe and Kozarich have proposed that C3' chemistry partitions to form a strand break with either a PGA residue or an alternative five-carbon fragment *(7)*. This partitioning is common in the oxidation of the other positions in deoxyribose, such as the two sets of products arising from 5'-oxidation: a nucleoside-5'-aldehyde residue or a 3'-formylphosphate residue *(8)*. The latter accounts for only 10% of the C5' chemistry produced by the enediyne antibiotic neocarzinostatin *(8)* so it is possible that the PGA residue is a minor lesion and that 3'-oxidation occurs more frequently than predicted by our results and by the solvent exposure model for deoxyribose oxidation *(9)*. The presence of the proposed 2-methylene-3(H)-furanone or some other yet to be identified C3' deoxyribose oxidation product remains to be proven in oxidative DNA damage. This question might be addressed using an oligonucleotide containing ^{13}C dR labeled in the 3' position and comparing total ion chromatograms for a labeled and unlabeled oligonucleotide and a chromatogram of mixture of both oligonucleotides. Also, the use of a modified oligodeoxynucleotide that serves as a model for C3' radicals in the deoxyribose as discussed in Chapter I section 2 *(10)* may serve as a model to study the products of C3' oxidation. Such studies are currently underway in the laboratory of Professor Amanda Bryant-Friedrich.

1. Detection of PGA in tissues. In order to detect PGA in tissues, either sensitivity levels of the current method have to be improved or PGA levels have to be higher than indicated by PGA levels measured in cells (see Chapter 6). The following discussion assumes the irradiation of a mouse with 1 Gy of γ-radiation. The average size

of a mouse liver is 1.5 g (wet weight) *(11)*, which for this discussion will serve as the target tissue. The extraction of DNA from tissues yields about 1 % of the wet weight of the liver using current protocols established by Ms Min Dong in our laboratory, which in this case results in a maximum yield of 15 mg of DNA. If linear extrapolation from the TK6 cell data obtained using acute high dose irradiations presented in Chapter 6 is applicable, the expected yield of PGA for 1 Gy is 0.0024 PGA molecules per 10^6 nt. The mouse genome has a size of 3 x 10^9 nt *(11)*. Taking into account the DNA yield from the mouse liver and the PGA yield from 1 Gy of radiation, the expected yield of PGA is 110 fmol per mouse liver. With the current limit of detection of the method established in Chapter 2 is 30 fmol. Therefore, the current method should be applicable to measure PGA in tissues, if the assumptions made in this section are correct. Tissues may exhibit higher backgrounds than observed for *in vitro* work, which would impact sensitivity levels. Recommendations made in Chapter 7 to optimize the current PGA quantification method for cell work are directly applicable to optimize PGA detection in tissues in order to increase sensitivity levels. However, to be applicable for clinical levels of radiation, which range from a few cGy to a few hundred cGy depending on the tissue treated, the sensitivity levels have to be improved by at least 1 order of magnitude, especially due to the limited amount of human tissue available for study.

2. REFERENCES

(1) Sitlani, A., Long, E.C., Pyle, A.M., Barton, J.K. (1992). DNA Photocleavage by Phenanthrenequinone Diimine Complexes of Rhodium(III): Shape-Selective Recognition and Reaction. *J. Am. Chem. Soc* ***114***, 2303-2312.

(2) Benites, P.J., Rawat, D.S., Zaleski, J.M. (2000). Metalloenediynes: ligand field control of thermal Bergman cyclization reactions. *J Am Chem Soc* ***122***, 7208-7217.

(3) Sugiyama, H., Tsutsumi, Y., Fujimoto, K., Saito, I. (1993). Photoinduced deoxyribose-C2' oxidation in DNA: Alkali-dependent cleavage of erythrose-containing sites via a retroaldol reaction. *J. Am. Chem. Soc.* ***115***, 4443-4448.

(4) Dizdaroglu, M., Jaruga, P., Birincioglu, M., Rodriguez, H. (2002). Free radical-induced damage to DNA: mechanisms and measurement. *Free radical biology & medicine.* ***32(11)***, 1102-1115.

(5) Lloyd, D.R., Phillips, D.H. (1999). Oxidative DNA damage mediated by copper(II), iron(II) and nickel(II) Fenton reactions: evidence for site-specific mechanisms in the formation of double-strand breaks, 8-hydroxydeoxyguanosine and putative intrastrand cross-links. *Mutation research.* ***424(1-2)***, 23-36.

(6) Lloyd, D.R., Carmichael, P.L., Phillips, D.H. (1998). Comparison of the formation of 8-hydroxy-2'-deoxyguanosine and single- and double-strand breaks in DNA mediated by Fenton reactions. *Chemical research in toxicology.* ***11(5)***, 420-427.

(7) Stubbe, J., Kozarich, J.W. (1987). Mechanisms of Bleomycin-Induced DNA Degradation. *Chem Rev* ***87***, 1107-1136.

(8) Dedon, P.C., Jiang, Z.W., Goldberg, I.H. (1992). Neocarzinostatin-mediated DNA damage in a model AGT.ACT site: mechanistic studies of thiol-sensitive partitioning of C4' DNA damage products. *Biochemistry* ***31***, 1917-1927.

(9) Balasubramanian, B., Pogozelski, W.K., Tullius, T.D. (1998). DNA strand breaking by the hydroxyl radical is governed by the accessible surface areas of the hydrogen atoms of the DNA backbone. *Proc. Natl. Acad. Sci. U S A* ***95***, 9738-9743.

(10) Koerner, S., Bryant-Friedrich, A., Giese, B. (1999). C-3'-branched thymidines as precursors for the selective generation of C-3'-nucleoside radicals. *J. Org. Chem.* ***64***, 1559-1564.

(11) Bult, C.J., Blake, J.A., Richardson, J.E., Kadin, J.A., Eppig, J.T., Baldarelli, R.M., et al. (2004). The Mouse Genome Database (MGD): integrating biology with the genome. *Nucleic acids research.* ***32(1)***, D476-481.